Study of Electrostatic Modes and Potential of a Projectile in a Hot Magnetized Non-Maxwellian Dusty Plasma

BY

FARAH DEEBA
Regd No. 03-GCU-PH.D-PHY-06
SESSION 2006-2011

DEPARTMENT OF PHYSICS
GC UNIVERSITY
LAHORE PAKISTAN

2011

This work is submitted as a thesis in
partial fulfillment for the award of the degree of

DOCTOR OF PHILOSOPHY

in

PHYSICS

By

FARAH DEEBA
Regd No. 03-GCU-PH.D-PHY-06
SESSION 2006-2011

Department of Physics
GC University
Lahore, Pakistan

CERTIFICATE

Certified that the research work contained in this thesis entitled "**Study of Electrostatic Modes and Potential of a Projectile in a Hot Magnetized Non-Maxwellian Dusty Plasma"** has been carried out by **Farah Deeba**, Regd No. **03-GCU-PH.D-PHY-06** under my supervision during her PhD (Physics) studies.

Supervisor:

Prof. Dr. G. Murtaza

Salam Chair in Physics
Govt. College University
Lahore, Pakistan

Submitted Through:

Prof. Dr. Riaz Ahmad

Chairman
Department of Physics
Govt. College University
Lahore, Pakistan

The present study is based on the following publications:

1. "Electrostatic potentials and energy loss due to a projectile propagating through a Non-Maxwellian dusty plasma" Phys. Plasmas, **13**, 082108 (2006)
   (**F. Deeba**, Z. Ahmad and G. Murtaza)

2. "Generalized Dispersion Relation for Electron Bernstein Waves in a non-Maxwellian Magnetized Anisotropic Plasma" Phys. Plasmas, **17**, 102114 (2010)
   (**F. Deeba**, Z. Ahmad and G. Murtaza)

3. "Dispersion Relation for Pure Dust Bernstein Waves in a non-Maxwellian Magnetized Dusty Plasma"
   Phys. Plasmas, Phys. Plasmas, **18**, 072104 (2011)
   (**F. Deeba,** Z. Ahmad and G. Murtaza)

Publications in Conference Proceedings:

4. "Debye Potential and wake field due to a projectile propagating through a Non-Maxwellian Plasma", 12^{th} Regional Conference on Mathematical Physics March 27-April 1, 2006 National Centre for Physics, Islamabad Pakistan
   (**F. Deeba,** Z. Ahmad and G. Murtaza)

ACKNOWLEDGEMENT

All praise to *ALMIGHTY ALLAH*, the most benevolent and merciful, the creator of the whole universe, who enabled me to complete this research work.

First and foremost, I want to express my deepest gratitude towards my respectable supervisor Prof. Dr. G. Murtaza, for his kind and invaluable guidance during research work. His sympathetic attitude and encouraging discussions enabled me in broadening and improving my capabilities not only in physics, but also in other fields of life.

My immense gratitude goes to Dr. Badar Suleman, Member (Sciences), PAEC, who graciously extended me every possible help whenever required. He has stimulated my imagination and gave me insight of research. Very special thanks are due to Prof. Dr. H. A. Shah for his encouraging attitude.

I am grateful to Prof. Dr. Riaz Ahmad, Chairman, Department of Physics, for providing me research facilities and moral support.

The cooperation of the teaching faculty and secretarial staff of the Salam Chair and Physics Department *GC University* is duly acknowledged. Many thanks to each member of Plasma Physics Group at Salam Chair, who helped me in one way or other.

Last but not the least I wish to record my deepest obligations to my brothers, sister and especially to my parents and in-laws, for their love and patience.

In the last stage of thesis write up my mother in-law is passed away and I missed her prayers and love.

(Farah Deeba)

DEDICATED TO

My daughter Fatima
(Who sacrificed the most)

And

My Husband
(Who suffered the most)

DECLARATION

I, **Farah Deeba**, Reg. No.**03-GCU-PH.D-PHY-06**, student of PhD in the subject of **Physics** session **2006-2011** here by declared that the matter printed in the thesis titled **"Study of Electrostatic Modes and Potential of a Projectile in a Hot Magnetized Non-Maxwellian Dusty Plasma"**is my own work and has not been printed, published and submitted as research work, thesis or publication in any form in any University, Research Institution etc. in Pakistan or abroad.

Dated: _____ Signature of Deponent

Abstract

The electrostatic potentials (Debye and wake) and energy loss due to a charged projectile propagating through an dusty plasma are derived employing kappa and generalized (r,q) velocity distributions for the Dust Acoustic Wave (DAW). It is found that these quantities in general differ from their Maxwellian counterparts and are sensitive to the values of spectral index, kappa in case of kappa distribution and to r, q in case of generalized (r,q) distribution. The amplitudes of these quantities are less for small values of the spectral index (kappa, r=0, q) but approach to the Maxwellian in the limit $\kappa \to \infty$ (for kappa distribution) and for r=0, $q \to \infty$ (for generalized (r, q) distribution). For any non-zero value of r, the potential and the energy loss grow beyond the Maxwellian results. The effect of kappa and generalized (r, q) distributions on potential and energy loss is also studied numerically and the results are compared with those of the Maxwellian distribution.

A generalized dielectric constant for the electron Bernstein waves using non-Maxwellian distribution functions is derived in a collisionless, uniform magnetized plasma. Using Neumann's series expansion for the products of Bessel functions, we can derive dispersion relations for both kappa and the generalized (r,q) distributions in a straight forward manner. The dispersion relations now become dependent upon the spectral indices κ and (r,q) for the kappa and the generalized (r,q) distribution respectively. Our results show how the non-Maxwellian dispersion curves deviate from the Maxwellian depending upon the values of the spectral indices chosen. Pure dust Bernstein waves are also investigated using non-Maxwellian kappa and (r,q) distribution functions. Dispersion relations for both distributions are derived considering waves whose frequency is of the order of dust cyclotron frequency and dispersion curves are plotted. It is observed that the propagation band for dust Bernstein waves is rather narrow as compared with the electron Bernstein waves. However the band width increases for higher harmonics, for both kappa and (r,q) distributions. Effect of dust charge on dispersion curves is also studied and one observes that with increasing dust charge, the dispersion curves shift toward the lower frequencies. Increasing the dust to ion density ratio causes the dispersion curve to shift toward the higher frequencies. Relevance of this work can be found in astrophysical dusty plasmas where non-Maxwellian distribution is present along with the dust particles.

Contents

1 Introduction **3**

1.1 The Term Plasma 3

1.2 Brief history of the Plasma 4

1.3 Plasma Types 4

1.3.1 Unmagnetized Plasmas 5

1.3.2 Magnetized Plasmas 5

1.3.3 Thermal Plasmas 6

1.4 Plasma Waves 6

1.5 Kinetic Theory of Plasmas 8

1.5.1 Maxwellian Distribution Function 9

1.6 Non-Maxwellian Distribution functions 9

1.7 Motivation 11

1.8 Layout of the Thesis 14

2 Electrostatic Potentials and Energy Loss of a Projectile in Non-Maxwellian Dusty Plasmas **16**

2.1 Introduction 16

2.2 Mathematical formulation of the problem 17

2.3 Derivation of Electrostatic potentials 19

2.3.1 Electrostatic potentials of Kappa Velocity Distribution 19

2.3.2 Electrostatic potentials of Generalized (r, q) Velocity Distribution 27

2.4 Energy loss of a projectile in Non-Maxwellian Plasma 32
2.4.1 Energy loss for Kappa Velocity Distribution 33
2.4.2 Energy loss for Generalized (r, q) Distribution Function 38
2.5 Numerical Results and Discussion 43

3 Generalized Dispersion Relation of Electron Bernstein Waves in Magnetized Non-Maxwellian Plasmas 52
3.1 Introduction 52
3.2 Generalized Dielectric Constant in Magnetized Non-Maxwellian Plasmas 53
3.2.1 Dispersion relation of electron Bernstein waves for kappa Distribution Function 56
3.2.2 Parallel Propagation in Terms of Kappa Distribution 59
3.2.3 Dispersion relation of electron Bernstein waves for (r, q) Distribution 62
3.2.4 Parallel Propagation for (r, q) Distribution 66
3.3 Summary and Conclusions 71

4 Pure Dust Bernstein Waves in Magnetized Non-Maxwellian Plasmas 73
4.1 Introduction 73
4.2 Mathematical formulation of the pure dust Bernstein waves 74
4.2.1 Dispersion relation of pure dust Bernstein waves for kappa distribution function 74
4.2.2 Dispersion relation of pure dust Bernstein waves for (r, q) distribution function 78
4.3 Summary and Conclusion 83

5 Summary of the Results and Recommendations for Future Research Work 87

Chapter 1

Introduction

1.1 The Term Plasma

Matter naturally exists in four states: solid, liquid, gas and plasma. In a solid, the atoms are closely packed and form a rigid lattice structure. When energy is added to the system, the atoms gain energy and break the bonds that hold them in structure. Thus a process of phase transition from a solid state to a liquid state occur. In the liquid state, the atoms are closely spaced but they do not hold a fixed shape. As more energy is added, another phase transition from liquid to gas occur. In the gas state, the atoms are spread and interact very weakly. If more energy is added, electrons within the atoms gain enough energy to become free from the atoms forming an ionized gas. This quasi-neutral collection of ions, electrons and neutral particles makes up the final, and most common state of matter is called as plasma [1]. 95% (in some literature it is 99%) of the universe is in plasma state. Plasmas phenomena are complex and plasmas exist in a wide variety of situations. An important situation where plasmas do not normally exist or known is ordinary human experience. Consequently, common people do not have much experience or knowledge of plasma behavior as they have for solids, liquids and gases.

1.2 Brief history of the Plasma

American scientists Irving Langmuir and his colleague Lewi Tonks were the first who used the term plasma to describe an ionized gas in 1927. They worked on the gaseous electron tubes. During his research Langmuir discovered that certain regions of a plasma discharge tube exhibit periodic variations of the electron density. This phenomenon is known as Langmuir waves. At the same time study on the effect of ionospheric plasma on long distance shortwave radio propagation was started. In 1940's Hannes Alfvén developed a theory of hydromagnetic waves (called Alfvén waves) and suggested that these waves would be important in the study and understanding of the astrophysical plasmas [2]. In 1950's plasma based research on magnetic confinement fusion energy was stared in USA, UK and Soviet Union. The concept of tokamak was evolved in Soviet Union in those years. Soon it was spread in many other countries.

James A. Van Allen discovered the Van Allen radiation belts surrounding the Earth in 1958. This started the systematic research on the understanding of the Earth's magnetosphere and opened up another branch of plasma known as space plasma physics [3]. In the 1960's with the development of high power lasers, field of laser plasma physics was established. When a laser beam strikes a solid target, material is ablated, and a plasma is formed at the boundary between the beam and the target surface. Laser plasmas tend to have fairly extreme properties (e.g., high densities and high temperature) which are not found in conventional plasmas. Inertial confinement fusion is one of the out come of laser plasma physics as a scheme of fusion energy.

1.3 Plasma Types

Plasmas can be subdivided in to the following three types.

1.3.1 Unmagnetized Plasmas

Unmagnetized plasmas are considered first as have no equilibrium magnetic field and they are isotropic i.e., same in all direction and the waves that such a plasma will support are either high frequency electromagnetic waves which see the plasma as a simple dielectric due to the response of the electrons only to the wave (ions are generally considered immobile), or sound-type waves. In a cold plasma, the latter waves become a simple oscillation at the plasma frequency. Below this frequency electromagnetic waves do not propagate. In a thermal plasma there are sound-like waves near this frequency, In a plasma with different electron and ion temperatures considering $T_e >> T_i$, there is even a kind of hybrid sound wave that depends on the electron temperature and the ion mass [4].

1.3.2 Magnetized Plasmas

Almost in all of the realistic plasmas (laboratory, ionospheric and astrophysical) magnetic field is present . Inclusion of the magnetic field effects can add new phenomenon to the plasma waves, like anisotropy (as now there is preferred direction for propagation). Some kind of waves are excited only in a magnetized plasma e.g. Alfven waves and finite Larmor orbit effects due to thermal motions around the magnetic field lines. Although in a cold plasma the thermal effects are absent, however number of wave types excited by the inclusion of the magnetic field is large, and wave types vary greatly with the angle of propagation with respect to the magnetic field. We can find waves which are guided by the magnetic field in certain frequency ranges, and cases where the phase and group velocities are nearly normal to one another. In a cold unmagnetized plasma, the only parameter that may lead to inhomogeneities is the plasma density. Magnetic field not only adds new source of inhomogeneity, but also the gradients in the magnetic field may appear in different directions.

1.3.3 Thermal Plasmas

When thermal effects are added to the plasma dynamics, the plasma is called thermal plasma. This new phenomena can be grouped into two general categories: acoustic wave phenomena due to various kinds of sound waves; and kinetic phenomena due to the fact that in a thermal distribution, there are some particles moving at the phase velocity. These particles have resonant interactions with the waves due to their long interaction time. These interactions can lead to either collisionless wave damping or to instabilities and wave growth. When coupled with magnetic field effects, finite Larmor orbit effects lead to some new wave types and instabilities.

1.4 Plasma Waves

Plasma waves are discussed with two models; fluid model and kinetic model. Kinetic model present the most general theory to study the wave phenomenon in the plasma. Kinetic model takes explicit care of the properties of the particle distribution function. Therefore new effects will appear in this model which cannot be covered by the fluid approach for plasma [5]. In kinetic model/theory we deal with distribution functions and their evolution, the mass conservation, momentum conservation and energy conservation equations of fluid model are replaced by the set of Vlasov equations for the different components of the plasma. The field equations remain the same in both models. In this thesis we will concentrate only on kinetic theory leaving the fluid theory. As the kinetic theory is based upon the statistical approach, therefore it takes into account, the properties of the particle distribution function, its variations and the correlations between particles and fields.

In plasma usually two types of waves are dealt, transverse electromagnetic waves and longitudinal electrostatic waves. The latter are nothing but oscillations of the electrostatic potential and are not accompanied by magnetic field fluctuations. These oscillations of the electrostatic potential can be maintained only inside the plasma boundaries that is

why electrostatic modes are confined to the plasma [6]. Examples of electrostatic waves are, magnetized Langmuir and Ion-Acoustic waves, Electron Bernstein waves, Upper-Hybrid waves, Ion Bernstein waves, Lower-Hybrid waves etc. If we are dealing with the dusty plasma there exists new waves that are associated with the dust particle dynamics, e.g. dust acoustic waves (DAW) and dust ion acoustic wave (DIAW), will also be present. Below is the brief description of each of them.

Magnetized Langmuir and Ion-Acoustic waves: If one considers parallel propagation, at high frequencies the only wave present is the Langmuir wave. Magnetized ion-acoustic waves can be treated like the Langmuir waves. The only difference is that in Langmuir waves the electron plasma dispersion function is expanded in the small argument limit, whereas in the former case the ion dispersion function is expanded in the large argument limit.

Electron Bernstein waves: When we consider strictly perpendicular (or transverse) propagation in to plasma, we find electrostatic electron-cyclotron waves or Bernstein waves. Bernstein waves are high frequency gyroharmonics and there is no wave propagation below the first cyclotron harmonic. Electron Bernstein waves are ordered into electron-cyclotron harmonic bands.

Upper-Hybrid waves: The resonant frequency which is greater than the electron cyclotron or plasma frequencies is called the upper hybrid frequency.

Ion Bernstein waves: These waves are electrostatic ion-cyclotron resonances and are further sub-divided into pure and neutralized ion Bernstein waves. Pure ion Bernstein waves propagate in a plasma perpendicular to the magnetic field like electron Bernstein waves. However neutralized ion Bernstein waves have parallel component as well. Electrostatic ion-cyclotron waves are ordered into ion-cyclotron harmonic bands in a similar fashion as electron Bernstein waves.

Lower-Hybrid waves: The resonant frequency,which lies between the electron and ion cyclotron frequencies is called the lower hybrid frequency.

Dust acoustic waves (DAW): These waves are acoustic modes and the most fun-

damental excitation present in a uniform, unmagnetized, collisionless dusty plasmas. The phase velocity of the DA waves is much smaller than the electron and ion thermal speeds [7].

Dust ion-acoustic waves (DIAW): These are also acoustics modes in dusty plasma. The phase velocity of the DIA waves is much smaller than the electron thermal speed and is much larger than ion and dust thermal speeds.

1.5 Kinetic Theory of Plasmas

Fluid model does not give information about the velocity distribution of the particles since the fluid variables depend upon the position and time only and is independent of the velocities. The physical property of the plasma which describes the microscopic details in six-dimensional $(\mathbf{r}, \mathbf{v})$ space. Thus we deal with the distribution function $f_\alpha(\mathbf{r}, \mathbf{v}, t)$ which is the function of seven variables depend upon the density of particles in $(\mathbf{r}, \mathbf{v})$ space at time t. Therefore the existance of the distribution function is described by the kinetic theory.

In statistical mechanics, the generalized Boltzmann equation which satisfies the distribution function $f_\alpha(\mathbf{r}, \mathbf{v}, t)$ depends upon the position $\mathbf{r}$, velocity $\mathbf{v}$ and time t is written as

$$\partial_t f_\alpha + (\mathbf{v}.\boldsymbol{\nabla}) f_\alpha + \mathbf{a}.\boldsymbol{\nabla}_v f_\alpha = \left(\frac{\partial f}{\partial t}\right)_c$$

where the Lorentz force is related as

$$\mathbf{a} = \frac{q_\alpha}{m_\alpha}\left(\mathbf{E} + \frac{\mathbf{v}\times\mathbf{B}}{c}\right)$$

$\left(\frac{\partial f}{\partial t}\right)_c$ is the collisional operator which includes all types of collisions. The collision term can be neglected as compared to the high thermal velocities of the plasma particles and the Boltzmann equation can be written in the fundamental kinetic equation which

is called Vlasov equation and is given by

$$\partial_t f_\alpha + (\mathbf{v}.\boldsymbol{\nabla})\, f_\alpha + \mathbf{a}.\boldsymbol{\nabla}_v f_\alpha = 0$$

which is the basic equation in collisionless space plasmas such as solar wind and planetary magnetospheres.

1.5.1 Maxwellian Distribution Function

One of the important equilibrium velocity distribution function is called Maxwellian distribution which shows that there is no energy exchange processes occur between the particles in plasmas and there is no more free energy in thermal equilibrium state. In such type of distribution collisions dominate. In other words, system of particles with excess energy would Maxwellize through collisions in a certain time known as relaxation time. The isotropic Maxwellian distribution function is given by

$$f\,(v) = \left(\frac{M}{2\pi T}\right) \exp\left(\frac{-Mv^2}{2T}\right)$$

where M is the mass of the plasma species and T is the temperature.

1.6 Non-Maxwellian Distribution functions

It has been observed that the Maxwellian is not a realistic distribution under all circumstances. Other distributions such as kappa or generalized (r, q) distribution which are the subject of the present work may fit better with the data available for many environs in space plasmas such as the planetary magnetospheres, astrophysical plasmas and the solar wind. In such cases, the plasmas are generally observed to possess a Non-Maxwellian high energy tail[8]. Vasyliunas [9] was the first to employ the general form of the kappa distribution and note its relation with the Maxwellian. Mace *et al.* [10] found that superthermal particles have higher levels of electrostatic fluctuations and

shorter Debye lengths than plasmas with Maxwellian velocity distributions. It is also well known that space plasmas frequently contain particle components that exhibit high or superthermal energy tails with approximate power law distributions in velocity space. Such nonthermal distributions with overabundance of fast particles can be better fitted for supra and superthermal velocities, by generalized Lorentzian or kappa distribution than by Maxwellian [11]. A three dimensional anisotropic kappa distribution [8] is given by

$$f_\kappa = \frac{1}{\pi^{3/2}\theta_{\perp\alpha}^2\theta_{\parallel\alpha}}\left(\frac{\Gamma\left(\kappa+1\right)}{\kappa^{3/2}\Gamma\left(\kappa-\frac{1}{2}\right)}\right)\left[1+\frac{v_\parallel^2}{\kappa\theta_{\parallel\alpha}^2}+\frac{v_\perp^2}{\kappa\theta_{\perp\alpha}^2}\right]^{-\kappa-1}$$

where κ is the spectral index. The thermal speed θ is related to the particle temperature T by

$$\theta_{\parallel\alpha}^2 = \left(\frac{2\kappa-3}{\kappa}\right)v_{T_{\parallel\alpha}}^2;\ \theta_{\perp\alpha}^2 = \left(\frac{2\kappa-3}{\kappa}\right)v_{T\perp\alpha}^2$$

with

$$v_{T(\parallel,\perp)\alpha}^2 = \frac{T_{(\parallel,\perp)\alpha}}{m_\alpha}$$

where Γ is the gamma function; and f_κ has been normalized so that $\int f_\kappa d^3v = 1$. Here it is worth mentioning that the value of κ must be greater than $\frac{3}{2}$ which is dictated by the condition of normalization and the definition of temperature for the distribution function [8]. Important features of kappa distribution are that, first at high velocities this distribution obeys an inverse power law and second in the limit when the spectral index $\kappa \to \infty$, the distribution approaches the Maxwellian distribution. In this sense, the kappa distribution is a generalization of Maxwellian distribution.

In the present work we also consider another three dimensional anisotropic distribution called generalized (r, q) distribution which was first introduced by Qureshi *et al.* [12]. They have employed it to study parallel propagating waves in general and for Alfven waves in particular. This distribution function is of a more general form than the above

mentioned kappa distribution and is given by [12]

$$f_{(r,q)} = \left(\frac{3}{4\pi\psi_{\perp\alpha}^2\psi_{\parallel\alpha}}\right)\left(\frac{\Gamma(q)}{(q-1)^{\frac{3}{2+2r}}\,\Gamma\left(q-\frac{3}{2+2r}\right)\Gamma\left(1+\frac{3}{2+2r}\right)}\right) \times\left[1+\frac{1}{q-1}\left(\frac{v_\parallel^2}{\psi_{\parallel\alpha}^2}+\frac{v_\perp^2}{\psi_{\perp\alpha}^2}\right)^{r+1}\right]^{-q}$$

where q and r are the spectral indices. The thermal speed $\psi_{(\parallel,\perp)\alpha}$ is related to the particle thermal velocity by v_T in the following manner.

$$\psi_{\parallel\alpha}^2 = \left(\frac{3\,(q-1)^{\frac{-1}{r+1}}\,\Gamma\left(q-\frac{3}{2+2r}\right)\Gamma\left(\frac{3}{2+2r}\right)}{\Gamma\left(\frac{5}{2+2r}\right)\Gamma\left(q-\frac{5}{2+2r}\right)}\right)v_{T_{\parallel\alpha}}^2$$

and

$$\psi_{\perp\alpha}^2 = \left(\frac{3\,(q-1)^{\frac{-1}{r+1}}\,\Gamma\left(q-\frac{3}{2+2r}\right)\Gamma\left(\frac{3}{2+2r}\right)}{\Gamma\left(\frac{5}{2+2r}\right)\Gamma\left(q-\frac{5}{2+2r}\right)}\right)v_{T_{\perp\alpha}}^2$$

where the specific forms of $\psi_{(\parallel,\perp)\alpha}$ have been obtained in a manner similar to that used for obtaining $\theta_{(\parallel,\perp)\alpha}$ in the kappa distribution function. The spectral indices r, q are constrained to $q > 1$ and $q\,(1+r) > \frac{5}{2}$, the conditions which emerge from the normalization and the definition of temperature. $f_{(r,q)}$ has been normalized so that $\int f_{(r,q)} d^3v = 1$. This distribution reduces to kappa distribution function if $r = 0$ and $q = \kappa + 1$ and to a Maxwellian if $r = 0$ and $q \to \infty$.

These two well known distribution functions exist in planetary magnetospheres, astrophysical plasmas, and the solar wind [13, 14].

1.7 Motivation

Dusty plasmas are common in cosmic and space environments [15, 16, 17, 18, 19, 20, 21, 22, 23, 24, 25, 26]. Dust particles are also observed by the wave instruments installed on the spacecraft missions sent to the outer planets [27, 28, 29, 30, 31]. Dusty plasmas are not

only observed in space but are also observed in industrial applications (microelectronics, carbon nanotubes, growth of carbon layer as diamond structure etc) [32, 33, 34, 35, 36] and in fusion plasmas [37, 38]. Wakefield arises due to the resonance interaction between the dust ion-acoustic and dust acoustic waves and a test dust charge that moves with a speed close to the DIA or DA speeds. Nambu and his collaborators [39, 40] were the first to introduce the concept of the wake potential due to a test charge for ion-electron plasmas and for dusty plasmas. It has been noted that the wake potential plays an important role in generating attractive forces among the like polarity dust grains [41]. The physics of charged dust attraction is rather similar to the Cooper pairing of electrons in superconductors, in which electron attraction occurs due to presence of phonons. In the case of dusty plasmas, phonons are replaced by a dust acoustic wave. In this way the charged dust particles rearrange themselves at the location where they experience net zero field [42]. At the same time the energy loss of a dust projectile moving through a dusty plasma has gained much attention which was first proposed by Nasim *et al.* [43]. Their work was then followed by other studies [44, 45] in which many effects, like dust-neutral collision, correlation effect of a pair of projectiles, the dust charge fluctuation effect on the energy loss and so on were studied. Using kappa and generalized (r, q) distribution, Zaheer *et al.* [46] calculated the real frequencies and the growth rate of some fundamental modes such as Langmuir waves, dust ion acoustic waves, and dust-acoustic waves. Sarwar *et al.* [47] studied the shielded potential and energy loss of $N \times M$ projectile using kappa distribution for the isotropic case. More recently, effects of charge fluctuation of dust particles on the dispersion characteristics of low frequency wave were investigated using kappa and generalized (r, q) distribution functions [48, 49].

In many space and laboratory plasmas it is found that the Maxwellian velocity distribution is not a realistic one under all circumstances [13, 14, 50]. Similarly in laboratory plasmas, tokamak edge plasma shows non-Maxwellian behavior when Lower Hybrid (LH) waves are applied for current drive [51]. In such cases, the plasmas are generally observed to exhibit high- or suprathermal-energy tails with power-law like distributions in veloc-

ity space. These nonthermal distributions with overabundance of fast particles can be better fitted for supra and superthermal velocities, by generalized Lorentzian or kappa distribution than by Maxwellian. Krivenski [52] shows that the discrepancies between electron cyclotron emission (ECE) and Thomson scattering (TS) temperature measurements can be used to identify the presence of non-Maxwellian distribution functions in FTU (Frascati Tokamak Upgrade)- like parameters. In tokamaks, high density and high temperature are desired so as to increase the reaction rate in the core region. For that purpose wave heating is used. However, high plasma density hinders such wave heating like for example, the Electron Cyclotron Resonance Heating (ECRH) as it can not penetrate beyond a certain density limit [53, 54]. On the other hand, Electron Bernstein Waves (EBW) [55] are strongly supported for heating and current drive in high beta plasmas like Spherical Tokamaks (ST) as they are free from the density constraint and can therefore access plasmas of arbitrary densities at the high, fundamental and low harmonics of the Electron Cyclotron (EC) frequency [56, 57, 58]. EBWs therefore are a preferred source of plasma heating.

Electron Bernstein waves are also a useful diagnostic tool for spherical tokamaks and can be used for measurement of the local electron temperature if one can detect their intensities and identify their birth positions [59].

Presence of electron Bernstein waves in laboratory plasma were reported by Crawford [60] and by Leuterer [61]. In space these waves have also been routinely observed by spacecraft emitted from magnetized plasma of Jupiter's moon Io [62]. Mace [13] has studied the electron Bernstein waves for isotropic Kappa distribution and derived the dispersion relation using Gordeyev-type integral. Later he [63] extended the work for interpreting the banded emission in planetary magnetospheres. Meyer-Vernet et al.[64] showed that the weakly banded emission from the Jupitor's magnetosphere between consecutive gyroharmonics frequency are quasi-thermal noise in Bernstein waves.

Electron Bernstein waves are undamped, whereas electrostatic waves propagating in an unmagnetized plasma exhibit collisionless Landau damping [65]. It means that tran-

sition between magnetized and unmagnetized situations is discontinues. This Bernstein-Landau paradox is of great interest for many authors. Sukhorukov et al., [66] presented an analytical solution for perturbations perpendicular to the magnetic field when external field becomes small. Time evolution of electrostatic wave propagating perpendicularly to the back ground magnetic field was numerically studied by Valentini et al. [67]. It is shown that external magnetic field plays different roles depending upon the initial amplitude of the wave. Later they have studied frequency and damping rate of Langmuir waves [68].

Ion Bernstein wave is used to heat the plasma in tokamak [69]. Salimullah studied low-frequency dust-lower hybrid modes in a magnetized dusty plasma [70] and showed that no mode can exist for $\omega < \omega_{cd}$ with perpendicular propagation. But, when $\omega \sim \omega_{cd}$, low-frequency dust Bernstein modes may exist in the dusty plasma. Here ω_{cd} is cyclotron frequency of dust particles. Verheest et al. [71] investigated dust Bernstein modes at lowest possible frequency using fluid model with strictly perpendicular propagation. Dust Bernstein modes can be applicable in interstellar space, molecular clouds, planetary magnetospheres, etc. [72].

1.8 Layout of the Thesis

The Chapter 1 gives the introduction of the plasma waves, kinetic model/theory, non-Maxwellian distribution function and some back ground of the electrostatic potentials and energy loss of a projectile. It also contain some history of the electron, ion and dust Bernstein waves. Chapter 2 deals with the wake and Debye potential of a test charge particle moving in a non-Mawellian dusty plasma. The numerical results are plotted for debye and wake potentials with different values of kappa and r, q. We also studied the energy loss of a projectile in a non-Maxwellian plasma using kappa and generalized (r, q) distributions. Effect of different values of kappa and r, q on energy loss is also studied numerically. In Chapter 3 we have derived the dielectric constant of the electron

Bernstein waves using non-Maxwellian velocity distributions in a magnetized plasma. Cases of perpendicular and parallel propagations are discussed. The numerical results of dispersion relation are plotted for several harmonics with different values of kappa and r,q. Chapter 4 deals with the case of dust Bernstein waves in a non-Maxwellian magnetized dusty plasma. Dispersion relations are derived and the results are plotted for different values of kappa and r, q. Effect of dust charge and dust density on the dispersion curves is also studied. In Chapter 5 we have discussed and summarized the results. Also the suggestion for the future work are proposed.

Chapter 2

Electrostatic Potentials and Energy Loss of a Projectile in Non-Maxwellian Dusty Plasmas

2.1 Introduction

Dusty plasmas have attracted a great deal of attention in the last two decades due to their important role in the laboratory as well as space plasmas. It is well known that the charged particulates having the same polarity can attract each other due to collective interactions involving the dust acoustic waves. This suggests the possibility of lattice formation in a Coulomb system. The test charge approach is the most appropriate technique used to calculate the electrostatic potential of a projectile moving through plasma and is an active area of research because of its applications such as wake field accelerator, formation of regular crystalline structure and dust particle coagulation in space and astrophysical plasmas[41, 73, 17]. The Debye and wake potentials as well as the energy loss due to a dust projectile propagating through a dusty plasma were determined. But this was based on Maxwellian velocity distribution for plasma species.

To understand how Non-Maxwellian velocity distributions such as kappa and general-

ized (r, q) might effect the electrostatic potentials and the energy loss, we have calculated these quantities for a dust projectile moving through an unmagnetized, collisionless dusty plasma. We have also compared the results with those of Maxwellian distribution.

The chapter 2 is organized in the following fashion. In section (2.2) we calculate the dielectric constant by using the linearized Vlasov model for multicomponent dusty plasma. The electrostatic potentials for a single projectile is calculated both analytically and numerically using Non-Maxwellian distribution in section (2.3) and energy loss for Non-Maxwellian distribution function is calculated in section (2.4) . In section (2.5), we summarize and discuss the results.

2.2 Mathematical formulation of the problem

Consider an unmagnetized collisionless dusty plasma whose constituents are electrons, singly ionized positive ions and micron-sized negatively charged dust grains. This dusty plasma is characterized by equilibrium number density $n_{\alpha 0}$, temperature T_α, and mass m_α where $\alpha = i$, e, d denote the plasma species namely ions, electrons and dust grains respectively. The quasineutrality condition is $n_{i0} = n_{e0} + Z_{d0} n_{d0}$, where Z_{d0} is the equilibrium charge number of the dust species. The plasma particles are assumed to be point charges as long as the dust grain size and the intergrain spacings are small as compared with the characteristic scale lengths (the effective dusty plasma Debye length, the particle mean free path, gyroradii etc).

We use the Vlasov-Poisson coupled set of equations to calculate the electrostatic potentials and energy loss due to a test charge $Z_t e$ moving through a multicomponent dusty plasma, with velocity $\mathbf{v}_t$ in the $z-$direction.

The linearized form of the Vlasov and Poisson equations for collisionless and field free plasma are

$$(\partial_t + \mathbf{v}.\boldsymbol{\nabla}) f_{\alpha 1} - \frac{q_\alpha}{m_\alpha} \boldsymbol{\nabla} \phi_1 . \boldsymbol{\nabla}_v f_{\alpha 0} = 0 \tag{2.1}$$

and

$$-\nabla^2\phi_1 = 4\pi\sum_\alpha \overline{n}_\alpha q_\alpha \int f_{\alpha 1} d\mathbf{v} + 4\pi Z_t e\delta(\mathbf{r}-\mathbf{v}_t t) \tag{2.2}$$

where $Z_t e\delta(\mathbf{r}-\mathbf{v}_t t)$ is the charge density of the test charge moving in a dusty plasma and $\delta(\mathbf{r}-\mathbf{v}_t t)$ denotes the three dimensional Dirac delta function.

Applying Space-Time Fourier Transformation, Eq. (2.1) and Eq. (2.2) can be written as

$$\left(-i\omega + i\mathbf{k}.\mathbf{v}\right)\widetilde{f}_{\alpha 1}(\mathbf{k},\omega) - \frac{q_\alpha}{m_\alpha} i\mathbf{k}.\boldsymbol{\nabla}_v f_{\alpha 0}\widetilde{\phi}_1\left(\mathbf{k},\omega\right) = 0$$

or

$$\widetilde{f}_{\alpha 1}(\mathbf{k},\omega) = \frac{-q_\alpha}{m_\alpha}\frac{\mathbf{k}.\boldsymbol{\nabla}_v f_{\alpha 0}}{(\omega-\mathbf{k}.\mathbf{v})}\widetilde{\phi}_1(\mathbf{k},\omega) \tag{2.3}$$

and

$$k^2\widetilde{\phi}_1(\mathbf{k},\omega) = 4\pi\sum_\alpha \overline{n}_\alpha q_\alpha \int \widetilde{f}_{\alpha 1} d\mathbf{v} + 4\pi Z_t e\int\int \exp\left[-i\left(\mathbf{k}.\mathbf{r}-\omega t\right)\right]\delta(\mathbf{r}-\mathbf{v}_t t) d\mathbf{r}dt$$

Substituting value of $\widetilde{f}_{\alpha 1}(\mathbf{k},\omega)$ from Eq. (2.3)in above equation we get

$$k^2\widetilde{\phi}_1(\mathbf{k},\omega) + \sum_\alpha \omega_{p\alpha}^2 \int \frac{\mathbf{k}.\boldsymbol{\nabla}_v f_{\alpha 0}}{(\omega-\mathbf{k}.\mathbf{v})}\widetilde{\phi}_1(\mathbf{k},\omega) d\mathbf{v} = 4\pi Z_t e\int\int \exp\left[-i\left(\mathbf{k}.\mathbf{r}-\omega t\right)\right]\delta(\mathbf{r}-\mathbf{v}_t t) d\mathbf{r}dt$$

where $\omega_{p\alpha}^2 = \frac{4\pi\overline{n}_\alpha q_\alpha^2}{m_\alpha}$ is the plasma frequency of $\alpha-$species.

Using the following property of $\delta-$function

$$\int f(x)\,\delta(x-x')\,dx = f(x') \qquad \text{at} \quad x = x'$$

we obtain

$$k^2\widetilde{\phi}_1(\mathbf{k},\omega)\left[1 + \sum_\alpha \frac{\omega_{p\alpha}^2}{k^2}\int \frac{\mathbf{k}.\boldsymbol{\nabla}_v f_{\alpha 0}}{(\omega-\mathbf{k}.\mathbf{v})} d\mathbf{v}\right] = 4\pi Z_t e\int \exp\left[i\left(\omega-\mathbf{k}.\mathbf{v_t}\right)t\right] dt$$

where

$$\varepsilon\left(\mathbf{k},\omega\right)=1+\sum_{\alpha}\frac{\omega_{p\alpha}^{2}}{k^{2}}\int\frac{\mathbf{k}.\boldsymbol{\nabla}_{v}f_{\alpha0}}{\left(\omega-\mathbf{k}.\mathbf{v}\right)}\mathbf{dv} \tag{2.4}$$

Again use another $\delta-$function property which is given by

$$\delta(\omega-\mathbf{k}.\mathbf{v}_{t})=\frac{1}{2\pi}\int\exp\left[i\left(\omega-\mathbf{k}.\mathbf{v_{t}}\right)t\right]dt$$

Therefore

$$\widetilde{\phi}_{1}(\mathbf{k},\omega)=\frac{8\pi^{2}Z_{t}e\delta(\omega-\mathbf{k}.\mathbf{v}_{t})}{k^{2}\varepsilon\left(\mathbf{k},\omega\right)} \tag{2.5}$$

We use Inverse Space-Time Fourier Transformation and obtain perturbed electrostatic potential $\phi_1(\mathbf{r},t)$

$$\phi_{1}(\mathbf{r},t)=\frac{1}{\left(2\pi\right)^{4}}\int\int\frac{8\pi^{2}Z_{t}e\exp\left[i\left(\mathbf{k}.\mathbf{r}-\omega t\right)\right]\delta(\omega-\mathbf{k}.\mathbf{v}_{t})d\mathbf{k}d\omega}{k^{2}\varepsilon\left(\mathbf{k},\omega\right)}$$

or

$$=\frac{Z_{t}e}{2\pi^{2}}\int\frac{\exp[i\mathbf{k}.\left(\mathbf{r}-\mathbf{v}_{t}t\right)]}{k^{2}\varepsilon\left(k,\mathbf{k}.\mathbf{v}_{t}\right)}d\mathbf{k}\qquad\text{at}\qquad\omega=\mathbf{k}.\mathbf{v}_{t} \tag{2.6}$$

2.3 Derivation of Electrostatic potentials

In the following, we proceed to calculate the Debye potential and the wake field due to a projectile propagating through a Non-Maxwellian dusty plasma.

2.3.1 Electrostatic potentials of Kappa Velocity Distribution

Using kappa distribution function in Eq. (2.4) we obtain

$$\varepsilon\left(k,\mathbf{k}.\mathbf{v}_t\right) = 1+\sum_{\alpha}\frac{4\omega_{p\alpha}^2}{k^2\sqrt{\pi}\theta_{\perp\alpha}^2\theta_{\parallel\alpha}^3}\left(\frac{\left(\kappa+1\right)\Gamma\left(\kappa+1\right)}{\kappa^{5/2}\Gamma\left(\kappa-\frac{1}{2}\right)}\right)\int_{-\infty}^{\infty}\left(\frac{v_\parallel}{v_\parallel-v_t}\right)dv_\parallel$$
$$\int_0^{\infty}v_\perp\left(1+\frac{v_\parallel^2}{\kappa\theta_{\parallel\alpha}^2}+\frac{v_\perp^2}{\kappa\theta_{\perp\alpha}^2}\right)^{-\kappa-2}dv_\perp$$

After performing the perpendicular integration, the dielectric constant is written as

$$\varepsilon\left(k,\mathbf{k}.\mathbf{v}_t\right)=1+\sum_{\alpha}\frac{2\omega_{p\alpha}^2}{k^2\sqrt{\pi}\theta_{\parallel\alpha}^3}\left(\frac{\Gamma\left(\kappa+1\right)}{\kappa^{5/2}\Gamma\left(\kappa-\frac{1}{2}\right)}\right)\int_{-\infty}^{\infty}\left(\frac{v_\parallel}{v_\parallel-v_t}\right)\left(1+\frac{v_\parallel^2}{\kappa\theta_{\parallel\alpha}^2}\right)^{-\kappa-1}dv_\parallel$$

where

$$\int_0^{\infty}v_\perp\left(1+\frac{v_\parallel^2}{\kappa\theta_{\parallel\alpha}^2}+\frac{v_\perp^2}{\kappa\theta_{\perp\alpha}^2}\right)^{-\kappa-2}dv_\perp=\frac{\kappa\theta_{\perp\alpha}^2\left(1+\frac{v_\parallel^2}{\kappa\theta_{\parallel\alpha}^2}\right)^{-\kappa-1}}{2\left(\kappa+1\right)}$$

For the dust acoustic wave with phase velocity constraint $v_{Td_\parallel}<\omega/k<v_{Ti_\parallel},v_{Te_\parallel}$, the velocity integral for dust is given by

$$I_d=\int_{-\infty}^{\infty}\left(\frac{v_\parallel}{v_\parallel-v_t}\right)\left(1+\frac{v_\parallel^2}{\kappa\theta_{\parallel d}^2}\right)^{-\kappa-1}dv_\parallel$$

$$=-\int_{-\infty}^{\infty}\left(\frac{v_\parallel}{v_t}\right)\left(1+\frac{v_\parallel^2}{\kappa\theta_{\parallel d}^2}\right)^{-\kappa-1}\left(1+\frac{v_\parallel}{v_t}+\frac{v_\parallel^2}{v_t^2}+---\right)dv_\parallel$$

where

$$\int_{-\infty}^{\infty}\left(\frac{v_\parallel}{v_t}\right)\left(1+\frac{v_\parallel^2}{\kappa\theta_{\parallel d}^2}\right)^{-\kappa-1}dv_\parallel=0$$

and

$$\int_{-\infty}^{\infty}\left(\frac{v_\parallel^2}{v_t^2}\right)\left(1+\frac{v_\parallel^2}{\kappa\theta_{\parallel d}^2}\right)^{-\kappa-1}dv_\parallel=\frac{\sqrt{\pi}\theta_{\parallel d}^3}{2v_t^2}\left(\frac{\kappa^{3/2}\Gamma\left(\kappa-\frac{1}{2}\right)}{\Gamma\left(\kappa+1\right)}\right)$$

Therefore

$$I_d = -\frac{\sqrt{\pi}\theta_{\|d}^3}{2v_t^2}\left(\frac{\kappa^{3/2}\Gamma\left(\kappa-\frac{1}{2}\right)}{\Gamma\left(\kappa+1\right)}\right)$$

The velocity integral for electron is written as

$$I_e = \int_{-\infty}^{\infty} \frac{\left(1+\frac{v_\|^2}{\kappa\theta_{\|e}^2}\right)^{-\kappa-1}}{\left(1-\frac{v_t}{v_\|}\right)} dv_\|$$

$$= \int_{-\infty}^{\infty}\left(1+\frac{v_\|^2}{\kappa\theta_{\|e}^2}\right)^{-\kappa-1}\left(1+\frac{v_t}{v_\|}+\frac{v_t^2}{v_\|^2}+---\right)dv_\|$$

where

$$\int_{-\infty}^{\infty}\left(1+\frac{v_\|^2}{\kappa\theta_{\|e}^2}\right)^{-\kappa-1} dv_\| = \sqrt{\pi}\theta_{\|e}\left(\frac{\kappa^{1/2}\Gamma\left(\kappa-\frac{1}{2}\right)}{\Gamma\left(\kappa+1\right)}\right)$$

Thus

$$I_e = \sqrt{\pi}\theta_{\|e}\left(\frac{\kappa^{1/2}\Gamma\left(\kappa-\frac{1}{2}\right)}{\Gamma\left(\kappa+1\right)}\right)$$

Similarly we calculate for ions

$$I_i = \sqrt{\pi}\theta_{\|i}\left(\frac{\kappa^{1/2}\Gamma\left(\kappa-\frac{1}{2}\right)}{\Gamma\left(\kappa+1\right)}\right)$$

So that the dielectric constant in terms of dust, ions and electron is written as

$$\varepsilon(k,\mathbf{k}.\mathbf{v}_t) = 1+\frac{2\omega_{pe}^2}{k^2\theta_{\|e}^2}\left(\frac{\Gamma\left(\kappa+\frac{1}{2}\right)}{\kappa\Gamma\left(\kappa-\frac{1}{2}\right)}\right)+\frac{2\omega_{pi}^2}{k^2\theta_{\|i}^2}\left(\frac{\Gamma\left(\kappa+\frac{1}{2}\right)}{\kappa\Gamma\left(\kappa-\frac{1}{2}\right)}\right)-\frac{\omega_{pd}^2}{k^2v_t^2}$$

$$= 1 + \frac{1}{k^2\lambda_{Deff}^2}\left(\frac{\Gamma\left(\kappa+\frac{1}{2}\right)}{\left(\kappa-\frac{3}{2}\right)\Gamma\left(\kappa-\frac{1}{2}\right)}\right) - \frac{\omega_{pd}^2}{k^2v_t^2}$$

where

$$\lambda_{Deff} = (\lambda_{De}^{-2} + \lambda_{Di}^{-2})^{-1/2}$$

is the effective Debye length of electrons and ions.

Now the inverse of the dielectric constant is given as

$$\frac{1}{\varepsilon(k, \mathbf{k}.\mathbf{v}_t)} = \left(\frac{k^2\lambda_{Deff}^2}{k^2\lambda_{Deff}^2 + \left(\frac{\Gamma(\kappa+1/2)}{(\kappa-3/2)\Gamma(\kappa-1/2)}\right) - \frac{\omega_{pd}^2k^2\lambda_{Deff}^2}{k^2v_t^2}}\right)$$

or

$$= \left(\frac{k^2\lambda_{Deff}^2}{\left\{k^2\lambda_{Deff}^2 + \left(\frac{\Gamma(\kappa+1/2)}{(\kappa-3/2)\Gamma(\kappa-1/2)}\right)\right\}\left\{1 - \frac{\omega_{pd}^2k^2\lambda_{Deff}^2}{k^2v_t^2\left[k^2\lambda_{Deff}^2+\left(\frac{\Gamma(\kappa+1/2)}{(\kappa-3/2)\Gamma(\kappa-1/2)}\right)\right]}\right\}}\right)$$

or

$$= \left(\frac{k^2\lambda_{Deff}^2}{\left\{k^2\lambda_{Deff}^2 + \left(\frac{\Gamma(\kappa+1/2)}{(\kappa-3/2)\Gamma(\kappa-1/2)}\right)\right\}\left\{1 - \frac{\omega_{k1}^2}{k^2v_t^2}\right\}}\right)$$

$$= \left(\frac{k^2\lambda_{Deff}^2}{k^2\lambda_{Deff}^2 + \left(\frac{\Gamma(\kappa+1/2)}{(\kappa-3/2)\Gamma(\kappa-1/2)}\right)}\right)\left(\frac{k^2v_t^2}{k^2v_t^2 - \omega_{k1}^2}\right)$$

$$\frac{1}{\varepsilon(k, \mathbf{k}.\mathbf{v}_t)} = \left(\frac{k^2\lambda_{Deff}^2}{k^2\lambda_{Deff}^2 + \left(\frac{\Gamma(\kappa+1/2)}{(\kappa-3/2)\Gamma(\kappa-1/2)}\right)}\right)\left(1 + \frac{\omega_{k1}^2}{(\mathbf{k}.\mathbf{v}_t)^2 - \omega_{k1}^2}\right) \tag{2.7}$$

ω_{k1}^2 is the dispersion frequency of the dust acoustic wave (DAW) for kappa velocity

distribution which can be written as,

$$\omega_{k1}^2 = \frac{\omega_{pd}^2 k^2 \lambda_{Deff}^2}{\left[k^2\lambda_{Deff}^2 + \left(\frac{\Gamma(\kappa+1/2)}{(\kappa-3/2)\Gamma(\kappa-1/2)}\right)\right]}$$

here $\omega_{pd}^2 = 4\pi n_{d0} Z_d^2 e^2/m_d$ is the plasma frequency of dust particles. Using Eq. (2.7) in Eq. (2.6), the electrostatic potential becomes

$$\phi_1(\mathbf{r},t) = \frac{Z_t e}{2\pi^2}\int \frac{\exp\left[i\mathbf{k}.(\mathbf{r}-\mathbf{v}_t t)\right]}{\left[k^2 + k_{Deff}^2\left(\frac{\Gamma(\kappa+1/2)}{(\kappa-3/2)\Gamma(\kappa-1/2)}\right)\right]}\left[1 + \frac{\omega_{k1}^2}{\left(\mathbf{k}.\mathbf{v}_t\right)^2 - \omega_{k1}^2}\right] d\mathbf{k} \qquad (2.8)$$

In Eq. (2.8), the first term represents the Debye potential and the second term shows the wake potential in terms of kappa distribution function.

From Eq. (2.8), we extract the Debye potential by using spherical polar coordinates which can be written as

$$\phi_D(\mathbf{r},t) = \frac{Z_t e}{\pi}\int_0^\infty \int_0^\pi \frac{k^2 \exp\left[ik\mu\xi\right]\sin\left[\theta_k\right] d\theta_k dk J_0\left(k\rho\sqrt{1-\mu^2}\right)}{\left[k^2 + k_{Deff}^2\left(\frac{\Gamma(\kappa+1/2)}{(\kappa-3/2)\Gamma(\kappa-1/2)}\right)\right]}$$

where ϕ_k integration is given by

$$\int_0^{2\pi} \exp\left[ik\rho\sqrt{1-\mu^2}\cos\left[\phi_k\right]\right] d\phi_k = 2\pi J_0\left(k\rho\sqrt{1-\mu^2}\right)$$

Further simplification yields

$$\phi_D(\mathbf{r},t) = \frac{Z_t e}{\pi}\int_0^\infty \int_{-1}^{+1} \frac{k^2 \cos\left[k\mu\xi\right] J_0\left(k\rho\sqrt{1-\mu^2}\right) d\mu dk}{\left[k^2 + k_{Deff}^2\left(\frac{\Gamma(\kappa+1/2)}{(\kappa-3/2)\Gamma(\kappa-1/2)}\right)\right]}$$

where

$$\int_0^1 J_0\left(k\rho\sqrt{1-\mu^2}\right)\cos\left[k\mu\xi\right] d\mu = \frac{\sin\left[k\sqrt{\rho^2+\xi^2}\right]}{\sqrt{k^2\rho^2 + k^2\xi^2}}$$

and

$$\int_0^\infty \frac{k\sin\left[k\sqrt{\rho^2+\xi^2}\right]dk}{\left[k^2+k_{Deff}^2\left(\frac{\Gamma(\kappa+1/2)}{(\kappa-3/2)\Gamma(\kappa-1/2)}\right)\right]} = \frac{\pi}{2}\exp\left[-k_{Deff}\sqrt{\rho^2+\xi^2}\left(\frac{\Gamma\left(\kappa+1/2\right)}{\left(\kappa-3/2\right)\Gamma\left(\kappa-1/2\right)}\right)\right]$$

Finally the Debye potential with the kappa distribution is written as

$$\phi_D(\mathbf{r},t) = \frac{Z_t e}{R}\exp\left[-\frac{R\left(\frac{\Gamma(\kappa+1/2)}{(\kappa-3/2)\Gamma(\kappa-1/2)}\right)^{1/2}}{\lambda_{Deff}}\right] \tag{2.8a}$$

where $\mu = \cos\theta_k$, and $R = \sqrt{\rho^2+\xi^2}$ is the distance of the projectile from the observation point $\mathbf{r}$. Here $\xi = z - v_t t$ is the axial distance with $z = r\cos\theta_r$ and $\rho = r\sin\theta_r$ is the perpendicular distance of the point of observation from the z-axis.

The second part of the Eq. (2.8) represents the wake potential which is solved by using cylindrical coordinatesand is given by

$$\phi_W(\rho,\xi) = \frac{Z_t e}{2\pi^2}\int_{-\infty}^{\infty}\int_0^{\infty}\int_0^{2\pi}\frac{\exp\left[i\left(k_\perp\rho\cos\left[\phi_k\right]+k_\parallel\xi\right)\right]\lambda_{Deff}^2}{\left[k^2\lambda_{Deff}^2+\left(\frac{\Gamma(\kappa+1/2)}{(\kappa-3/2)\Gamma(\kappa-1/2)}\right)\right]}\left[\frac{\omega_{k1}^2}{\left(\mathbf{k}.\mathbf{v}_t\right)^2-\omega_{k1}^2}\right]k_\perp dk_\perp dk_\parallel d\phi_k$$

$$= \frac{Z_t e}{\pi}\int_{-\infty}^{\infty}\int_0^{\infty}\frac{\exp\left[i\left(k_\parallel\xi\right)\right]\lambda_{Deff}^2 J_0\left(k_\perp\rho\right)k_\perp dk_\perp dk_\parallel}{\left[k^2\lambda_{Deff}^2+\left(\frac{\Gamma(\kappa+1/2)}{(\kappa-3/2)\Gamma(\kappa-1/2)}\right)\right]}$$
$$\left[\frac{\omega_{pd}^2k^2\lambda_{Deff}^2}{\left(1+k^2\lambda_{Deff}^2\right)\left(\mathbf{k}.\mathbf{v}_t\right)^2-\omega_{pd}^2k^2\lambda_{Deff}^2}\right]$$

Introducing K such that

$$K_\perp = k_\perp\lambda_{Deff}$$

$$K_\parallel = k_\parallel\lambda_{Deff}$$

we obtain

$$= \frac{Z_t e}{\pi \lambda_{Deff}} \int_{-\infty}^{\infty} \int_{0}^{\infty} \frac{K_\perp \exp\left[\frac{iK_\parallel \xi}{\lambda_{Deff}}\right] J_0\left(\frac{K_\perp \rho}{\lambda_{Deff}}\right) (C_D^2/v_t^2) \left(K_\perp^2 + K_\parallel^2\right) dK_\perp dK_\parallel}{\left[K_\perp^2 + K_\parallel^2 + \left(\frac{\Gamma(\kappa+1/2)}{(\kappa-3/2)\Gamma(\kappa-1/2)}\right)\right] \left(K_\parallel^2 - K_+^2\right) \left(K_\parallel^2 + K_-^2\right)}$$

Note that pole at $K_\parallel = \pm iK_-$ represents the non-oscillating part that change the effective Debye shielding in plasmas whereas oscillating part arise from the residue at pole $K_\parallel = \pm K_+$

Solving biquardratic equation in $K_\parallel^2$, we get

$$K_\parallel^2 = \frac{-\left(1 + K_\perp^2 - \frac{\omega_{pd}^2 \lambda_{Deff}^2}{v_t^2}\right) \pm \sqrt{\left(1 + K_\perp^2 - \frac{\omega_{pd}^2 \lambda_{Deff}^2}{v_t^2}\right)^2 + \frac{4\omega_{pd}^2 \lambda_{Deff}^2 K_\perp^2}{v_t^2}}}{2}$$

where K_+^2 and $-K_-^2$ are the roots of $K_\parallel^2$ and are given by

$$K_+^2 = \frac{-\left(1 + K_\perp^2 - \frac{\omega_{pd}^2 \lambda_{Deff}^2}{v_t^2}\right) + \sqrt{\left(1 + K_\perp^2 - \frac{\omega_{pd}^2 \lambda_{Deff}^2}{v_t^2}\right)^2 + \frac{4\omega_{pd}^2 \lambda_{Deff}^2 K_\perp^2}{v_t^2}}}{2}$$

and

$$-K_-^2 = \frac{\left(1 + K_\perp^2 - \frac{\omega_{pd}^2 \lambda_{Deff}^2}{v_t^2}\right) + \sqrt{\left(1 + K_\perp^2 - \frac{\omega_{pd}^2 \lambda_{Deff}^2}{v_t^2}\right)^2 + \frac{4\omega_{pd}^2 \lambda_{Deff}^2 K_\perp^2}{v_t^2}}}{2}$$

For $K_\perp^2 << 1$, $K_\pm^2$ become

$$K_+^2 \simeq \frac{\omega_{pd}^2 \lambda_{Deff}^2 K_\perp^2}{v_t^2}$$

and

$$K_-^2 \simeq 1 - \frac{\omega_{pd}^2 \lambda_{Deff}^2}{v_t^2}$$

On carrying out the integration over $K_{\parallel}$,

$$\begin{aligned}
&\int_{-\infty}^{\infty} \frac{\exp\left[\frac{iK_{\parallel}\xi}{\lambda_{Deff}}\right]\left(K_{\perp}^2+K_{\parallel}^2\right)dK_{\parallel}}{\left[K_{\perp}^2+K_{\parallel}^2+\left(\frac{\Gamma(\kappa+1/2)}{(\kappa-3/2)\Gamma(\kappa-1/2)}\right)\right]\left(K_{\parallel}^2-K_{+}^2\right)\left(K_{\parallel}^2+K_{-}^2\right)} \\
= &\frac{-2\pi K_{\perp}\left(1+\frac{\omega_{pd}^2\lambda_{Deff}^2}{v_t^2}\right)\sin\left(\frac{\omega_{pd}K_{\perp}\xi}{v_t}\right)}{\left(1-\frac{\omega_{pd}^2\lambda_{Deff}^2}{v_t^2}\right)\left(\frac{\Gamma(\kappa+1/2)}{(\kappa-3/2)\Gamma(\kappa-1/2)}\right)\left(\frac{\omega_{pd}\lambda_{Deff}}{v_t}\right)}
\end{aligned}$$

The wake potential is now given by

$$\begin{aligned}
\phi_W(\rho &= 0,\xi) = -\frac{2Z_te}{\lambda_{Deff}}\left(\frac{C_D}{v_t}\right)\left(\frac{1}{\left(\frac{\Gamma(\kappa+1/2)}{(\kappa-3/2)\Gamma(\kappa-1/2)}\right)}\right)\left(\frac{1+\frac{\omega_{pd}^2\lambda_{Deff}^2}{v_t^2}}{1-\frac{\omega_{pd}^2\lambda_{Deff}^2}{v_t^2}}\right) \\
&\times\int_0^{\infty} K_{\perp}^2 J_0\left(\frac{K_{\perp}\rho}{\lambda_{Deff}}\right)\sin\left(\frac{\omega_{pd}K_{\perp}\xi}{v_t}\right)dK_{\perp}
\end{aligned}$$

Since $K_{\perp}\rho < 1$, therefore $J_0\left(\frac{K_{\perp}\rho}{\lambda_{Deff}}\right) \to 1$

$$\begin{aligned}
\phi_W(\rho &= 0,\xi) = -\frac{2Z_te}{\lambda_{Deff}}\left(\frac{C_D}{v_t}\right)\left(\frac{1}{\left(\frac{\Gamma(\kappa+1/2)}{(\kappa-3/2)\Gamma(\kappa-1/2)}\right)}\right)\left(\frac{1+\frac{\omega_{pd}^2\lambda_{Deff}^2}{v_t^2}}{1-\frac{\omega_{pd}^2\lambda_{Deff}^2}{v_t^2}}\right) \\
&\times\int_0^{\infty} K_{\perp}^2 \sin\left(\frac{\omega_{pd}K_{\perp}\xi}{v_t}\right)dK_{\perp}
\end{aligned}$$

Performing the perpendicular integration

$$\int_0^{\infty} K_{\perp}^2 \sin\left(\frac{\omega_{pd}K_{\perp}\xi}{v_t}\right)dK_{\perp} = \frac{-\cos\left(\frac{\omega_{pd}\xi}{v_t}\right)}{\left(\frac{\omega_{pd}\xi}{v_t}\right)}$$

Therefore we obtain the expression for the wake potential with kappa distribution

function as follows

$$\phi_W(\rho=0,\xi) = \frac{2Z_t e\omega_{pd}}{v_t\left(\frac{\Gamma(\kappa+1/2)}{(\kappa-3/2)\Gamma(\kappa-1/2)}\right)}\left(\frac{1+C_{DA}^2/v_t^2}{1-C_{DA}^2/v_t^2}\right)\frac{\cos\theta_1}{\theta_1} \tag{2.8b}$$

where $C_{DA}^2 = \omega_{pd}^2\lambda_{Deff}^2$ is the dust acoustic speed and $\theta_1 = \left(\frac{\omega_{pd}\xi}{v_t}\right)$.

It may be noted that the Debye and the wake potentials differ from the Maxwellian results by a factor $\left(\frac{\Gamma(\kappa+1/2)}{(\kappa-3/2)\Gamma(\kappa-1/2)}\right)$involving the spectral index kappa (κ).

2.3.2 Electrostatic potentials of Generalized (r,q) Velocity Distribution

In this section, we use the generalized (r,q) distribution function to evaluate the Debye and wake potential using the same procedure as in the preceding section.

Inserting (r,q) distribution function in Eq. (2.4) the dielectric constant is written as

$$\begin{aligned}\varepsilon(k,\mathbf{k}.\mathbf{v}_t) &= 1+\sum_\alpha \frac{3\omega_{p\alpha}^2}{k^2\psi_{\perp\alpha}^2\psi_{\|\alpha}^3}\left(\frac{q\,(1+r)\,\Gamma\,(q)}{(q-1)^{1+\frac{3}{2+2r}}\,\Gamma\left(q-\frac{3}{2+2r}\right)\Gamma\left(1+\frac{3}{2+2r}\right)}\right)\\ &\quad\times\int_{-\infty}^{\infty}\left(\frac{v_\|}{v_\|-v_t}\right)dv_\|\\ &\quad\times\int_0^\infty v_\perp\left(\frac{v_\|^2}{\psi_{\|\alpha}^2}+\frac{v_\perp^2}{\psi_{\perp\alpha}^2}\right)^r\left[1+\frac{1}{(q-1)}\left(\frac{v_\|^2}{\psi_{\|\alpha}^2}+\frac{v_\perp^2}{\psi_{\perp\alpha}^2}\right)^{r+1}\right]^{-q-1}dv_\perp\end{aligned}$$

Taking the perpendicular integral

$$\begin{aligned}&\int_0^\infty v_\perp\left(\frac{v_\|^2}{\psi_{\|\alpha}^2}+\frac{v_\perp^2}{\psi_{\perp\alpha}^2}\right)^r\left[1+\frac{1}{(q-1)}\left(\frac{v_\|^2}{\psi_{\|\alpha}^2}+\frac{v_\perp^2}{\psi_{\perp\alpha}^2}\right)^{r+1}\right]^{-q-1}dv_\perp\\ =\;&\frac{\psi_{\perp\alpha}^2}{2}\frac{\left[1+(q-1)\left(\frac{v_\|^2}{\psi_{\|\alpha}^2}\right)^{-r-1}\right]^{-q}\left(\frac{v_\|^2}{\psi_{\|\alpha}^2}\right)^{-q(r+1)}}{(q-1)^{-q-1}\,q\,(1+r)}\end{aligned}$$

Therefore the dielectric constant simplifies

$$\begin{aligned}\varepsilon(k,\mathbf{k}.\mathbf{v}_t) &= 1+\sum_{\alpha}\frac{3\omega_{p\alpha}^2}{2k^2\psi_{\|\alpha}^3}\left(\frac{\Gamma(q)}{(q-1)^{-q+\frac{3}{2+2r}}\,\Gamma\left(q-\frac{3}{2+2r}\right)\Gamma\left(1+\frac{3}{2+2r}\right)}\right)\\ &\quad\times\int_{-\infty}^{\infty}\left(\frac{v_{\|}}{v_{\|}-v_t}\right)\left[1+(q-1)\left(\frac{v_{\|}^2}{\psi_{\|\alpha}^2}\right)^{-r-1}\right]^{-q}\left(\frac{v_{\|}^2}{\psi_{\|\alpha}^2}\right)^{-q(r+1)}dv_{\|}\end{aligned}$$

By applying the condition of dust acoustic wave

The dust integral is written as

$$\begin{aligned}I_d &= -\int_{-\infty}^{\infty}\left(\frac{v_{\|}}{v_t}\right)\left[1+(q-1)\left(\frac{v_{\|}^2}{\psi_{\|d}^2}\right)^{-r-1}\right]^{-q}\left(\frac{v_{\|}^2}{\psi_{\|d}^2}\right)^{-q(r+1)}\\ &\quad\times\left(1+\frac{v_{\|}}{v_t}+\frac{v_{\|}^2}{v_t^2}+---\right)dv_{\|}\end{aligned}$$

where

$$\begin{aligned}&\int_{-\infty}^{\infty}\left(\frac{v_{\|}^2}{v_t^2}\right)\left[1+(q-1)\left(\frac{v_{\|}^2}{\psi_{\|d}^2}\right)^{-r-1}\right]^{-q}\left(\frac{v_{\|}^2}{\psi_{\|d}^2}\right)^{-q(r+1)}\\ &= \frac{2}{3v_t^2}\left(\frac{1}{\psi_{\|d}^2}\right)^{\frac{-3}{2}}\left(\frac{\Gamma\left(1+\frac{3}{2+2r}\right)\Gamma\left(q-\frac{3}{2+2r}\right)}{\Gamma(q)\,(q-1)^{q-\frac{3}{2+2r}}}\right)\end{aligned}$$

Therefore

$$I_d=-\frac{2\psi_{\|d}^3}{3v_t^2}\left(\frac{\Gamma\left(1+\frac{3}{2+2r}\right)\Gamma\left(q-\frac{3}{2+2r}\right)}{(q-1)^{q-\frac{3}{2+2r}}\,\Gamma(q)}\right)$$

The velocity integral for electron is given by

$$I_e = \int_{-\infty}^{\infty} \left[1 + (q-1)\left(\frac{v_\parallel^2}{\psi_{\parallel e}^2}\right)^{-r-1}\right]^{-q} \left(\frac{v_\parallel^2}{\psi_{\parallel e}^2}\right)^{-q(r+1)} \left[1 + \frac{v_t}{v_\parallel} + \frac{v_t^2}{v_\parallel^2} + --\right] dv_\parallel$$

Taking the leading order term in the expansion

$$\begin{aligned} & \int_{-\infty}^{\infty} \left[1 + (q-1)\left(\frac{v_\parallel^2}{\psi_{\parallel e}^2}\right)^{-r-1}\right]^{-q} \left(\frac{v_\parallel^2}{\psi_{\parallel e}^2}\right)^{-q(r+1)} \\ = \; & 2\left(\frac{1}{\psi_{\parallel e}^2}\right)^{\frac{-1}{2}} \left(\frac{\Gamma\left(q - \frac{1}{2+2r}\right)\Gamma\left(1 + \frac{1}{2+2r}\right)}{(q-1)^{q-\frac{1}{2+2r}}\,\Gamma(q)}\right) \end{aligned}$$

$$I_e = 2\psi_{\parallel e}\left(\frac{\Gamma\left(q - \frac{1}{2+2r}\right)\Gamma\left(1 + \frac{1}{2+2r}\right)}{(q-1)^{q-\frac{1}{2+2r}}\,\Gamma(q)}\right)$$

Similarly for ions

$$I_i = 2\psi_{\parallel i}\left(\frac{\Gamma\left(q - \frac{1}{2+2r}\right)\Gamma\left(1 + \frac{1}{2+2r}\right)}{(q-1)^{q-\frac{1}{2+2r}}\,\Gamma(q)}\right)$$

By substituting the values of integrals in the above equation, the dielectric constant becomes

$$\begin{aligned} \varepsilon(k, \mathbf{k}.\mathbf{v}_t) \; = \; & 1 + \frac{3\omega_{pe}^2}{k^2\psi_{\parallel e}^2}\left(\frac{\Gamma\left(q - \frac{1}{2+2r}\right)\Gamma\left(1 + \frac{1}{2+2r}\right)}{(q-1)^{\frac{1}{1+r}}\,\Gamma\left(q - \frac{3}{2+2r}\right)\Gamma\left(1 + \frac{3}{2+2r}\right)}\right) \\ & + \frac{3\omega_{pi}^2}{k^2\psi_{\parallel i}^2}\left(\frac{\Gamma\left(q - \frac{1}{2+2r}\right)\Gamma\left(1 + \frac{1}{2+2r}\right)}{(q-1)^{\frac{1}{1+r}}\,\Gamma\left(q - \frac{3}{2+2r}\right)\Gamma\left(1 + \frac{3}{2+2r}\right)}\right) - \frac{\omega_{pd}^2}{k^2 v_t^2} \end{aligned}$$

The inverse of dielectric constant becomes

$$\frac{1}{\varepsilon(k,\mathbf{k}.\mathbf{v}_t)} = \left(\frac{k^2\lambda_{Deff}^2}{k^2\lambda_{Deff}^2+A}\right)\left(1+\frac{\omega_{k2}^2}{\left(\mathbf{k}.\mathbf{v}_t\right)^2-\omega_{k2}^2}\right)$$

where

$$A = \frac{\Gamma\left(\frac{5}{2+2r}\right)\Gamma\left(q-\frac{5}{2+2r}\right)\Gamma\left(q-\frac{1}{2+2r}\right)\Gamma\left(1+\frac{1}{2+2r}\right)}{\left[\Gamma\left(q-\frac{3}{2+2r}\right)\right]^2\Gamma\left(\frac{3}{2+2r}\right)\Gamma\left(1+\frac{3}{2+2r}\right)}$$

ω_{k2}^2 is the dispersion frequency of the DAW for the generalized (r,q) distribution function and is given by

$$\omega_{k2}^2 = \frac{\omega_{pd}^2 k^2\lambda_{Deff}^2}{\left[k^2\lambda_{Deff}^2+A\right]} \tag{2.9}$$

The electrostatic potential for (r,q) velocity distribution thus becomes

$$\phi_1(\mathbf{r},t) = \frac{Z_t e}{2\pi^2}\int \frac{\exp\left[i\mathbf{k}.(\mathbf{r}-\mathbf{v}_t t)\right]}{\left[k^2+k_{Deff}^2 A\right]}\left[1+\frac{\omega_{k2}^2}{\left(\mathbf{k}.\mathbf{v}_t\right)^2-\omega_{k2}^2}\right]d\mathbf{k} \tag{2.10}$$

From this expression, we can separate the Debye and the wake potentials for dust acoustic mode as

$$\begin{aligned}\phi_1(\mathbf{r},t) &= \frac{Z_t e}{2\pi^2}\int \frac{\exp\left[i\mathbf{k}.(\mathbf{r}-\mathbf{v}_t t)\right]}{\left[k^2+k_{Deff}^2 A\right]}d\mathbf{k} \\ &\quad + \frac{Z_t e}{2\pi^2}\int \frac{\exp\left[i\mathbf{k}.(\mathbf{r}-\mathbf{v}_t t)\right]}{\left[k^2+k_{Deff}^2 A\right]}\left(\frac{\omega_{k2}^2}{\left(\mathbf{k}.\mathbf{v}_t\right)^2-\omega_{k2}^2}\right)d\mathbf{k}\end{aligned}$$

Debye potential is obtained by using the spherical polar coordinates and is given by

$$\phi_D(\mathbf{r},t) = \frac{Z_t e}{\pi}\int_0^\infty\int_{-1}^{+1} \frac{\exp\left[ik\mu\xi\right]J_0\left(k\rho\sqrt{1-\mu^2}\right)k^2 dk d\mu}{\left[k^2+k_{Deff}^2 A\right]}$$

or

$$= \frac{Z_t e}{\pi} \int_0^\infty \frac{\sin\left[k\sqrt{\rho^2+\xi^2}\right] k^2 dk}{\left[k^2 + k_{Deff}^2 A\right]\sqrt{k^2\rho^2 + k^2\xi^2}}$$

Finally

$$\phi_D(\mathbf{r},t) = \frac{Z_t e}{R} \exp\left[-\frac{R\,(A)^{1/2}}{\lambda_{Deff}}\right] \tag{2.10a}$$

and again following the same procedure as described before,using the cylindrical coordinates

$$\phi_W(\rho,\xi) = \frac{Z_t e}{\pi} \int_{-\infty}^{\infty}\int_0^\infty \frac{\exp\left[ik_\parallel \xi\right] \lambda_{Deff}^2 J_0\left(k_\perp \rho\right) k_\perp dk_\perp dk_\parallel}{\left[k^2 + k_{Deff}^2 A\right]} \left(\frac{\omega_{k2}^2}{\left(\mathbf{k}.\mathbf{v}_t\right)^2 - \omega_{k2}^2}\right)$$

$$\begin{aligned} = \quad & \frac{Z_t e}{\pi\lambda_{Deff}} \int_0^\infty K_\perp J_0\left(\frac{K_\perp \rho}{\lambda_{Deff}}\right) dK_\perp \\ & \times \int_{-\infty}^{\infty} \frac{\exp\left[\frac{iK_\parallel \xi}{\lambda_{Deff}}\right] \left(\frac{C_D^2}{v_t^2}\right) \left(K_\parallel^2 + K_\perp^2\right) dK_\parallel}{\left(K_\parallel^2 + K_\perp^2 + A\right)\left(K_\parallel^2 - K_+^2\right)\left(K_\parallel^2 + K_-^2\right)} \end{aligned}$$

Further simplification yields

$$\phi_W(\rho=0,\xi) = \frac{-2Z_t e}{\lambda_{Deff} A} \left(\frac{\omega_{pd}\lambda_{Deff}}{v_t}\right) \left(\frac{1 + \frac{\omega_{pd}^2 \lambda_{Deff}^2}{v_t^2}}{1 - \frac{\omega_{pd}^2 \lambda_{Deff}^2}{v_t^2}}\right) \int_0^\infty K_\perp^2 \sin\left(\frac{\omega_{pd} K_\perp \xi}{v_t}\right) dK_\perp$$

Therefore the wake potential in terms of (r, q) distribution is given by

$$\phi_W(\rho=0,\xi) = \frac{2Z_t e\omega_{pd}}{v_t A} \left(\frac{1 + C_{DA}^2/v_t^2}{1 - C_{DA}^2/v_t^2}\right) \frac{\cos\theta_1}{\theta_1} \tag{2.10b}$$

Here we note that both the Debye and wake potential are modified by a factor A which depends upon gamma functions and spectral indices (r, q). It is easy to see that for the

limit $r = 0, q \to \infty$, the potential produced by the (r, q) distribution approaches that of the Maxwellian.

2.4 Energy loss of a projectile in Non-Maxwellian Plasma

The energy loss per unit path length of the projectile is the force that a charge particulate experiences in its own induced field, i.e.,

$$S = \frac{-d\varpi}{dx}$$

$$= Z_t e \frac{\partial \phi_1(\mathbf{r}, t)}{\partial \mathbf{r}} \mid_{\mathbf{r}=\mathbf{v}_t t}$$

Substituting the value of potential from Eq. (2.6), S becomes

$$S = \frac{Z_t^2 e^2}{2\pi^2} \frac{\partial}{\partial \mathbf{r}} \int \frac{\exp[i\mathbf{k}.(\mathbf{r} - \mathbf{v}_t t)]}{k^2 \varepsilon(k, \mathbf{k}.\mathbf{v}_t)} d\mathbf{k} \mid_{\mathbf{r}=\mathbf{v}_t t}$$

Using spherical polar coordinates and performing ϕ-integration, we get

$$= \frac{Z_t^2 e^2}{\pi} \frac{\partial}{\partial \mathbf{r}} \left[\int_0^\infty \int_0^\pi \frac{\exp[ik\mu\xi] \sin[\theta_k] J_0\left(k\rho\sqrt{1-\mu^2}\right) dk d\theta_k}{\varepsilon(k, \mathbf{k}.\mathbf{v}_t)} \right] \mid_{\mathbf{r}=\mathbf{v}_t t}$$

where

$$J_0\left(k\rho\sqrt{1-\mu^2}\right) << 1$$

or

$$J_0(0) \simeq 1$$

$$S = \frac{Z_t^2 e^2}{\pi} \frac{\partial}{\partial z} \left[\int_0^{k\max} dk \int_{-1}^{+1} \frac{\exp\left[ik\mu\xi\right] d\mu}{\varepsilon\left(k, \mathbf{k}.\mathbf{v}_t\right)} \right] |_{z=\mathbf{v}_t t}$$

$$= \frac{Z_t^2 e^2}{\pi} \int_0^{k\max} dk \int_{-1}^{+1} \frac{ik\mu d\mu}{\varepsilon\left(k, \mathbf{k}.\mathbf{v}_t\right)}$$

Finally the energy loss of a projectile through a dusty plasma is given by

$$S = \frac{Z_t^2 e^2}{\pi} \int_0^{k\max} k dk \int_{-1}^{+1} \mu d\mu \, \mathrm{Im} \left[\frac{1}{\varepsilon(k, \mathbf{k}.\mathbf{v}_t)} \right] \tag{2.11}$$

where

$$\mu = \cos\theta_k$$

and

$$\xi = z - v_t t$$

2.4.1 Energy loss for Kappa Velocity Distribution

By using cylindrical coordinates, the dielectric constant given in Eq. (2.4) in terms of kappa distribution is written as

$$\begin{aligned} \varepsilon(k, \mathbf{k}.\mathbf{v}_t) &= 1 + \sum_\alpha \frac{4\pi\omega_{p\alpha}^2}{k^2 \pi^{3/2} \theta_{\|\alpha}^3 \theta_{\perp\alpha}^2} \left(\frac{(\kappa+1)\,\Gamma\left(\kappa+1\right)}{\kappa^{5/2}\Gamma\left(\kappa - \frac{1}{2}\right)} \right) \int_{-\infty}^{\infty} \left(\frac{v_\|}{v_\| - \frac{\mathbf{k}.\mathbf{v}_t}{k}} \right) dv_\| \\ &\times \int_0^{\infty} v_\perp \left(1 + \frac{v_\|^2}{\kappa\theta_{\|\alpha}^2} + \frac{v_\perp^2}{\kappa\theta_{\perp\alpha}^2} \right)^{-\kappa-2} dv_\perp \end{aligned}$$

where

$$\int_0^\infty v_\perp \left(1+\frac{v_\parallel^2}{\kappa\theta_{\parallel\alpha}^2}+\frac{v_\perp^2}{\kappa\theta_{\perp\alpha}^2}\right)^{-\kappa-2} dv_\perp = \frac{\kappa\theta_{\perp\alpha}^2\left(1+\frac{v_\parallel^2}{\kappa\theta_{\parallel\alpha}^2}\right)^{-\kappa-1}}{2\left(\kappa+1\right)}$$

After performing the perpendicular integration, we get

$$\varepsilon(k,\mathbf{k}.\mathbf{v}_t) = 1+\sum_\alpha \frac{2\omega_{p\alpha}^2}{k^2\theta_{\parallel\alpha}^2}\left[\frac{\Gamma\left(\kappa+\frac{1}{2}\right)}{\kappa\Gamma\left(\kappa-\frac{1}{2}\right)}+\xi_1 Z_\kappa^*\left(\xi_1\right)\right]$$

where

$$Z_\kappa^*\left(\xi_1\right) = \frac{1}{\sqrt{\pi}}\left(\frac{\Gamma\left(\kappa+1\right)}{\kappa^{3/2}\Gamma\left(\kappa-1/2\right)}\right)\int_{-\infty}^{\infty}\frac{\left(1+\frac{s^2}{\kappa}\right)^{-\kappa-1} ds}{\left(s-\xi_1\right)}$$

is the plasma dispersion function for the kappa distribution with

$$\xi_1 = \frac{\mathbf{k}\cdot\mathbf{v}_t}{k\theta_{\parallel\alpha}}.$$

In the limiting cases, the plasma dispersion function is reduced to the following forms [11],

$$Z_\kappa^*\left(\xi_1\right) = \frac{i\sqrt{\pi}}{\kappa^{3/2}\Gamma\left(\kappa-1/2\right)}\sum_{n=0}^{\infty}\left(\frac{-1}{i\sqrt{\kappa}}\right)^n\frac{\Gamma\left[\kappa+\frac{1}{2}\left(n+2\right)\right]\xi_1^n}{\Gamma\left[\frac{1}{2}\left(n+2\right)\right]},\ \ \left|\xi_1\right|<1$$

and

$$\begin{aligned} Z_\kappa^*\left(\xi_1\right) &= \frac{-i\sqrt{\pi}\Gamma\left(\kappa+1\right)}{\kappa^{3/2}\Gamma\left(\kappa-1/2\right)\cos\left(\pi\kappa\right)}\left(\frac{\xi_1}{i\sqrt{\kappa}}-1\right)^{-(\kappa+1)}\left(\frac{\xi_1}{i\sqrt{\kappa}}+1\right)^{-(\kappa+1)} \\ &\quad -\left(\frac{2\kappa-1}{2\kappa}\right)\frac{1}{\xi_1}\sum_{n=0}^{\infty}\frac{\kappa^n\sqrt{\pi}\Gamma\left(-\kappa+\frac{1}{2}\right)\xi_1^{-2n}}{\Gamma\left(-\kappa+\frac{1}{2}+n\right)\Gamma\left(-n+\frac{1}{2}\right)},\ \ \left|\xi_1\right|>1 \end{aligned}$$

For dust acoustic wave, we use the expression of small argument of plasma disper-

sion function for electrons and ions, and large argument for dust species, therefore the dielectric constant can be written as

$$\begin{aligned}
\varepsilon(k,\mathbf{k}.\mathbf{v}_t) &= 1+\frac{2\omega_{pe}^2}{k^2\theta_{\|e}^2}\left[\frac{\Gamma\left(\kappa+\frac{1}{2}\right)}{\kappa\Gamma\left(\kappa-\frac{1}{2}\right)}+\xi_1\left\{\frac{i\sqrt{\pi}}{\kappa^{3/2}\Gamma\left(\kappa-1/2\right)}\right.\right.\\
&\left.\left.\times\left[\left(\frac{\Gamma\left(\kappa+1\right)}{\Gamma\left(1\right)}\right)-\frac{1}{i\sqrt{\kappa}}\left(\frac{\Gamma\left(\kappa+\frac{3}{2}\right)}{\Gamma\left(\frac{3}{2}\right)}\right)\xi_1+--\right]\right\}\right]\\
&+\frac{2\omega_{pi}^2}{k^2\theta_{\|i}^2}\left[\frac{\Gamma\left(\kappa+\frac{1}{2}\right)}{\kappa\Gamma\left(\kappa-\frac{1}{2}\right)}+\xi_1\left\{\frac{i\sqrt{\pi}}{\kappa^{3/2}\Gamma\left(\kappa-1/2\right)}\right.\right.\\
&\left.\left.\times\left[\left(\frac{\Gamma\left(\kappa+1\right)}{\Gamma\left(1\right)}\right)-\frac{1}{i\sqrt{\kappa}}\left(\frac{\Gamma\left(\kappa+\frac{3}{2}\right)}{\Gamma\left(\frac{3}{2}\right)}\right)\xi_1+--\right]\right\}\right]\\
&+\frac{2\omega_{pd}^2}{k^2\theta_{\|d}^2}\left[\frac{\Gamma\left(\kappa+\frac{1}{2}\right)}{\kappa\Gamma\left(\kappa-\frac{1}{2}\right)}+\xi_1 Z_\kappa^*\left(\xi_1\right)\right]
\end{aligned}$$

Further simplification yields,

$$\begin{aligned}
\varepsilon(k,\mathbf{k}.\mathbf{v}_t) &= 1+\frac{1}{k^2\lambda_{Deff}^2}\left(\frac{\Gamma\left(\kappa+\frac{1}{2}\right)}{\left(\kappa-\frac{3}{2}\right)\Gamma\left(\kappa-\frac{1}{2}\right)}\right)\\
&+\frac{1}{k^2\lambda_{Dd}^2}\left(\frac{\Gamma\left(\kappa+\frac{1}{2}\right)}{\left(\kappa-\frac{3}{2}\right)\Gamma\left(\kappa-\frac{1}{2}\right)}\right)\left[1+\left(\frac{2\kappa}{2\kappa-1}\right)\xi_1 Z_\kappa^*\left(\xi_1\right)\right]
\end{aligned}$$

In general the definition of $W-$function is given by

$$W\left(\xi\right)=1+\xi Z\left(\xi\right)$$

Since Z is complex, we may write

$$W\left(\xi\right)=X\left(\xi\right)+iY\left(\xi\right)$$

so that

$$X(\xi) = 1 + \xi \operatorname{Re} Z(\xi)$$

and

$$Y(\xi) = \xi \operatorname{Im} Z(\xi)$$

The inverse of the dielectric constant is given by

$$\frac{1}{\varepsilon(k, \mathbf{k}.\mathbf{v}_t)} = \frac{k^2}{k^2 + k_{Deff}^2 \left(\frac{\Gamma\left(\kappa+\frac{1}{2}\right)}{\left(\kappa-\frac{3}{2}\right)\Gamma\left(\kappa-\frac{1}{2}\right)} \right) + k_{Dd}^2 \left(\frac{2\kappa}{2\kappa-3} \right) X(\xi_1) - k_{Dd}^2 \left(\frac{1}{2\kappa-3} \right) + i k_{Dd}^2 Y(\xi_1) \left(\frac{2\kappa}{2\kappa-3} \right)}$$

which gives,

$$\operatorname{Im}\left[\frac{1}{\varepsilon(k, \mathbf{k}.\mathbf{v}_t)}\right] = \frac{-k^2 k_{Dd}^2 Y(\xi_1) \left(\frac{2\kappa}{2\kappa-3} \right)}{\left[k^2 + k_{Deff}^2 \frac{\Gamma\left(\kappa+\frac{1}{2}\right)}{\left(\kappa-\frac{3}{2}\right)\Gamma\left(\kappa-\frac{1}{2}\right)} + k_{Dd}^2 \left(\frac{2\kappa}{2\kappa-3} \right) X(\xi_1) - k_{Dd}^2 \left(\frac{1}{2\kappa-3} \right) \right]^2 + \left[k_{Dd}^2 Y(\xi_1) \left(\frac{2\kappa}{2\kappa-3} \right) \right]^2}$$

where

$$X(\xi_1) = \frac{1}{2\kappa} - \frac{1}{2\xi_1^2} - \frac{3\kappa}{2(2\kappa-3)\xi_1^4} + - - --$$

and

$$Y(\xi_1) = \frac{\sqrt{\pi}\Gamma(\kappa+1)\xi_1}{\kappa^{3/2}\Gamma\left(\kappa-\frac{1}{2}\right)} \left(1 + \frac{\xi_1^2}{\kappa}\right)^{-(\kappa+1)}$$

Substituting the value of $\operatorname{Im}\left[\frac{1}{\varepsilon(k, \mathbf{k}.\mathbf{v}_t)}\right]$ in Eq. (2.11) we get

$$S = \frac{-Z_t^2 e^2}{\pi} \int_0^{k\max} k^3 dk \int_{-1}^{+1} \frac{k_{Dd}^2 Y(\xi_1) \left(\frac{2\kappa}{2\kappa-3}\right) \mu d\mu}{\left[k^2 + \frac{k_{Deff}^2 \left(\Gamma\left(\kappa+\frac{1}{2}\right)\right)}{\left(\kappa-\frac{3}{2}\right)\Gamma\left(\kappa-\frac{1}{2}\right)} + \frac{k_{Dd}^2(2\kappa)}{(2\kappa-3)} X(\xi_1) - k_{Dd}^2 \left(\frac{1}{2\kappa-3}\right)\right]^2 + \left[k_{Dd}^2 Y(\xi_1) \left(\frac{2\kappa}{2\kappa-3}\right)\right]^2}$$

Performing k-integration yields

$$\begin{aligned} & \int_0^{k\max} \frac{x^3 dx}{\left[(x^2+a_1)^2 + b_1^2\right]} \\ = \; & \ln(k_{\max}) + \frac{1}{4} \ln \left[\frac{\left(1+\frac{a_1}{k_{\max}^2}\right)^2 + \left(\frac{b_1}{k_{\max}^2}\right)^2}{(a_1^2+b_1^2)}\right] \\ & - \left(\frac{a_1}{2b_1}\right) \left[\tan^{-1}\left(\frac{k_{\max}^2+a_1}{b_1}\right) - \tan^{-1}\left(\frac{a_1}{b_1}\right)\right] \end{aligned}$$

where

$$\begin{aligned} a_1 &= \frac{k_{Deff}^2 \left(\Gamma\left(\kappa+\frac{1}{2}\right)\right)}{\left(\kappa-\frac{3}{2}\right)\Gamma\left(\kappa-\frac{1}{2}\right)} + \frac{k_{Dd}^2(2\kappa)}{(2\kappa-3)} X(\xi_1) - k_{Dd}^2 \left(\frac{1}{2\kappa-3}\right) \\ b_1 &= k_{Dd}^2 Y(\xi_1) \left(\frac{2\kappa}{2\kappa-3}\right) \end{aligned}$$

Therefore

$$S = \frac{-Z_t^2 e^2 k_{Dd}^2}{\pi v_t^2} \int_0^{v_t} \xi_1 d\xi_1 Y(\xi_1) \left(\frac{2\kappa}{2\kappa-3}\right) \{\ln(k_{\max})$$

$$+\frac{1}{4}\ln\left[\frac{\left\{1+\frac{\left(\frac{k^2_{Deff}\left(\Gamma\left(\kappa+\frac{1}{2}\right)\right)}{\left(\kappa-\frac{3}{2}\right)\Gamma\left(\kappa-\frac{1}{2}\right)}\right)+\left(\frac{k^2_{Dd}(2\kappa)}{(2\kappa-3)}\right)X(\xi_1)-\left(\frac{k^2_{Dd}}{2\kappa-3}\right)}{k^2_{\max}}\right\}^2+\left\{\frac{k^2_{Dd}Y(\xi_1)\left(\frac{2\kappa}{2\kappa-3}\right)}{k^2_{\max}}\right\}^2}{\left\{\left(\frac{k^2_{Deff}\left(\Gamma\left(\kappa+\frac{1}{2}\right)\right)}{\left(\kappa-\frac{3}{2}\right)\Gamma\left(\kappa-\frac{1}{2}\right)}\right)+\left(\frac{k^2_{Dd}(2\kappa)}{(2\kappa-3)}\right)X(\xi_1)-\left(\frac{k^2_{Dd}}{2\kappa-3}\right)\right\}^2+\left\{Y(\xi_1)\left(\frac{k^2_{Dd}(2\kappa)}{(2\kappa-3)}\right)\right\}^2}\right]$$
$$-\left(\frac{k^2_{Deff}\left(\frac{2\kappa-1}{2\kappa-3}\right)+k^2_{Dd}\left(\frac{2\kappa}{2\kappa-3}\right)X(\xi_1)-k^2_{Dd}\left(\frac{1}{2\kappa-3}\right)}{2k^2_{Dd}\left(\frac{2\kappa}{2\kappa-3}\right)Y(\xi_1)}\right)$$
$$\times\left[\tan^{-1}\left(\frac{k^2_{\max}+k^2_{Deff}\left(\frac{2\kappa-1}{2\kappa-3}\right)+k^2_{Dd}\left(\frac{2\kappa}{2\kappa-3}\right)X(\xi_1)-k^2_{Dd}\left(\frac{1}{2\kappa-3}\right)}{k^2_{Dd}\left(\frac{2\kappa}{2\kappa-3}\right)Y(\xi_1)}\right)\right.$$
$$\left.-\tan^{-1}\left(\frac{k^2_{Deff}\left(\frac{2\kappa-1}{2\kappa-3}\right)+k^2_{Dd}\left(\frac{2\kappa}{2\kappa-3}\right)X(\xi_1)-k^2_{Dd}\left(\frac{1}{2\kappa-3}\right)}{k^2_{Dd}\left(\frac{2\kappa}{2\kappa-3}\right)Y(\xi_1)}\right)\right]\Bigg\} \tag{2.12}$$

2.4.2 Energy loss for Generalized (r,q) Distribution Function

The dielectric constant in case of (r,q) distribution function after using the cylindrical coordinates is written as:

$$\begin{aligned}\varepsilon(k,\mathbf{k}.\mathbf{v}_t) &= 1+\sum_\alpha\frac{3\omega^2_{p\alpha}}{k^2\psi^3_{\parallel\alpha}\psi^2_{\perp\alpha}}\left(\frac{q(1+r)\Gamma(q)}{(q-1)^{1+\frac{3}{2+2r}}\Gamma\left(q-\frac{3}{2+2r}\right)\Gamma\left(1+\frac{3}{2+2r}\right)}\right)\int_{-\infty}^{\infty}\frac{v_\parallel dv_\parallel}{v_\parallel-\frac{\mathbf{k}.\mathbf{v}_t}{k}}\\ &\times\int_0^\infty v_\perp\left(\frac{v^2_\parallel}{\psi^2_{\parallel\alpha}}+\frac{v^2_\perp}{\psi^2_{\perp\alpha}}\right)\left[1+\frac{1}{(q-1)}\left(\frac{v^2_\parallel}{\psi^2_{\parallel\alpha}}+\frac{v^2_\perp}{\psi^2_{\perp\alpha}}\right)^{r+1}\right]^{-q-1}dv_\perp\end{aligned}$$

where

$$\begin{aligned}&\int_0^\infty v_\perp\left(\frac{v^2_\parallel}{\psi^2_{\parallel\alpha}}+\frac{v^2_\perp}{\psi^2_{\perp\alpha}}\right)\left[1+\frac{1}{(q-1)}\left(\frac{v^2_\parallel}{\psi^2_{\parallel\alpha}}+\frac{v^2_\perp}{\psi^2_{\perp\alpha}}\right)^{r+1}\right]^{-q-1}dv_\perp\\ &= \frac{\psi^2_{\perp\alpha}}{2}\left(\frac{(q-1)}{q(1+r)}\right)\left[1+\frac{1}{(q-1)}\left(\frac{v^2_\parallel}{\psi^2_{\parallel\alpha}}\right)^{r+1}\right]^{-q}\end{aligned}$$

$$\varepsilon(k,\mathbf{k}.\mathbf{v}_t)=1+\sum_{\alpha}\frac{2\omega_{p\alpha}^2}{k^2\psi_{\|\alpha}^2}\left[B+\xi_2 Z_1^{(r,q)}\left(\xi_2\right)\right]$$

where the plasma dispersion function is given by [12]

$$Z_1^{(r,q)}\left(\xi_2\right)=\frac{3\Gamma\left(q\right)}{4\left(q-1\right)^{\frac{3}{2+2r}}\Gamma\left(1+\frac{3}{2+2r}\right)\Gamma\left(q-\frac{3}{2+2r}\right)}\int_{-\infty}^{\infty}\frac{\left(1+\frac{s^{2(1+r)}}{(q-1)}\right)^{-q}ds}{\left(s-\xi_2\right)}$$

with

$$\xi_2=\frac{\mathbf{k}\cdot\mathbf{v}_t}{k\psi_{\|\alpha}},\qquad s=\frac{v_{\|}}{\psi_{\|\alpha}}$$

and

$$B=\left(\frac{3\Gamma\left(1+\frac{1}{2+2r}\right)\Gamma\left(q-\frac{1}{2+2r}\right)}{2\left(q-1\right)^{\frac{1}{1+r}}\Gamma\left(1+\frac{3}{2+2r}\right)\Gamma\left(q-\frac{3}{2+2r}\right)}\right).$$

This plasma dispersion function $Z_1^{(r,q)}\left(\xi_2\right)$ has the following limiting values

$$\begin{aligned}Z_1^{(r,q)}\left(\xi_2\right) &= \left(\frac{3\left(q-1\right)^{\frac{-3}{2+2r}}}{4\Gamma\left(q-\frac{3}{2+2r}\right)\Gamma\left(1+\frac{3}{2+2r}\right)}\right)\\ &\times\left\{\frac{-\sum_{n=1}^{\infty}\xi_2^{2n-1}\left(-1\right)^{-2n}\left(\frac{1}{q-1}\right)^{\frac{2n-1}{2+2r}}\Gamma\left(\frac{3-2n+2r}{2+2r}\right)\Gamma\left(q+\frac{2n-1}{2+2r}\right)\left[1+\left(-1\right)^{2n}\right]}{(2n-1)}\right\}\\ &+\pi i\left(\frac{3\left(q-1\right)^{\frac{-3}{2+2r}}\Gamma\left(q\right)}{4\Gamma\left(q-\frac{3}{2+2r}\right)\Gamma\left(1+\frac{3}{2+2r}\right)}\right)\left[1+\frac{\xi_2^{2(1+r)}}{(q-1)}\right]^{-q},|\xi_2|<1\end{aligned}$$

$$Z_1^{(r,q)}\left(\xi_2\right) = \left(\frac{3\left(q-1\right)^{\frac{-3}{2+2r}}}{4\Gamma\left(q-\frac{3}{2+2r}\right)\Gamma\left(1+\frac{3}{2+2r}\right)}\right)$$

$$\times\left\{\frac{\sum_{n=0}^{\infty}\left(\frac{-1}{\xi_2}\right)^{2n+1}\left(\frac{1}{q-1}\right)^{-\left(\frac{2n+1}{2+2r}\right)}\Gamma\left(\frac{3+2n+2r}{2+2r}\right)\Gamma\left(q-\frac{2n+1}{2+2r}\right)\left[1+(-1)^{2n}\right]}{(2n+1)}\right\}$$

$$+\pi i\left(\frac{3\left(q-1\right)^{\frac{-3}{2+2r}}\Gamma\left(q\right)}{4\Gamma\left(q-\frac{3}{2+2r}\right)\Gamma\left(1+\frac{3}{2+2r}\right)}\right)\left[1+\frac{\xi_2^{2(1+r)}}{(q-1)}\right]^{-q},|\xi_2|>1$$

Employing the condition of dust acoustic wave, the dielectric constant is written as

$$\begin{aligned}
\varepsilon(k,\mathbf{k}.\mathbf{v}_t) &= 1+\frac{2\omega_{pe}^2}{k^2\psi_{\|e}^2}\left[\frac{3\left(q-1\right)^{\frac{-1}{r+1}}\Gamma\left(q-\frac{1}{2+2r}\right)\Gamma\left(1+\frac{1}{2+2r}\right)}{2\Gamma\left(q-\frac{3}{2+2r}\right)\Gamma\left(1+\frac{3}{2+2r}\right)}\right.\\
&+\frac{3\pi i\left(q-1\right)^{\frac{-3}{2+2r}}\Gamma\left(q\right)\xi_2}{4\Gamma\left(q-\frac{3}{2+2r}\right)\Gamma\left(1+\frac{3}{2+2r}\right)}-\frac{3\Gamma\left(q-\frac{1}{2+2r}\right)\Gamma\left(q+\frac{1}{2+2r}\right)\xi_2^2}{2\Gamma\left(q-\frac{3}{2+2r}\right)\Gamma\left(1+\frac{3}{2+2r}\right)(q-1)^{\frac{2}{r+1}}}\\
&-\frac{3\pi iq\left(q-1\right)^{\frac{-3}{2r+2}-1}\Gamma\left(q\right)\xi_2^{3+2r}}{4\Gamma\left(q-\frac{3}{2+2r}\right)\Gamma\left(1+\frac{3}{2+2r}\right)}-\frac{\Gamma\left(1-\frac{3}{2+2r}\right)\Gamma\left(q+\frac{3}{2+2r}\right)\xi_2^4}{2\Gamma\left(q-\frac{3}{2+2r}\right)\Gamma\left(1+\frac{3}{2+2r}\right)(q-1)^{\frac{3}{r+1}}}\\
&\left.+\frac{3\pi iq\left(q+1\right)\left(q-1\right)^{\frac{-3}{2+2r}-2}\Gamma\left(q\right)\xi_2^{5+2r}}{8\Gamma\left(q-\frac{3}{2+2r}\right)\Gamma\left(1+\frac{3}{2+2r}\right)}+---\right]\\
&+\frac{2\omega_{pi}^2}{k^2\psi_{\|i}^2}\left[\frac{3\left(q-1\right)^{\frac{-1}{r+1}}\Gamma\left(q-\frac{1}{2+2r}\right)\Gamma\left(1+\frac{1}{2+2r}\right)}{2\Gamma\left(q-\frac{3}{2+2r}\right)\Gamma\left(1+\frac{3}{2+2r}\right)}\right.\\
&+\frac{3\pi i\left(q-1\right)^{\frac{-3}{2+2r}}\Gamma\left(q\right)\xi_2}{4\Gamma\left(q-\frac{3}{2+2r}\right)\Gamma\left(1+\frac{3}{2+2r}\right)}-\frac{3\Gamma\left(q-\frac{1}{2+2r}\right)\Gamma\left(q+\frac{1}{2+2r}\right)\xi_2^2}{2\Gamma\left(q-\frac{3}{2+2r}\right)\Gamma\left(1+\frac{3}{2+2r}\right)(q-1)^{\frac{2}{r+1}}}\\
&-\frac{3\pi iq\left(q-1\right)^{\frac{-3}{2r+2}-1}\Gamma\left(q\right)\xi_2^{3+2r}}{4\Gamma\left(q-\frac{3}{2+2r}\right)\Gamma\left(1+\frac{3}{2+2r}\right)}-\frac{\Gamma\left(1-\frac{3}{2+2r}\right)\Gamma\left(q+\frac{3}{2+2r}\right)\xi_2^4}{2\Gamma\left(q-\frac{3}{2+2r}\right)\Gamma\left(1+\frac{3}{2+2r}\right)(q-1)^{\frac{3}{r+1}}}\\
&\left.+\frac{3\pi iq\left(q+1\right)\left(q-1\right)^{\frac{-3}{2+2r}-2}\Gamma\left(q\right)\xi_2^{5+2r}}{8\Gamma\left(q-\frac{3}{2+2r}\right)\Gamma\left(1+\frac{3}{2+2r}\right)}+---\right]\\
&+\frac{2\omega_{pd}^2}{k^2\psi_{\|d}^2}\left[\frac{3\left(q-1\right)^{\frac{-1}{r+1}}\Gamma\left(q-\frac{1}{2+2r}\right)\Gamma\left(1+\frac{1}{2+2r}\right)}{2\Gamma\left(q-\frac{3}{2+2r}\right)\Gamma\left(1+\frac{3}{2+2r}\right)}+\xi_2 Z_1^{(r,q)}\left(\xi_2\right)\right]
\end{aligned}$$

Further simplify

$$\begin{aligned}\varepsilon(k,\mathbf{k}.\mathbf{v}_t) &= 1+\frac{\omega_{pe}^2}{k^2v_{T\|e}^2}\left[\frac{\Gamma\left(\frac{5}{2+2r}\right)\Gamma\left(q-\frac{5}{2+2r}\right)\Gamma\left(q-\frac{1}{2+2r}\right)\Gamma\left(1+\frac{1}{2+2r}\right)}{\Gamma\left(\frac{3}{2+2r}\right)\Gamma\left(q-\frac{3}{2+2r}\right)^2\Gamma\left(1+\frac{3}{2+2r}\right)}\right]\\ &+\frac{\omega_{pi}^2}{k^2v_{T\|i}^2}\left[\frac{\Gamma\left(\frac{5}{2+2r}\right)\Gamma\left(q-\frac{5}{2+2r}\right)\Gamma\left(q-\frac{1}{2+2r}\right)\Gamma\left(1+\frac{1}{2+2r}\right)}{\Gamma\left(\frac{3}{2+2r}\right)\Gamma\left(q-\frac{3}{2+2r}\right)^2\Gamma\left(1+\frac{3}{2+2r}\right)}\right]\\ &+\frac{\omega_{pd}^2}{k^2v_{T\|d}^2}\left[\frac{\Gamma\left(\frac{5}{2+2r}\right)\Gamma\left(q-\frac{5}{2+2r}\right)\Gamma\left(q-\frac{1}{2+2r}\right)\Gamma\left(1+\frac{1}{2+2r}\right)}{\Gamma\left(\frac{3}{2+2r}\right)\Gamma\left(q-\frac{3}{2+2r}\right)^2\Gamma\left(1+\frac{3}{2+2r}\right)}\right]\\ &\times\left[1+\frac{2\Gamma\left(q-\frac{3}{2+2r}\right)\Gamma\left(1+\frac{3}{2+2r}\right)\xi_2Z_1^{(r,q)}\left(\xi_2\right)}{3\left(q-1\right)^{\frac{-1}{r+1}}\Gamma\left(q-\frac{1}{2+2r}\right)\Gamma\left(1-\frac{1}{2+2r}\right)}\right]\end{aligned}$$

$$=1+\frac{C}{k^2\lambda_{Deff}^2}+\frac{C}{k^2\lambda_{Dd}^2}\left[1+\frac{2\Gamma\left(q-\frac{3}{2+2r}\right)\Gamma\left(1+\frac{3}{2+2r}\right)\xi_2Z_1^{(r,q)}\left(\xi_2\right)}{3\left(q-1\right)^{\frac{-1}{r+1}}\Gamma\left(q-\frac{1}{2+2r}\right)\Gamma\left(1-\frac{1}{2+2r}\right)}\right]$$

where

$$C=\frac{\Gamma\left(\frac{5}{2+2r}\right)\Gamma\left(q-\frac{5}{2+2r}\right)\Gamma\left(q-\frac{1}{2+2r}\right)\Gamma\left(1+\frac{1}{2+2r}\right)}{\left[\Gamma\left(q-\frac{3}{2+2r}\right)\right]^2\Gamma\left(\frac{3}{2+2r}\right)\Gamma\left(1+\frac{3}{2+2r}\right)}$$

The inverse of dielectric constant is written as

$$\begin{aligned}&\frac{1}{\varepsilon(k,\mathbf{k}.\mathbf{v}_t)}\\ =\ &\frac{k^2}{\left\{k^2+\left(\frac{\Gamma\left(\frac{5}{2+2r}\right)\Gamma\left(q-\frac{5}{2+2r}\right)\Gamma\left(q-\frac{1}{2+2r}\right)\Gamma\left(1+\frac{1}{2+2r}\right)k_{Deff}^2}{\left[\Gamma\left(q-\frac{3}{2+2r}\right)\right]^2\Gamma\left(\frac{3}{2+2r}\right)\Gamma\left(1+\frac{3}{2+2r}\right)}\right)\right.\\ &\left.+\left(\frac{2\Gamma\left(\frac{5}{2+2r}\right)\Gamma\left(q-\frac{5}{2+2r}\right)k_{Dd}^2}{3(q-1)^{\frac{-1}{r+1}}\Gamma\left(q-\frac{3}{2+2r}\right)\Gamma\left(\frac{3}{2+2r}\right)}\right)\left[1-\left\{1-\frac{(q-1)^{\frac{-1}{r+1}}\Gamma\left(\frac{1}{2+2r}\right)\Gamma\left(q-\frac{1}{2+2r}\right)}{2\Gamma\left(\frac{3}{2+2r}\right)\Gamma\left(q-\frac{3}{2+2r}\right)}\right\}+\xi_2Z_1^{(r,q)}\left(\xi_2\right)\right]\right\}\end{aligned}$$

or

$$= \frac{k^2}{\left\{k^2 + \left(\frac{\Gamma\left(\frac{5}{2+2r}\right)\Gamma\left(q-\frac{5}{2+2r}\right)\Gamma\left(q-\frac{1}{2+2r}\right)\Gamma\left(1+\frac{1}{2+2r}\right)k_{Deff}^2}{\left[\Gamma\left(q-\frac{3}{2+2r}\right)\right]^2\Gamma\left(\frac{3}{2+2r}\right)\Gamma\left(1+\frac{3}{2+2r}\right)}\right)\right.}$$
$$+\left(\frac{2\Gamma\left(\frac{5}{2+2r}\right)\Gamma\left(q-\frac{5}{2+2r}\right)k_{Dd}^2}{3(q-1)^{\frac{-1}{r+1}}\Gamma\left(q-\frac{3}{2+2r}\right)\Gamma\left(\frac{3}{2+2r}\right)}\right)X\left(\xi_2\right)$$
$$-\left(\frac{2\Gamma\left(\frac{5}{2+2r}\right)\Gamma\left(q-\frac{5}{2+2r}\right)k_{Dd}^2}{3(q-1)^{\frac{-1}{r+1}}\Gamma\left(q-\frac{3}{2+2r}\right)\Gamma\left(\frac{3}{2+2r}\right)}\right)\left\{1-\frac{(q-1)^{\frac{-1}{r+1}}\Gamma\left(\frac{1}{2+2r}\right)\Gamma\left(q-\frac{1}{2+2r}\right)}{2\Gamma\left(\frac{3}{2+2r}\right)\Gamma\left(q-\frac{3}{2+2r}\right)}\right\}$$
$$\left.+ik_{Dd}^2\left(\frac{2\Gamma\left(\frac{5}{2+2r}\right)\Gamma\left(q-\frac{5}{2+2r}\right)k_{Dd}^2}{3(q-1)^{\frac{-1}{r+1}}\Gamma\left(q-\frac{3}{2+2r}\right)\Gamma\left(\frac{3}{2+2r}\right)}\right)Y\left(\xi_2\right)\right\}$$

so that

$$\mathrm{Im}\left[\frac{1}{\varepsilon(k,\mathbf{k}.\mathbf{v}_t)}\right] = \frac{-k^2k_{Dd}^2Y\left(\xi_2\right)D}{\left[k^2+k_{Deff}^2C+k_{Dd}^2X\left(\xi_2\right)D-k_{Dd}^2DE\right]^2+\left[k_{Dd}^2Y\left(\xi_2\right)D\right]^2}$$

The values of $X\left(\xi_2\right)$ and $Y\left(\xi_2\right)$ are

$$X\left(\xi_2\right) = 1-\frac{3}{2}\left(\frac{\Gamma\left(q-\frac{1}{2+2r}\right)\Gamma\left(1+\frac{1}{2+2r}\right)}{(q-1)^{\frac{1}{r+1}}\Gamma\left(q-\frac{3}{2+2r}\right)\Gamma\left(1+\frac{3}{2+2r}\right)}\right)-\frac{1}{2\xi_2^2}+---$$

and

$$Y\left(\xi_2\right) = \frac{3\pi\xi_2}{4}\left[\frac{(q-1)^{\frac{-3}{2+2r}}\Gamma\left(q\right)}{\Gamma\left(q-\frac{3}{2+2r}\right)\Gamma\left(1+\frac{3}{2+2r}\right)}\right]\left(1+\frac{\xi_2^{2(1+r)}}{(q-1)}\right)^{-q}$$

The energy loss in case of (r,q) distribution function therefore, is written as

$$S = \frac{-Z_t^2e^2}{\pi}\int_0^{k\max}k^3dk$$
$$\int_{-1}^{+1}\frac{k_{Dd}^2Y\left(\xi_2\right)D\mu d\mu}{\left[k^2+k_{Deff}^2C+k_{Dd}^2X\left(\xi_2\right)D-k_{Dd}^2DE\right]^2+\left[k_{Dd}^2Y\left(\xi_2\right)D\right]^2}$$

with

$$D = \frac{2\Gamma\left(\frac{5}{2+2r}\right)\Gamma\left(q-\frac{5}{2+2r}\right)}{3\left(q-1\right)^{\frac{-1}{r+1}}\Gamma\left(q-\frac{3}{2+2r}\right)\Gamma\left(\frac{3}{2+2r}\right)}$$

and

$$E = 1 - \frac{\left(q-1\right)^{\frac{-1}{r+1}}\Gamma\left(q-\frac{1}{2+2r}\right)\Gamma\left(\frac{1}{2+2r}\right)}{2\Gamma\left(\frac{3}{2+2r}\right)\Gamma\left(q-\frac{3}{2+2r}\right)}$$

On performing k-integration, S becomes

$$\begin{aligned}
S &= \frac{-Z_t^2 e^2 k_{Dd}^2}{\pi v_t^2}\int_0^{v_t}\xi_2 d\xi_2 Y\left(\xi_2\right)D \\
&\times\left\{\ln\left(k_{\max}\right)+\frac{1}{4}\ln\left[\frac{\left\{1+\frac{k_{Deff}^2 C+k_{Dd}^2 DX(\xi_2)-k_{Dd}^2 DE}{k_{\max}^2}\right\}^2+\left\{\frac{k_{Dd}^2 Y(\xi_2)D}{k_{\max}^2}\right\}^2}{\left\{k_{Deff}^2 C+k_{Dd}^2 DX\left(\xi_2\right)-k_{Dd}^2 DE\right\}^2+\left\{k_{Dd}^2 Y\left(\xi_2\right)D\right\}^2}\right]\right. \\
&-\left(\frac{k_{Deff}^2 C+k_{Dd}^2 DX\left(\xi_2\right)-k_{Dd}^2 DE}{2k_{Dd}^2 DY\left(\xi_2\right)}\right) \\
&\times\left[\tan^{-1}\left(\frac{k_{\max}^2+k_{Deff}^2 C+k_{Dd}^2 DX\left(\xi_2\right)-k_{Dd}^2 DE}{k_{Dd}^2 DY\left(\xi_2\right)}\right)\right. \\
&\left.\left.-\tan^{-1}\left(\frac{k_{Deff}^2 C+k_{Dd}^2 DX\left(\xi_2\right)-k_{Dd}^2 DE}{k_{Dd}^2 DY\left(\xi_2\right)}\right)\right]\right\} \qquad (2.13)
\end{aligned}$$

Equations (2.12) and (2.13) give the energy loss for κ and generalized (r,q)velocity distributions respectively which we shall analyze numerically in the next section.

2.5 Numerical Results and Discussion

We have numerically solved the equations of the Debye potential (2.9,2.11) and wake field (2.9,2.11) for kappa and generalized (r,q) velocity distribution by using some typical values of parameters [46, 74]: $T_{d_\parallel} = 0.1eV$, $T_{i_\parallel}$=$0.11eV$, $T_{e_\parallel} = 1.0eV$, $n_{i0} = 10^9 cm^{-3}$,

$n_{d0} = 10^5 cm^{-3}$, $n_{e0} = 9.8 \times 10^8 cm^{-3}$, $Z_d = 200$ and $m_d = 10^8 m_p$, where m_p is the mass of the proton. The variables are normalized with the dust parameters, i.e., $v_t^{'} \rightarrow v_t/v_{td}$, $t^{'} \rightarrow t\omega_{pd}$, $\phi^{'} \rightarrow Z_d e\phi_1/T_d$, $S^{'} \rightarrow 2\pi^2 S/Z_t^2 e^2$, $Z_t^{'} \rightarrow Z_t/N_d Z_d$, where $N_d = \frac{4\pi n_{do}\lambda_{Dd}^3}{3}$ is the number of dust particles in the Debye sphere. Fig (2-1) shows the 3D profiles of Debye potential plotted against normalized axial position $\xi' = \xi/\lambda_d$ and the normalized radial position $\rho' = \rho/\lambda_d$, for the case of Maxwellian and Non-Maxwellian distributions. Fig (2-1 a) shows the profile for Maxwellian distribution and Fig (2-1 b) shows the profile for kappa distribution with $\kappa = 3$. Note that the value of $\kappa = 3$ is consistent with the condition $\kappa > 3/2$. Fig (2-1 c) and Fig (2-1 d) are for (r, q) distribution with $r = 0$, $q = 5$ and $r = 2$, $q = 5$. From Fig (2-1) we can see that the value of the Debye potential is smaller in the case of $\kappa = 3$ and $r = 0$, $q = 5$ while it is higher in the case $r = 2$, $q = 5$ as compared to the Maxwellian. This is due to the fact that for small values of κ and q ($r = 0$), the Debye length is much smaller than in the Maxwellian case, due to the presence of high energy particles and consequently the Debye potential is reduced. In Fig (2-2 a-f), the wake potential is plotted against ξ' for kappa and (r, q) distributions and the results are compared with those of Maxwellian distribution. Fig (2-2 a) is plotted for different values of κ starting from 3. It is seen that at low values of kappa the amplitude of wake potential is smaller as compared to the Maxwellian. On the other hand, for larger values of kappa, the contribution from the high energy particles is reduced and thus the Debye potential and the amplitude of wake potential are enhanced and eventually approach to the Maxwellian in the limit $\kappa \rightarrow \infty$. Fig (2-2 b) is plotted for the (r, q) distribution function keeping $r = 0$ and varying the value of q ($q > 5/2$) from 5. Again we see the same behavior i.e., for smaller values of q, the amplitude of wake potential is small as compared to that of Maxwellian while for large values of q, the amplitude of wake field approaches to the Maxwellian. Fig (2-2 c) is plotted for the wake potential keeping the value of q fixed at 5 and varying the value of r from 0 to 2. It is evident from the graph that although for $q = 5$ at $r = 0$, the amplitude of wake potential is smaller than Maxwellian but as soon as the value of r exceeds zero, its amplitude becomes larger

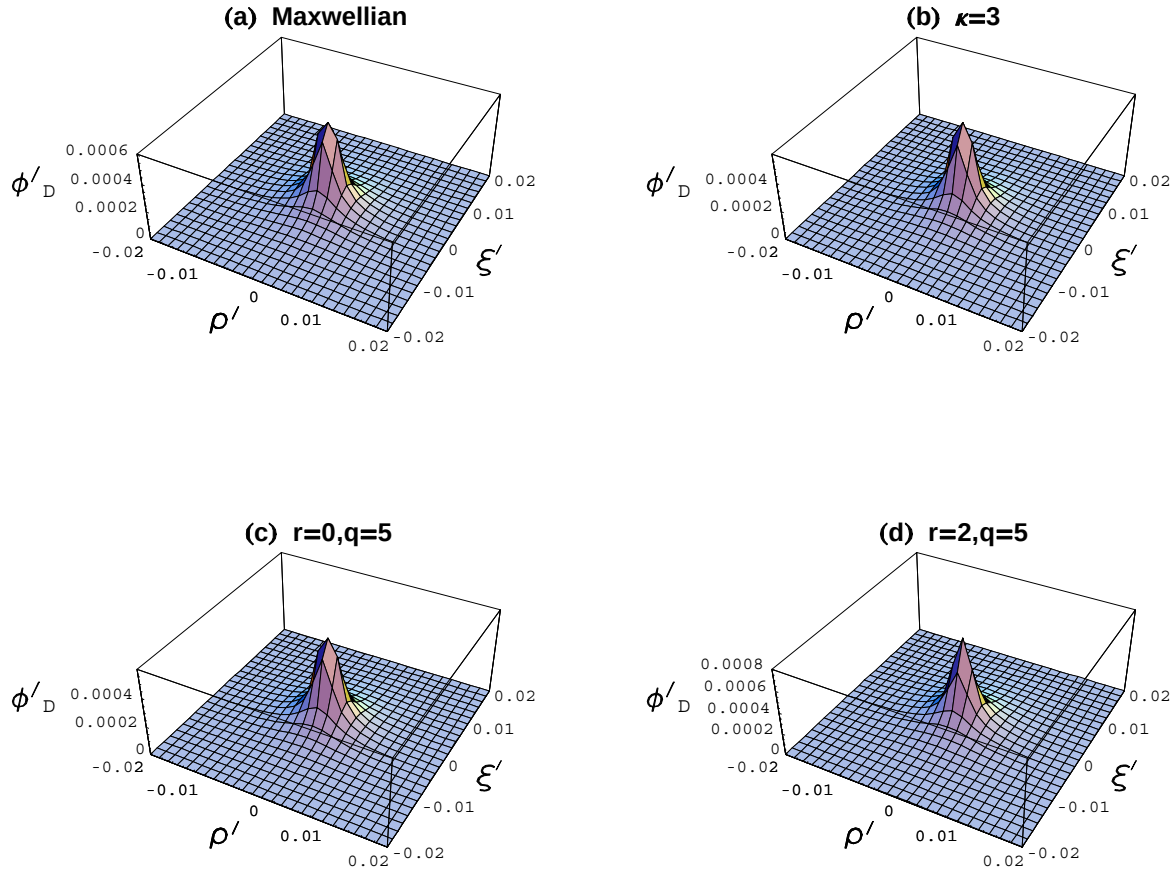

Figure 2-1: $3D$ plots of the normalized Debye potential $\phi'_D = (e\phi_D Z_d/T_d)$ of a projectile vs the normalized axial position $\xi' = \xi/\lambda_d$ and the normalized radial position $\rho' = \rho/\lambda_d$ showing the comparison of Maxwellian with Non-Maxwellian distributions: kappa and (r, q) for spectral index $\kappa = 3$, $(r = 0, q = 5)$ and $(r = 2, q = 5)$.

than the Maxwellian distribution. This behavior is obvious from the Fig (2-2 d). In Fig (2-2 e), we observe the effect of small values of r on the wake potential where q varies as $1/r$. Although this graph is plotted for the small values of r however it still fulfills the criterion $q\ (1 + r) > 5/2$. Fig (2-2 f) is plotted for different values of q, keeping r fixed at $r = 1$. We thus see that with $r = 1$ the amplitude of wake field is higher than the Maxwellian and it continues to rise as q is increased. This result may prove useful for dust plasma crystal formation in some regions of space.

We have also numerically solved the equations (2.12 and 2.13) of the energy loss for

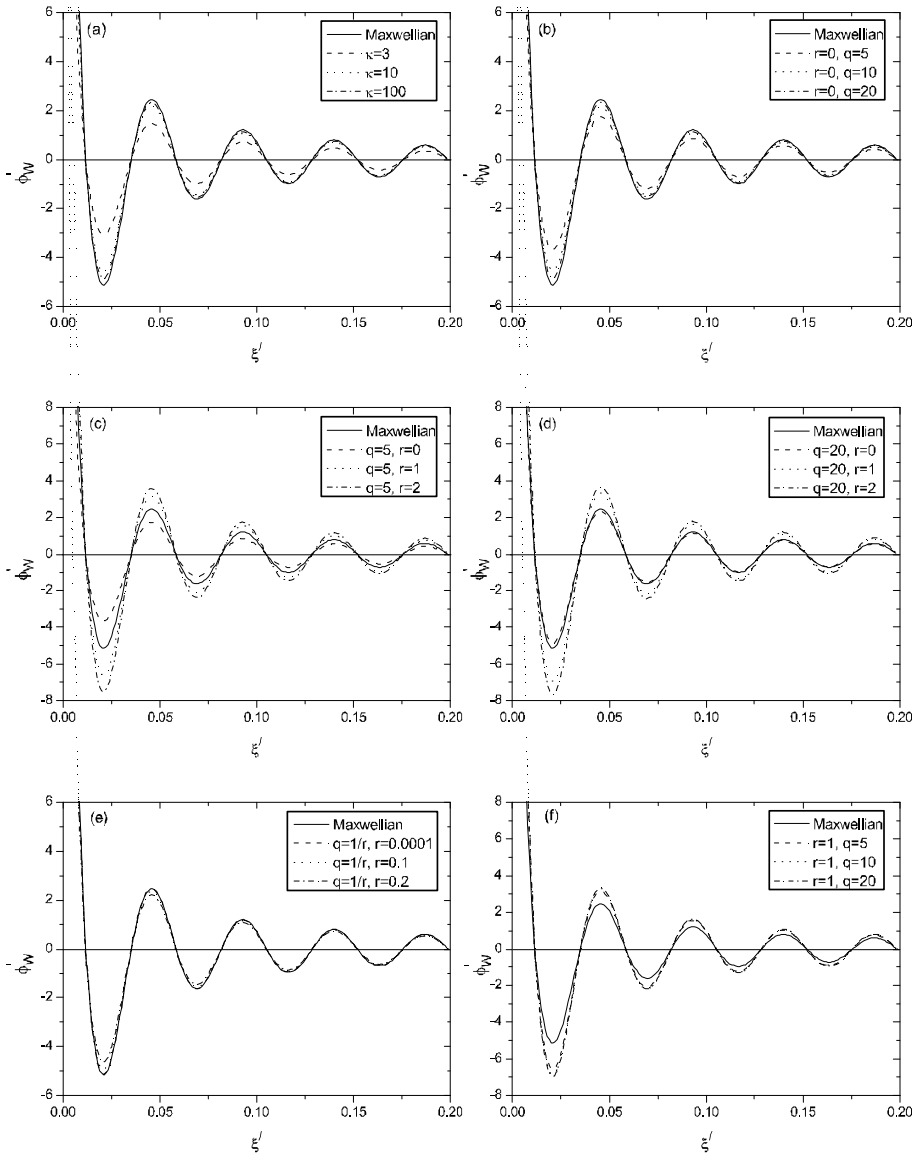

Figure 2-2: The normalized wake potential $\phi'_W = e\phi_W Z_d/T_d$ of a projectile vs normalized axial position $\xi' = \xi/\lambda_d$ for DAW showing the comparison of Maxwellian with non-Maxwellian distributions for different values of spectral indices κ or q and r.

kappa and generalized (r, q) velocity distribution by using the same parameters as above. Fig (2-3) is plotted for the normalized energy loss S' of a test charge vs the normalized test charge velocity V_t' for different values of kappa and the results are compared with the Maxwellian. We observe that for small value of κ $(= 2)$, the energy loss of the test particle is small but approaches to the Maxwellian for large values of kappa. In Fig (2-4) we have plotted the same for different values of q with $r = 0$ for generalized (r, q) distribution, and again we see the same behavior i.e., for small values of q the energy loss is less and can approach to the Maxwellian in the limit of $q \to \infty$. Fig (2-5) and Fig (2-6) are plotted for fixed values of $q = 5, 100$ and varying the value of r. From Fig (2-5), we observe that although for $r = 0, q = 5$, the energy loss is smaller than the Maxwellian but when we increase the value of r to 1 with fixed q the energy loss becomes larger than the Maxwellian which shows strong dependence of the energy loss on r and q values. Finally, Fig (2-6) shows that for $q = 100$ and $r = 0$ the energy loss is the same as that of the Maxwellian but as r increases, it grows higher than the Maxwellian. We may therefore conclude that the electrostatic potential and the energy loss due to a test charge propagating in a dusty plasma is sensitive to the choice of the velocity distribution function.

This work may be relevant to study space plasma in particular in those regions where strongly coupled plasmas are usually found, for example in highly evolved stars, white dwarfs, planetary rings (narrow rings of Uranus and Neptune) and in the Jovian interior.

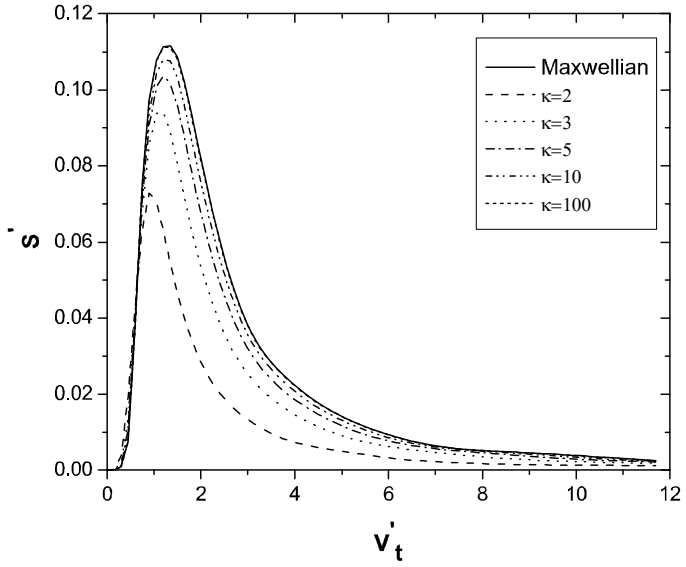

Figure 2-3: Normalized energy loss S' of a test charge in the units of $Z_t^2 e^2/2\pi^2$ vs the normalized test charge velocity V_t' (in the units of V_{td}), with $T_{e\|} = 1.0eV$, $T_{i\|} = 0.11eV$, $T_{d\|} = 0.1eV$, $n_{i0} = 10^9 cm^{-3}$, $n_{d0}/n_{i0} = 10^{-5}$, $Z_d = Z_t = 200$, with effective normalized Debye wave number $K_{Deffe} = 0.5$ in the units of λ_{Dd}^{-1} for different values of kappa ($\kappa > 2$).

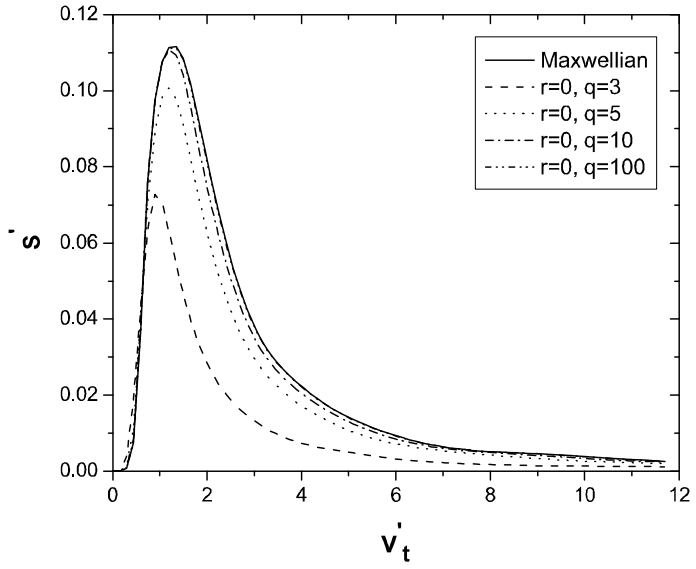

Figure 2-4: Normalized energy loss S' of a test charge in the units of $Z_t^2 e^2/2\pi^2$ vs the normalized test charge velocity V_t' (in the units of V_{td}), for the same parameters as in Fig.2-3 for generalized (r, q) velocity distribution function with $r = 0$ and different values of q.

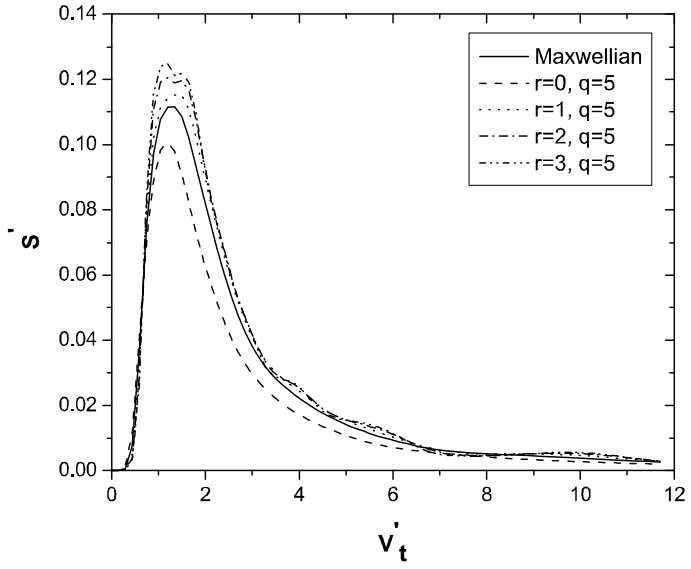

Figure 2-5: Normalized energy loss S' of a test charge in the units of $Z_t^2 e^2/2\pi^2$ vs the normalized test charge velocity V_t' (in the units of V_{td}), for the same parameters as in Fig.2-3 for generalized (r, q) velocity distribution function with $q = 5$ and different values of r.

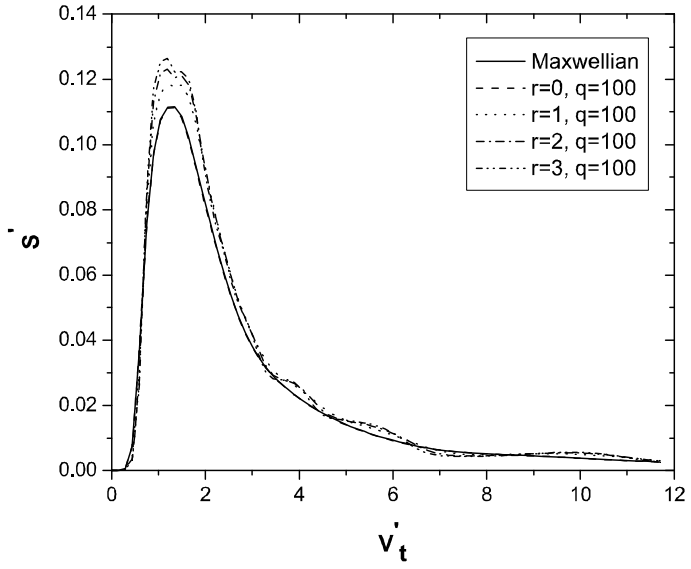

Figure 2-6: Normalized energy loss S' of a test charge in the units of $Z_t^2 e^2/2\pi^2$ vs the normalized test charge velocity V_t' (in the units of V_{td}), for the same parameters as in Fig.2-3 for generalized (r, q) velocity distribution function with $q = 100$ and different values of r.

Chapter 3

Generalized Dispersion Relation of Electron Bernstein Waves in Magnetized Non-Maxwellian Plasmas

3.1 Introduction

Bernstein waves are electrostatic waves, sustained by the electron gyration in an ambient magnetic field. These waves propagate without damping between gyroharmonics, perpendicular to ambient magnetic field[75]. Presence of electron Bernstein waves in laboratory plasma were reported by Crawford [60] and by Leuterer [61]. In space these waves have also been routinely observed by spacecraft emitted from magnetized plasma of Jupiter's moon Io[62]. Mace[13] has studied the electron Bernstein waves for isotropic Kappa distribution and derived the dispersion relation using Gordeyev-type integral. Later he [63] extended the work for interpreting the banded emission in planetary magnetospheres. Meyer-Vernet et al.[64] showed that the weakly banded emission from the Jupitor's magnetosphere between consecutive gyroharmonics frequency are quasi-thermal

noise in Bernstein waves.

The present work investigates the propagation characteristics of electron Bernstein waves for non-Maxwellian (kappa and generalized (r, q)) velocity distributions. Instead of dealing with Gordeyev-type integral, we make use of Neumann's series expansion for the products of Bessel functions [76] and derive the dispersion relation for the perpendicular propagation. We also plot the dispersion curves for both kappa and generalized (r, q) distribution. These results reduce to the standard Maxwellian case in the appropriate limits of $\kappa \to \infty$ and $r = 0, q \to \infty$ for the kappa and (r, q) distribution respectively.

Chapter 3 is organized in the following manner In section (3.2) we have presented mathematical model for Bernstein waves using the linearized Vlasov model and have obtained generalized dielectric constant for a magnetized non-Maxwellian plasma. In subsection (3.2.1) we calculate the dispersion relation for kappa and Maxwellian distributions for the generalized electron Bernstein wave and also present results graphically. Subsection (3.2.3) studies the dispersion relation for the generalized (r, q) distribution and draws its numerical results. Subsections (3.2.2) and (3.2.4) consists of parallel propagation for both kappa and (r, q) distributions respectively. In section (3.3), we summarize the results.

3.2 Generalized Dielectric Constant in Magnetized Non-Maxwellian Plasmas

Bernstein waves are electrostatic waves perpendicularly propagating in a magnetized plasma and are undamped. As mentioned earlier, to study Bernstein waves we have made use of two distribution functions namely kappa and generalized (r, q).We consider collisionless, uniform and infinite plasma embedded in a constant, uniform magnetic field. The direction of magnetic field $\mathbf{B}_0 = B_0 e_z$, is chosen along the $z-axis$, while the direction of wave propagation, $\mathbf{k}$, is confined to the $x - z$ plane, at an angle ϕ with the magnetic field, such that $k_z = k_{\|} = k\cos\phi$, $k_x = k_{\perp} = k\sin\phi$, and $k_y = 0$.

The Vlasov equation with Lorentz force can be written as

$$\partial_t f_\alpha + \mathbf{v}.\nabla_x f_\alpha + \mathbf{a}.\nabla_v f_\alpha = 0$$

where the acceleration is given by

$$\mathbf{a} = \frac{q_\alpha}{m_\alpha}\left(\mathbf{E} + \frac{1}{c}(\mathbf{v}\times\mathbf{B})\right)$$

On linearizing and using Fourier Laplace Transformation we get [77]

$$\partial_\phi f_{\alpha 1} - \frac{(s + i\mathbf{k}.\mathbf{v})f_{\alpha 1}}{\omega_{c\alpha}} = \frac{\Phi(\phi)}{\omega_{c\alpha}} \tag{3.1}$$

which is the first order linear differential equation for f. Here $s = -i\omega$ and $\omega_{c\alpha} = eB_0/mc$ is the cyclotron frequency. The solution of Eq. (3.1) can be written as

$$f_{\alpha 1} = \int_{\pm\infty}^{\phi} \frac{G(\phi^{'})\Phi(\phi^{'})d\phi^{'}}{\omega_{c\alpha}}$$

where

$$\Phi(\phi^{'}) = \frac{-iq\mathbf{k}.\nabla_v f_{\alpha 0}}{m_\alpha}\phi_1.$$

and

$$\begin{aligned} G(\phi^{'}) &= \exp[\frac{1}{\omega_{c\alpha}}\int_{\phi^{'}}^{\phi}(s + i\mathbf{k}.\mathbf{v}^{'})d\phi^{'}] \\ &= \exp[\frac{1}{\omega_{c\alpha}}\{(s + ik_\parallel v_\parallel)(\phi - \phi^{'}) + ik_\perp v_\perp(\sin\phi - \sin\phi^{'})\}] \end{aligned}$$

Substituting the values of $G(\phi^{'})$ and $\Phi(\phi^{'})$ in $f_{\alpha 1}$, we get

$$f_{\alpha 1} = \frac{iq_\alpha \phi_1}{m_\alpha \omega_{c\alpha}} \int_{-\infty}^{\infty} \left(k_\perp \frac{\partial f_{\alpha 0}}{\partial v_\perp} \cos(\phi - \beta) + k_\parallel \frac{\partial f_{\alpha 0}}{\partial v_\parallel} \right) \exp\left[\frac{\left(s + ik_\parallel v_\parallel\right)\beta}{\omega_{c\alpha}} \right]$$
$$\times \exp\left[-\frac{ik_\perp v_\perp}{\omega_{c\alpha}} \left(\sin(\phi - \beta) - \sin\phi \right) \right] d\beta$$

Performing the $\beta-$ integration and using the Bessel function identities [77] we get

$$f_{\alpha 1} = \frac{iq_\alpha \phi_1}{m_\alpha \omega_{c\alpha}} \sum_{n=-\infty}^{\infty} \left[\frac{n\omega_{c\alpha}}{v_\perp} \frac{\partial f_{\alpha 0}}{\partial v_\perp} + k_\parallel \frac{\partial f_{\alpha 0}}{\partial v_\parallel} \right] J_n^2 \left(\frac{k_\perp v_\perp}{\omega_{c\alpha}} \right) \left(\frac{\omega_{c\alpha}}{s + ik_\parallel v_\parallel + in\omega_{c\alpha}} \right)$$

where

$$\beta = \phi - \phi'$$

By using the Space Time Fourier Transformation, the linearized Poisson equation is written as

$$k^2 \widetilde{\phi}_1(\mathbf{k}, \omega) = 4\pi \sum_\alpha \overline{n}_\alpha q_\alpha \int \widetilde{f}_{\alpha 1} d\mathbf{v} + 8\pi^2 q_t \delta(\omega - \mathbf{k}.\mathbf{v}_t)$$

substituting the value of $f_{\alpha 1}$ in the above equation and simplify

$$\widetilde{\phi}_1(\mathbf{k}, \omega) = \frac{8\pi^2 q_t \delta(\omega - \mathbf{k}.\mathbf{v}_t)}{k^2 \left[1 - \sum_\alpha \sum_{n=-\infty}^{\infty} \frac{i\omega_{p\alpha}^2}{k^2} \int \left\{ \frac{(n\omega_{c\alpha}/v_\perp)\partial_{v_\perp} f_{\alpha 0} + k_\parallel \partial_{v_\parallel} f_{\alpha 0}}{s + ik_\parallel v_\parallel + in\omega_{c\alpha}} \right\} J_n^2(\frac{k_\perp v_\perp}{\omega_{c\alpha}}) d\mathbf{v} \right]}$$

After applying the Inverse Space Time Fourier Transformation, we obtain the perturbed potential $\phi_1(\mathbf{r}, t)$ as given below

$$\phi_1(\mathbf{r}, t) = \frac{q_t}{2\pi^2} \int \frac{\exp\left[\mathbf{k}.\left(\mathbf{r} - \mathbf{v}_t\right) t\right] d\mathbf{k}}{k^2 \varepsilon(k, \mathbf{k}.\mathbf{v}_t)}$$

where the generalized dielectric constant can be written as,

$$\varepsilon(\mathbf{k},\omega) = 1 - \sum_{\alpha} \sum_{n=-\infty}^{\infty} \frac{i\omega_{p\alpha}^2}{k^2} \int \left\{ \frac{(n\omega_{c\alpha}/v_\perp)\partial_{v_\perp} f_{\alpha 0} + k_\parallel \partial_{v_\parallel} f_{\alpha 0}}{s + ik_\parallel v_\parallel + in\omega_{c\alpha}} \right\} J_n^2(\frac{k_\perp v_\perp}{\omega_{c\alpha}}) d\mathbf{v}. \qquad (3.2)$$

We shall use this generalized dielectric constant to derive dispersion relations for both the non-Maxwellian distribution functions.

3.2.1 Dispersion relation of electron Bernstein waves for kappa Distribution Function

Inserting the value of kappa distribution function in Eq. (3.2), we obtain the expression for the generalized dielectric constant,

$$\begin{aligned} \varepsilon(k,\omega) &= 1 + \sum_{\alpha} \sum_{n=-\infty}^{\infty} \frac{i4\omega_{p\alpha}^2}{\sqrt{\pi} k^2 \theta_{\perp\alpha}^2 \theta_{\parallel\alpha}} \left(\frac{(\kappa+1)\Gamma(\kappa+1)}{\kappa^{5/2}\Gamma(\kappa-(1/2))} \right) \\ &\times \int_{-\infty}^{\infty} \left\{ \frac{(n\omega_{c\alpha}/\theta_{\perp\alpha}^2) + (k_\parallel v_\parallel/\theta_{\parallel\alpha}^2)}{s + ik_\parallel v_\parallel + in\omega_{c\alpha}} \right\} dv_\parallel \\ &\times \int_0^{\infty} v_\perp J_n^2(\frac{k_\perp v_\perp}{\omega_{c\alpha}}) \left[1 + \frac{v_\parallel^2}{\kappa\theta_\parallel^2} + \frac{v_\perp^2}{\kappa\theta_\perp^2} \right]^{-\kappa-2} dv_\perp \qquad (3.3) \end{aligned}$$

In the above equation it is difficult to perform the perpendicular integration in a straight forward fashion. We therefore use the following Neumann's series expansion for the products of Bessel functions defined in [76],

$$J_n^2(x) = \frac{x^{2n}}{n! 2^{2n}} \sum_{m=0}^{\infty} \frac{C_{n,m}}{(n+m)!} \frac{x^{2m}}{m! 2^{2m}}$$

where

$$C_{n,m} = \frac{(-1)^m \left[2\left(n+m\right)\right]! n!}{(2n+m)!\left(n+m\right)!}$$

Putting this value of $J_n^2(x)$ in Eq. (3.3), we have performed the perpendicular integration and obtained

$$\begin{aligned}
&\int_0^\infty v_\perp J_n^2\left(\frac{k_\perp v_\perp}{\omega_{c\alpha}}\right)\left[1+\frac{v_\parallel^2}{\kappa\theta_{\parallel\alpha}^2}+\frac{v_\perp^2}{\kappa\theta_{\perp\alpha}^2}\right]^{-\kappa-2} dv_\perp \\
= &\sum_{m=0}^{\infty}\frac{C_{n,m}}{m!n!}\left(\frac{k_\perp^2}{2^2\omega_{c\alpha}^2}\right)^{n+m}\left(1+\frac{v_\parallel^2}{\kappa\theta_{\parallel\alpha}^2}\right)^{-\kappa-1+n+m} \\
&\left(\frac{\left(\kappa\theta_{\perp\alpha}^2\right)^{n+m+1}\Gamma\left(\kappa+1-m-n\right)}{2\Gamma\left(\kappa+2\right)}\right)
\end{aligned}$$

For the perpendicular propagation $\left(i.e., k_\parallel = 0\right)$ and considering only electron species, the dielectric constant becomes

$$\begin{aligned}
\varepsilon(k,\omega) = &\ 1-\sum_{n=1}^{\infty}\frac{4\omega_{pe}^2}{\sqrt{\pi}k_\perp^2\theta_{\perp e}^2\theta_{\parallel e}}\sum_{m=0}^{\infty}\frac{C_{n,m}}{m!n!}\left(\frac{k_\perp^2}{2^2\omega_{ce}^2}\right)^{n+m} \\
&\times\left(\frac{\left(\kappa\theta_{\perp e}^2\right)^{n+m}\Gamma\left(\kappa+1-m-n\right)}{\kappa^{3/2}\Gamma(\kappa-(1/2))}\right) \\
&\times\left(\frac{n^2\omega_{ce}^2}{\omega^2-n^2\omega_{ce}^2}\right)\int_{-\infty}^{\infty}\left(1+\frac{v_\parallel^2}{\kappa\theta_{\parallel e}^2}\right)^{-\kappa-1+n+m} dv_\parallel \qquad (3.4)
\end{aligned}$$

Using the parallel integral

$$\int_{-\infty}^{\infty}\left(1+\frac{v_\parallel^2}{\kappa\theta_{\parallel e}^2}\right)^{-\kappa-1+n+m} dv_\parallel = \frac{\sqrt{\kappa\pi}\Gamma\left(\kappa+(1/2)-m-n\right)\theta_{\parallel e}}{\Gamma\left(\kappa+1-m-n\right)}$$

and rearranging the terms in Eq. (3.4), we obtain the dispersion relation as

$$1 = \sum_{n=1}^{\infty}\frac{4\omega_{pe}^2}{k_\perp^2\theta_{\perp e}^2}\sum_{m=0}^{\infty}\frac{C_{n,m}}{m!n!}\left(\frac{k_\perp^2\theta_{\perp e}^2}{2^2\omega_{ce}^2}\right)^{n+m}$$

$$\left(\frac{\kappa^{n+m-1}\Gamma\left(\kappa+(1/2)-m-n\right)}{\Gamma(\kappa-(1/2))}\right)\left(\frac{n^2\omega_{ce}^2}{\omega^2-n^2\omega_{ce}^2}\right)$$

Further simplification yields

$$\begin{aligned} 1 &= \sum_{n=1}^{\infty}\sum_{m=0}^{\infty}\frac{2k_{D\kappa}^2}{k_\perp^2}\frac{C_{n,m}}{m!n!}\left(\frac{b_\kappa}{2}\right)^{n+m} \\ &\left(\frac{\kappa^{n+m-1}\Gamma\left(\kappa+(1/2)-m-n\right)}{\Gamma(\kappa-(1/2))}\right)\left(\frac{n^2\omega_{ce}^2}{\omega^2-n^2\omega_{ce}^2}\right) \end{aligned} \tag{3.5}$$

This is the generalized dispersion relation of electron Bernstein waves in terms of kappa distribution function, b_κ and $k_{D\kappa}^2$ are given by

$$b_\kappa = b\left(\frac{2\kappa-3}{2\kappa}\right),\ k_{D\kappa}^2 = k_D^2\left(\frac{2\kappa}{2\kappa-3}\right)$$

where

$$b = \frac{k_\perp^2 v_{T_{\perp e}}^2}{2\omega_{ce}^2},\ k_D^2 = \frac{2\omega_{pe}^2}{v_{T_{\perp e}}^2}$$

Here ω_{pe}, ω_{ce}, and $v_{T_{\perp e}}$ are electron plasma frequency, electron cyclotron frequency and electron thermal velocity respectively. It may be noted that the hypergeometric functions which appear in the results of Mace[13, 63] are absent here in our expression of the dispersion relation for the electron Bernstein waves. Compared with his result, our Eq. (3.5) is compact and neat.

Before proceeding further, we may compare the result in Eq. (3.5) with the dispersion relation for the Maxwellian distribution given below

$$1 = \sum_{n=1}^{\infty}\sum_{m=0}^{\infty}\frac{C_{n,m}}{m!n!}\left(\frac{b}{2}\right)^{n+m}\left(\frac{k_D^2}{k_\perp^2}\right)\left(\frac{2n^2\omega_{ce}^2}{\omega^2-n^2\omega_{ce}^2}\right) \tag{3.6}$$

This expression has been obtained using the Neumann's series expansion for the product of Bessel function for small argument ($b \ll 1$) and is in agreement with the standard Maxwellian result. Using the above equation we have plotted the first few harmonics of

the electron Bernstein wave in Figure (3-1) for $b = 0.5$ and have compared the results with the known results of [55] and [1]. They are in full agreement as expected. The small value of b implies that Larmor radius is small compared with wavelength.

For large value of kappa i.e. $\kappa \to \infty$, Eq. (3.5) reduces to Eq. (3.6), which shows that our expression for electron Bernstein waves with kappa velocity distribution can be converted to that of the Maxwellian velocity distribution. This confirms the view that the Maxwellian distribution is a special case of the kappa distribution. In Figure (3-2), we have plotted different modes of the electron Bernstein waves for $\kappa = 3, 5, 7, 10$ taking $b = 0.5$ and compared the results with the Maxwellian distribution case. It is observed that for large values of κ, the results approach towards the Maxwellian distribution whereas smaller values of κ show larger deviation from the Maxwellian distribution which is due to the presence of high energy tail in electron distribution. Dispersion curves for small values of κ e.g., $\kappa = 3$ shows interesting features like backward Bernstein wave in the frequency bands $\omega_{ce} - 2\omega_{ce}$ and $3\omega_{ce} - 4\omega_{ce}$.

3.2.2 Parallel Propagation in Terms of Kappa Distribution

Inserting $k_\perp = 0$, in the Eq. (3.3), the argument of the Bessel functions vanishes and only the term $n = 0$ in the sum retained [5]. The dielectric constant now takes the form

$$\begin{aligned}\varepsilon(k_\parallel, \omega) &= 1 + \sum_\alpha \frac{4\omega_{p\alpha}^2}{k_\parallel^2 \theta_{\perp\alpha}^2 \theta_{\parallel\alpha}^3} \left(\frac{(\kappa+1)\,\Gamma(\kappa+1)}{\kappa^{5/2}\Gamma\left(\kappa - \frac{1}{2}\right)} \right) \int_{-\infty}^{\infty} \left(1 + \frac{\omega}{k_\parallel v_\parallel}\right) dv_\parallel \\ &\quad \times \int_0^{\infty} v_\perp \left(1 + \frac{v_\parallel^2}{\kappa\theta_{\parallel\alpha}^2} + \frac{v_\perp^2}{\kappa\theta_{\perp\alpha}^2}\right)^{-\kappa-2} dv_\perp\end{aligned}$$

After performing the perpendicular integration, we obtain

$$\varepsilon(k_\parallel, \omega) = 1 + \sum_\alpha \frac{2\omega_{p\alpha}^2}{\sqrt{\pi} k_\parallel^2 \theta_{\parallel\alpha}^3} \left(\frac{\Gamma(\kappa+1)}{\kappa^{3/2}\Gamma\left(\kappa - \frac{1}{2}\right)} \right) \int_{-\infty}^{\infty} \left(1 + \frac{\omega}{k_\parallel v_\parallel}\right) \left(1 + \frac{v_\parallel^2}{\kappa\theta_{\parallel\alpha}^2}\right)^{-\kappa-1} dv_\parallel$$

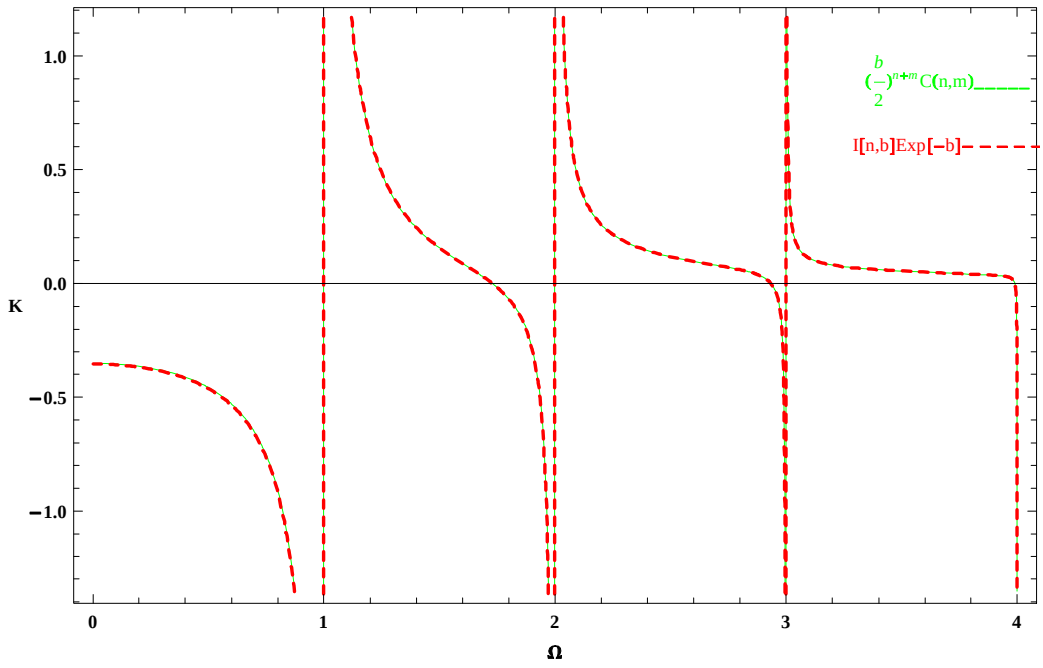

Figure 3-1: Plots of the electron Bernstein waves for $K\left(=\frac{k_\perp^2}{k_D^2}\right)$ versus $\Omega\left(=\frac{\omega}{\omega_{ce}}\right)$ using Maxwellian distribution ($b = 0.5$). Solid line shows the curve obtained from Eq. (3.6) and the dotted line shows the standard text book result (F.F. Chen).

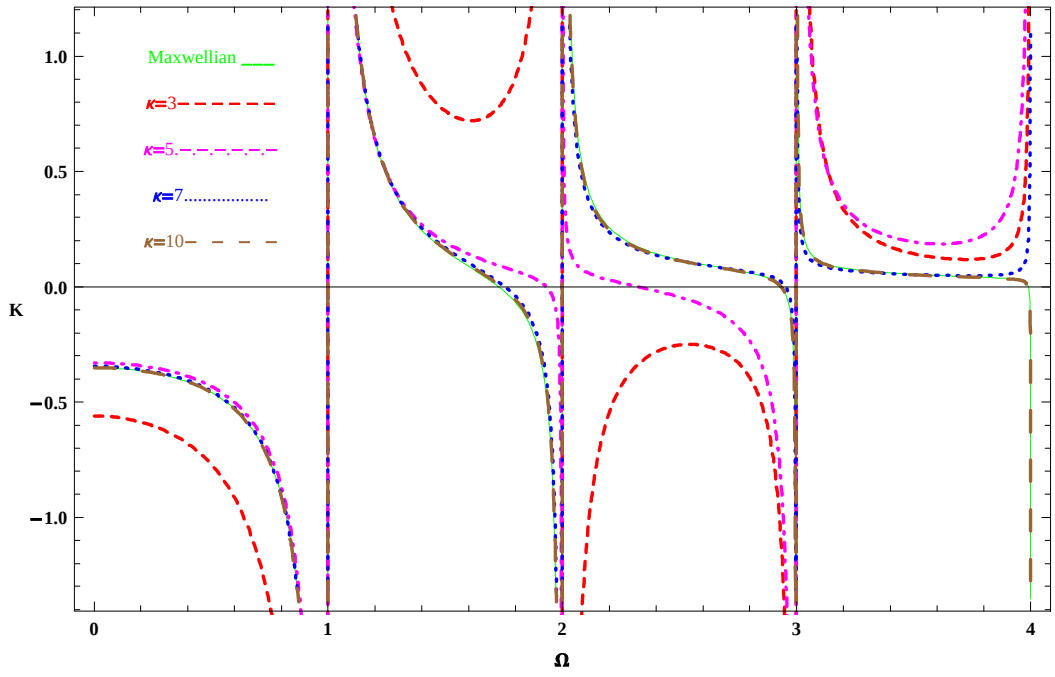

Figure 3-2: Dispersion plots of the electron Bernstein waves for different values of Kappa with $b = 0.5$. Dashed line shows a plot of $\kappa = 3$, dash-dot shows $\kappa = 5$, dotted line shows $\kappa = 7$, dash space dash line shows $\kappa = 10$, whereas Maxwellian is represented by a solid line.

where

$$\int_0^\infty v_\perp \left[1+\frac{v_\parallel^2}{\kappa\theta_{\parallel\alpha}^2}+\frac{v_\perp^2}{\kappa\theta_{\perp\alpha}^2}\right]^{-\kappa-2} dv_\perp = \frac{\kappa\theta_{\perp\alpha}^2}{2\left(\kappa+1\right)}\left(1+\frac{v_\parallel^2}{\kappa\theta_{\parallel\alpha}^2}\right)^{-\kappa-1}$$

Finally the dielectric constant in terms of kappa distribution function can be written as

$$\varepsilon(k_\parallel,\omega) = 1+\sum_\alpha \frac{2\omega_{p\alpha}^2}{k_\parallel^2\theta_{\parallel\alpha}^2}\left[\frac{\Gamma\left(\kappa+\frac{1}{2}\right)}{\kappa\Gamma\left(\kappa-\frac{1}{2}\right)}+\xi_1 Z_\kappa^*\left(\xi_1\right)\right] \tag{3.7}$$

The above result shows that the influence of the magnetic field on the waves disappear and we recover already obtained results in our early work of parallel propagation in unmagnetized anisotropic plasma with the kappa velocity distribution [50].

Here

$$Z_\kappa^*\left(\xi_1\right) = \frac{1}{\sqrt{\pi}}\left(\frac{\Gamma\left(\kappa+1\right)}{\kappa^{3/2}\Gamma\left(\kappa-\frac{1}{2}\right)}\right)\int_{-\infty}^{\infty}\frac{\left(1+\frac{w^2}{\kappa}\right)^{-\kappa-1}dw}{w-\xi_1}$$

is the plasma dispersion function with

$$w=\frac{v_\parallel}{\theta_{\parallel\alpha}}, \qquad\qquad \xi_1=\frac{\omega}{k_\parallel\theta_{\parallel\alpha}}$$

Eq. (3.7) can be further simplified to study Langmuir waves[11, 68]. Langmuir waves exhibit Landau damping where as Bernstein waves are undamped. This leads to one of the fundamental paradoxes called Bernstein-Landau paradox.

3.2.3 Dispersion relation of electron Bernstein waves for (r,q) Distribution

Using generalized (r,q) distribution function in Eq. (3.2), we obtain the generalized dielectric constant as

$$
\begin{aligned}
\varepsilon(k,\omega) &= 1+\sum_{\alpha}\sum_{n=-\infty}^{\infty}\frac{i3\omega_{p\alpha}^2}{k^2\psi_{\perp\alpha}^2\psi_{\|\alpha}}\left(\frac{q\,(1+r)\,\Gamma(q)}{(q-1)^{1+\frac{3}{2+2r}}\Gamma(q-\frac{3}{2+2r})\Gamma(1+\frac{3}{2+2r})}\right)\\
&\quad\int_{-\infty}^{\infty}\left\{\frac{(n\omega_{c\alpha}/\psi_{\perp\alpha}^2)+(k_{\|}v_{\|}/\psi_{\|\alpha}^2)}{s+ik_{\|}v_{\|}+in\omega_{c\alpha}}\right\}dv_{\|}\\
&\quad\times\int_0^{\infty}v_{\perp}J_n^2(\frac{k_{\perp}v_{\perp}}{\omega_{c\alpha}})\left(\frac{v_{\|}^2}{\psi_{\|\alpha}^2}+\frac{v_{\perp}^2}{\psi_{\perp\alpha}^2}\right)^r\\
&\quad\times\left[1+\frac{1}{(q-1)}\left(\frac{v_{\|}^2}{\psi_{\|\alpha}^2}+\frac{v_{\perp}^2}{\psi_{\perp\alpha}^2}\right)^{r+1}\right]^{-q-1}dv_{\perp}
\end{aligned}
\tag{3.8}
$$

Expanding $J_n^2(x)$ for small argument, we perform the perpendicular integration after using the binomial expansion to obtain,

$$
\begin{aligned}
&\int_0^{\infty}v_{\perp}J_n^2(\frac{k_{\perp}v_{\perp}}{\omega_{c\alpha}})\left(\frac{v_{\|}^2}{\psi_{\|\alpha}^2}+\frac{v_{\perp}^2}{\psi_{\perp\alpha}^2}\right)^r\\
&\times\left[1+\frac{1}{(q-1)}\left(\frac{v_{\|}^2}{\psi_{\|\alpha}^2}+\frac{v_{\perp}^2}{\psi_{\perp\alpha}^2}\right)^{r+1}\right]^{-q-1}dv_{\perp}\\
=\;&\frac{\psi_{\perp\alpha}^2}{2}\sum_{m=0}^{\infty}\frac{C_{n,m}}{m!n!}\left(\frac{k_{\perp}^2\psi_{\perp\alpha}^2}{2^2\omega_{c\alpha}^2}\right)^{n+m}\\
&\times\sum_{p=0}^{n+m}\frac{(-1)^p}{p!\,(n+m-p)!}\frac{(q-1)^{q+1}}{(1+r)}\left(\frac{\Gamma(q+\frac{p-m-n}{1+r})}{\Gamma(q+1+\frac{p-m-n}{1+r})}\right)\left(\frac{v_{\|}^2}{\psi_{\|}^2}\right)^{n+m-q-qr}\\
&\times{}_2F_1\left[q+1,q+\frac{p-m-n}{1+r};q+1+\frac{p-m-n}{1+r};-(q-1)\left(\frac{v_{\|}^2}{\psi_{\|}^2}\right)^{-1-r}\right]
\end{aligned}
$$

where ${}_2F_1$ is the usual hypergeometric function. Thus the dielectric constant can be written as,

$$
\begin{aligned}
\varepsilon(k,\omega) &= 1-\sum_{n=1}^{\infty}\frac{3\omega_{pe}^2}{k_\perp^2\psi_{\perp e}^2\psi_{\|e}}\left(\frac{q\Gamma(q)}{(q-1)^{-q+\frac{3}{2+2r}}\Gamma(q-\frac{3}{2+2r})\Gamma(1+\frac{3}{2+2r})}\right)\\
&\quad \sum_{p=0}^{n+m}\left(\frac{(-1)^p}{p!\,(n+m-p)!}\right)\left(\frac{1+r}{-m-n+p+q+qr}\right)\\
&\quad \sum_{m=0}^{\infty}\frac{C_{n,m}}{m!n!}\left(\frac{k_\perp^2\psi_{\perp e}^2}{2^2\omega_{ce}^2}\right)^{n+m}\left(\frac{n^2\omega_{ce}^2}{\omega^2-n^2\omega_{ce}^2}\right)\int_{-\infty}^{\infty}\left(\frac{v_\|^2}{\psi_{\|e}^2}\right)^{n+m-q-qr}\\
&\quad {}_2F_1\left[q+1,q+\left(\frac{p-n-m}{1+r}\right);q+1+\left(\frac{p-n-m}{1+r}\right);-(q-1)\left(\frac{v_\|^2}{\psi_{\|e}^2}\right)^{-1-r}\right]dv_\|
\end{aligned}
$$

The parallel integral now takes the form

$$
\begin{aligned}
&\int_{-\infty}^{\infty}\left(\frac{v_\|^2}{\psi_{\|e}^2}\right)^{n+m-q-qr}\\
&{}_2F_1\left[q+1,q+\left(\frac{p-n-m}{1+r}\right);q+1+\left(\frac{p-n-m}{1+r}\right);-(q-1)\left(\frac{v_\|^2}{\psi_{\|e}^2}\right)^{-1-r}\right]dv_\|\\
&= \frac{\psi_{\|e}\left(-m-n+p+q+qr\right)\Gamma\left(\frac{2p+1}{2+2r}\right)\Gamma\left(\frac{3+2n+2m+2r}{2+2r}\right)\Gamma\left(q-\left(\frac{1+2n+2m}{2+2r}\right)\right)}{(1+r)^2\,\Gamma\left(q+1\right)\Gamma\left(\frac{3+2p+2r}{2+2r}\right)(q-1)^{\left(q-\left(\frac{2n+2m+1}{2+2r}\right)\right)}}
\end{aligned}
$$

so that the dielectric constant finally becomes

$$
\begin{aligned}
\varepsilon(k,\omega) &= 1-\sum_{n=1}^{\infty}\frac{3\omega_{pe}^2}{k_\perp^2\psi_{\perp e}^2}\sum_{m=0}^{\infty}\frac{C_{n,m}}{m!n!}\left(\frac{k_\perp^2\psi_{\perp e}^2}{2^2\omega_{ce}^2}\right)^{n+m}\\
&\quad \sum_{p=0}^{n+m}\left(\frac{(-1)^p}{p!\,(n+m-p)!}\right)\left(\frac{2}{2p+1}\right)\left(\frac{n^2\omega_{ce}^2}{\omega^2-n^2\omega_{ce}^2}\right)\\
&\quad \left(\frac{\Gamma\left(\frac{3+2n+2m+2r}{2+2r}\right)\Gamma\left(q-\left(\frac{1+2n+2m}{2+2r}\right)\right)}{(q-1)^{\frac{1-n-m}{1+r}}\Gamma(q-\frac{3}{2+2r})\Gamma(1+\frac{3}{2+2r})\,(1+r)}\right)
\end{aligned}
$$

The dispersion relation for the electron Bernstein waves for generalized (r,q) distrib-

ution is therefore given by

$$
\begin{aligned}
1 &= \sum_{n=1}^{\infty} \frac{3k_{D(r,q)}^2}{k_\perp^2} \sum_{m=0}^{\infty} \frac{C_{n,m}}{m!n!} \left(\frac{b_{(r,q)}}{2}\right)^{n+m} \\
&\times \sum_{p=0}^{n+m} \left(\frac{(-1)^p}{p!\,(n+m-p)!\,(2p+1)}\right) \left(\frac{n^2\omega_{ce}^2}{\omega^2 - n^2\omega_{ce}^2}\right) \\
&\times \left(\frac{\Gamma\left(\frac{3+2n+2m+2r}{2+2r}\right)\Gamma\left(q-\left(\frac{1+2n+2m}{2+2r}\right)\right)}{(q-1)^{\frac{1-n-m}{1+r}}\Gamma(q-\frac{3}{2+2r})\Gamma(1+\frac{3}{2+2r})\,(1+r)}\right)
\end{aligned} \tag{3.9}
$$

where

$$
\begin{aligned}
k_{D(r,q)}^2 &= \frac{2k_D^2\Gamma\left(\frac{5}{2+2r}\right)\Gamma\left(q-\frac{5}{2+2r}\right)}{3\,(q-1)^{\frac{-1}{r+1}}\,\Gamma\left(q-\frac{3}{2+2r}\right)\Gamma\left(\frac{3}{2+2r}\right)}, \\
b_{(r,q)} &= b\left(\frac{3\,(q-1)^{\frac{-1}{r+1}}\,\Gamma\left(q-\frac{3}{2+2r}\right)\Gamma\left(\frac{3}{2+2r}\right)}{2\Gamma\left(\frac{5}{2+2r}\right)\Gamma\left(q-\frac{5}{2+2r}\right)}\right)
\end{aligned}
$$

It is interesting to note that above dispersion relation can be reduced to Eq. (3.5) for $r = 0, q = \kappa + 1$, which is the dispersion relation for the kappa distribution. One can say that (r, q) distribution is more generalized than the kappa distribution. Figure (3-3) shows $K\left(=\frac{k_\perp^2}{k_D^2}\right)$ versus $\Omega\left(=\frac{\omega}{\omega_{ce}}\right)$ for $r = 0$, $q = 4, 5, 7, 10$. One can see that at large values of q with $r = 0$, the dispersion curves approaches to the Maxwellian behavior like the kappa distribution. Figure (3-4) shows $K\left(=\frac{k_\perp^2}{k_D^2}\right)$ versus $\Omega\left(=\frac{\omega}{\omega_{ce}}\right)$ varying r from 1 to 3 and fixing q at 4. In Figure (3-5), we have plotted K vs Ω varying r from zero to 3, and fixing q at 10. We observe that at $r = 0$, $q = 10$, the curves become almost Maxwellian as expected. Figure (3-6) is a plot of dispersion curves for increasing the values of r and keeping q is fixed at 4. However increasing r value will shift the dispersion curves away from the Maxwellian and effect of supra thermal electrons will appear in the dispersion curves. One can notice that there is no propagation between $(0-1)\Omega$. Curves for $(1-2)\Omega$ starts from the higher side (2Ω) and tend to reach lower

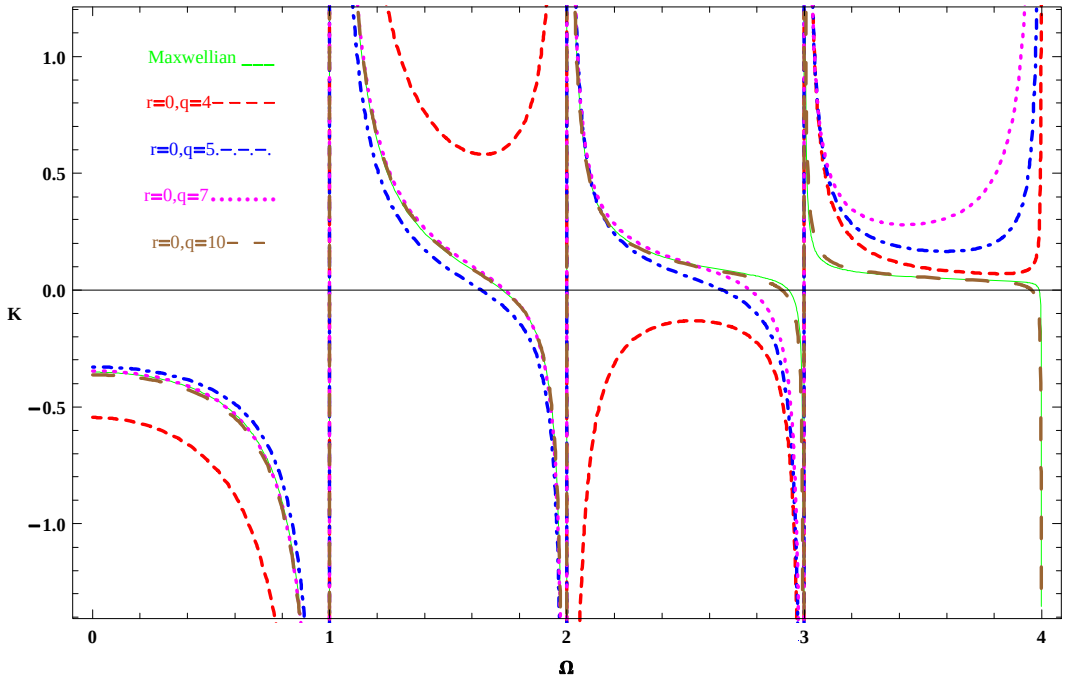

Figure 3-3: Dispersion plots of the electron Bernstein waves for different values of q with $r = 0$ using the Generalized (r, q) distribution. Dashed line shows plot of $q = 4$, dash-dot shows $q = 5$, dotted line shows $q = 7$, and dash-space-dash shows plot for $q = 10$, whereas Maxwellian is represented by a solid line.

side (Ω) with increase of b. In dispersion curves $(2-3)\Omega$, Maxwellian curve starts at 2.45Ω (upper hybrid frequency) goes towards bit higher side with the increase of b but remains in the same frequency range. Similar behavior is seen for $(3-4)\Omega$.

3.2.4 Parallel Propagation for (r, q) Distribution

Substituting $k_\perp = 0$, in the Eq. (3.8), the dielectric constant can be written as

$$\begin{aligned}\varepsilon(k_\parallel,\omega) &= 1+\sum_\alpha \frac{3\omega_{p\alpha}^2}{k_\parallel^2\psi_{\perp\alpha}^2\psi_{\parallel\alpha}^3}\left(\frac{q\,(1+r)\,\Gamma(q)}{(q-1)^{1+\frac{3}{2+2r}}\Gamma(q-\frac{3}{2+2r})\Gamma(1+\frac{3}{2+2r})}\right)\\ &\quad\times\int_{-\infty}^{\infty}\left(\frac{k_\parallel v_\parallel}{k_\parallel v_\parallel-\omega}\right)dv_\parallel\end{aligned}$$

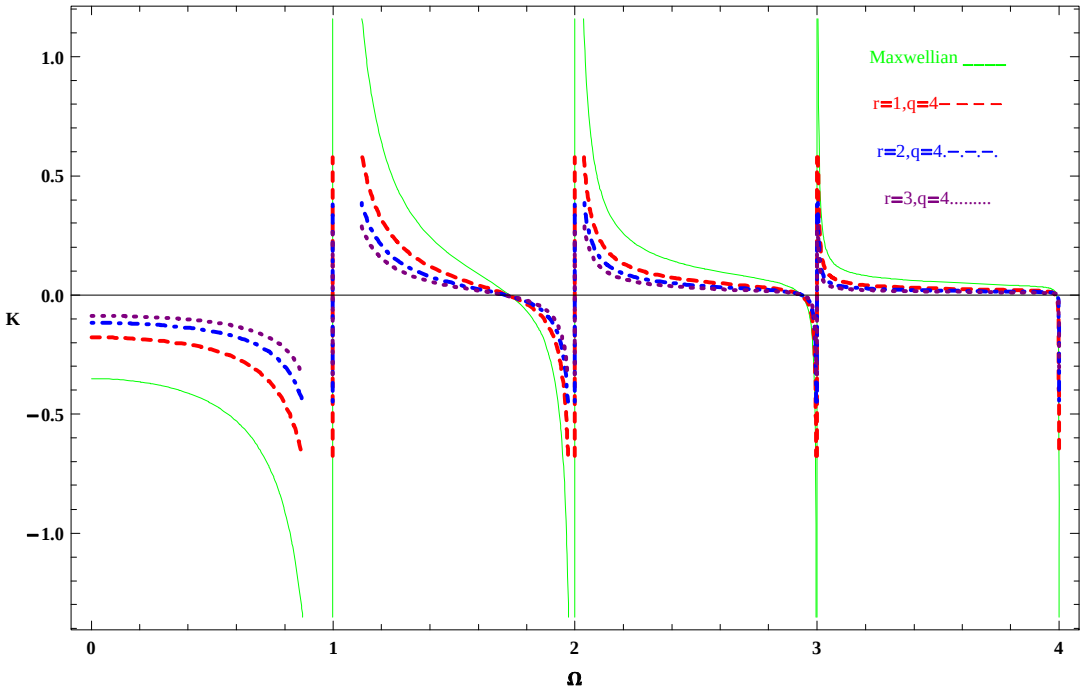

Figure 3-4: Dispersion plots of the electron Bernstein waves varying the values of r with fixed $q = 4$ using the Generalized (r, q) distribution. Dashed line shows plot of $r = 1$, dash-dot shows $r = 2$, dotted line shows $r = 3$, whereas Maxwellian is represented by a solid line.

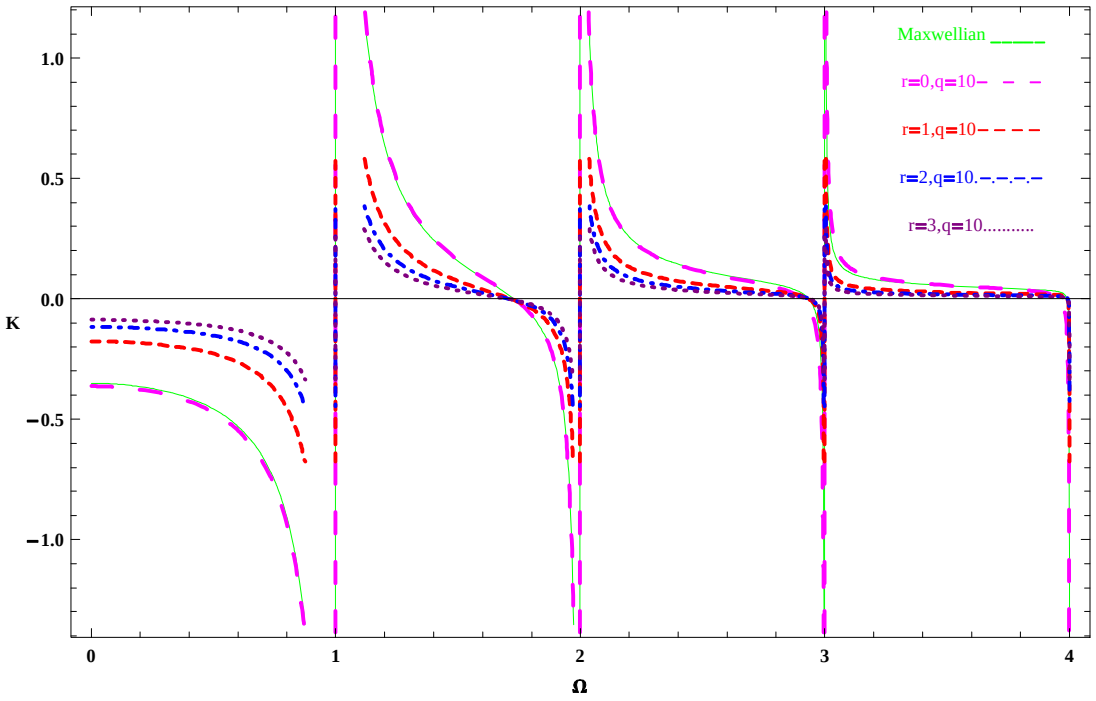

Figure 3-5: Dispersion plots of the electron Bernstein waves for different values of r with $q = 10$ using the Generalized (r, q) distribution. Dash space dash line shows $r = 0$, dashed line shows $r = 1$, dash-dot shows $r = 2$, dotted line shows $r = 3$, whereas Maxwellian is represented by a solid line.

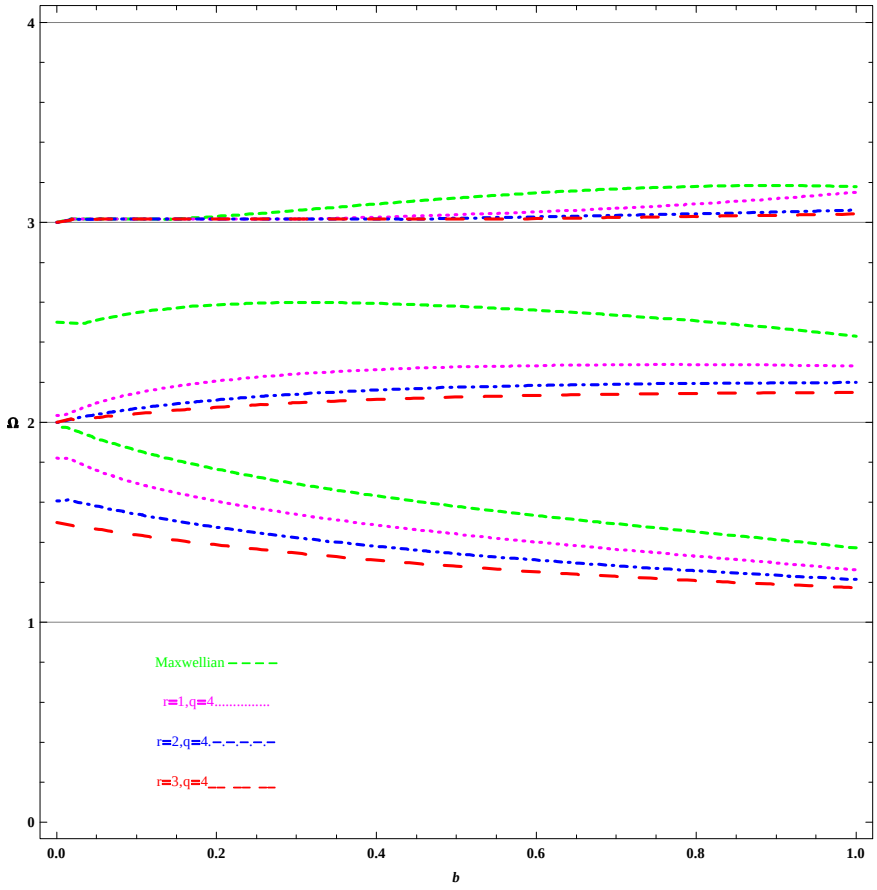

Figure 3-6: Plots of $\Omega\left(=\frac{\omega}{\omega_{ce}}\right)$ against b for different values of r with $q = 4$ using the Generalized (r, q) distribution. Dashed line shows plot of Maxwellian, dotted line shows $r = 1$, dash-dot shows $r = 2$, whereas $r = 3$ is represented by dash space dash line.

$$\times \int_0^\infty v_\perp \left(\frac{v_\parallel^2}{\psi_{\parallel\alpha}^2}+\frac{v_\perp^2}{\psi_{\perp\alpha}^2}\right)^r \left[1+\frac{1}{(q-1)}\left(\frac{v_\parallel^2}{\psi_{\parallel\alpha}^2}+\frac{v_\perp^2}{\psi_{\perp\alpha}^2}\right)^{r+1}\right]^{-q-1} dv_\perp$$

Performing the perpendicular integration

$$\begin{aligned}
&\int_0^\infty v_\perp \left(\frac{v_\parallel^2}{\psi_{\parallel\alpha}^2}+\frac{v_\perp^2}{\psi_{\perp\alpha}^2}\right)^r \left[1+\frac{1}{(q-1)}\left(\frac{v_\parallel^2}{\psi_{\parallel\alpha}^2}+\frac{v_\perp^2}{\psi_{\perp\alpha}^2}\right)^{r+1}\right]^{-q-1} dv_\perp \\
= \;& \frac{\psi_{\perp\alpha}^2}{2}\left(\frac{(q-1)}{q\,(1+r)}\right)\left[1+\frac{1}{(q-1)}\left(\frac{v_\parallel^2}{\psi_{\parallel\alpha}^2}\right)^{r+1}\right]^{-q}
\end{aligned}$$

Finally the dielectric constant is written as

$$\begin{aligned}
\varepsilon(k_\parallel,\omega) \;=\; & 1+\sum_\alpha \frac{3\omega_{p\alpha}^2}{2k_\parallel^2\psi_{\parallel\alpha}^3}\left(\frac{\Gamma(q)}{(q-1)^{\frac{3}{2+2r}}\Gamma(q-\frac{3}{2+2r})\Gamma(1+\frac{3}{2+2r})}\right) \\
& \int_{-\infty}^\infty \left(1+\frac{\omega}{k_\parallel v_\parallel-\omega}\right)\left[1+\frac{1}{(q-1)}\left(\frac{v_\parallel^2}{\psi_{\parallel\alpha}^2}\right)^{r+1}\right]^{-q} dv_\parallel
\end{aligned}$$

$$\begin{aligned}
= \;& 1+\sum_\alpha \frac{2\omega_{p\alpha}^2}{k_\parallel^2\psi_{\parallel\alpha}^2}\left\{\frac{3}{2}\left(\frac{\Gamma\left(1+\frac{1}{2+2r}\right)\Gamma\left(q-\frac{1}{2+2r}\right)}{(q-1)^{\frac{1}{1+r}}\Gamma(q-\frac{3}{2+2r})\Gamma(1+\frac{3}{2+2r})}\right)+\right. \\
& \left.\xi_2\left(\frac{3}{4}\right)\left(\frac{\Gamma\left(q\right)}{(q-1)^{\frac{3}{2+2r}}\Gamma(1+\frac{3}{2+2r})\Gamma(q-\frac{3}{2+2r})}\right)\int_{-\infty}^\infty \frac{\left(1+\frac{\left(u^2\right)^{1+r}}{(q-1)}\right)^{-q} ds}{u-\xi_1}\right\}
\end{aligned}$$

$$\varepsilon(k_\parallel,\omega)=1+\sum_\alpha \frac{2\omega_{p\alpha}^2}{k_\parallel^2\psi_{\parallel\alpha}^2}\left[B+\xi_2 Z_1^{(r,q)}\left(\xi_1\right)\right]$$

is the dielectric constant in unmagnetized parallel propagation plasma[50].

where

$$B = \frac{3}{2}\left(\frac{\Gamma\left(1+\frac{1}{2+2r}\right)\Gamma\left(q-\frac{1}{2+2r}\right)}{(q-1)^{\frac{1}{1+r}}\Gamma(q-\frac{3}{2+2r})\Gamma(1+\frac{3}{2+2r})}\right)$$

$$Z_1^{(r,q)}(\xi_2) = \left(\frac{3}{4}\right)\left(\frac{\Gamma(q)}{(q-1)^{\frac{3}{2+2r}}\Gamma(1+\frac{3}{2+2r})\Gamma(q-\frac{3}{2+2r})}\right)\int_{-\infty}^{\infty}\frac{\left(1+\frac{\left(u^2\right)^{1+r}}{(q-1)}\right)^{-q}ds}{s-\xi_2}$$

with

$$\xi_2 = \frac{\omega}{k_\parallel \psi_{\parallel\alpha}}, \qquad u = \frac{v_\parallel}{\psi_{\parallel\alpha}}$$

The growth rate and the real part of the frequency for the Langmuir waves has been described in [46]

3.3 Summary and Conclusions

Using the kinetic model we have presented the generalized dielectric constant in a magnetized non-Maxwellian anisotropic plasma. We have derived the dispersion relation for the (r, q) distribution function using Neumann's expansion for the products of Bessel function and compared the results with the kappa distribution in the limit $r = 0$, $q = \kappa + 1$ and to the Maxwellian for $\kappa -> \infty$.

Plotting $K\left(=\frac{k_\perp^2}{k_D^2}\right)$ versus $\Omega\left(=\frac{\omega}{\omega_{ce}}\right)$, figure (3-1) shows the comparison of the first few harmonics of electron Bernstein wave for $b = 0.5$. Solid line represents the curve obtained from Eq. (3.6) and the dotted line shows the standard text book result [1]. Figure (3-2) shows different modes of the electron Bernstein waves for $\kappa = 3, 5, 7, 10$ taking $b = 0.5$ and compared the results with the Maxwellian distribution. For small values of κ e.g., $\kappa = 3$ the dispersion curves show an interesting feature like backward Bernstein wave in the frequency bands $\omega_{ce} - 2\omega_{ce}$ and $3\omega_{ce} - 4\omega_{ce}$. On the other hand,

for larger values of κ, the contribution from the high energy particles is reduced and eventually approach to the Maxwellian in the limit $\kappa -> \infty$. Figure (3-3) shows the plot for the (r, q) distribution keeping $r = 0$ and varying $q = 4, 5, 7, 10$, the dispersion curves approach the Maxwellian behavior like the kappa distribution did for large κ. In figures (3-4) and (3-5), we keep q fixed at $q = 4, 10$ and allow r to vary From figure (3-4), we have observed that as we increase the value of r from 1 to 3, keeping $q = 4$, the dispersion curves move away from the Maxwellian case, which shows the strong dependence of the dispersion relation on the spectral indices r and q. Figure (3-5), shows the same behavior as that of the fig (3-4), for large values of q say 10 is fixed and increasing the value of r from zero to 3. Figure (3-6) depicts the plots of $\Omega \left(= \frac{\omega}{\omega_{ce}}\right)$ against b for different values of r keeping $q = 4$, for the first few Bernstein modes. It is observed that for r varying from 1 to 3, the dispersion curve depart away from the Maxwellian. As mentioned in the Introduction, our calculations will be useful for the non-Maxwellian plasmas with high energy tails following power-law like velocity distribution.

Although our main focus is on the electron Bernstein waves which are perpendicularly propagating electrostatic waves in the back ground magnetic field. However we have also discussed a limiting case of parallel propagation for both kappa and generalized (r, q) distribution and have obtained the Langmuir waves.

Present work is relevant to the space plasma where banded emissions have been observed and possess the high energy tail particle distribution functions. Non-Maxwellian particle velocity distributions are commonly observed in various space plasma scenarios such as solar wind, planetary magnetospheres and astrophysical plasmas wherein the temperature anisotropy is also present. In the laboratory plasma it has relevance with Tokamak edge plasma and beam plasma which contain non Maxwellian anisotropic velocity distributions.

Chapter 4

Pure Dust Bernstein Waves in Magnetized Non-Maxwellian Plasmas

4.1 Introduction

In dusty plasma the size distribution of dust particles indicate the presence of kappa and generalized Lorentzian distribution [78]. Electron Bernstein waves with isotropic kappa velocity distribution have been studied to explain the banded emission from the magnetosphere [13, 63]. In chapter 3, we studied electron Bernstein waves using anisotropic kappa and generalized (r, q) velocity distributions [79]. In this chapter we are presenting the case of Bernstein waves in the presence of dust particles using non-Maxwellian velocity distributions [80]. The relevance of this work can be found in astrophysical dusty plasmas where non-Maxwellian distribution is present along with the dust particles.

The chapter 4 is organized in the following fashion. Section (4.2) explains the mathematical formulation of the dust Bernstein waves subsections (4.2.1) , (4.2.2) describe the dispersion relations of dust Bernstein waves for kappa and generalized (r, q) distributions respectively. Section (4.3) summarizes and concludes the results.

4.2 Mathematical formulation of the pure dust Bernstein waves

Pure Bernstein waves are the electrostatic waves which propagate perpendicular to the ambient magnetic field. We have made use of two non-Maxwellian distribution functions namely, kappa and generalized (r, q).We consider a dusty plasma embedded in an ambient magnetic field $B_0 \| \widehat{z}$, whose constituents are electrons, singly ionized positive ions and micron sized negatively charged dust grains. The quasineutrality condition is $n_{i0} = n_{e0} + Z_{d0} n_{d0}$, where n_{i0}, n_{e0} and n_{d0} are the equilibrium number densities of ions, electrons and dust. Z_{d0} is the equilibrium charge number of the dust species. In the present work we investigate the dust Bernstein waves propagating perpendicular to the external magnetic field in a non-Maxwellian magnetized dusty plasma, the wave frequency is of the order of dust cyclotron frequency and the wavelength is of the order of dust Larmor radius.

The generalized dielectric constant for electrostatic waves in a uniform magnetized multiple species plasma, using kinetic model is given by [79]

$$\varepsilon(k,\omega) = 1 - \sum_{\alpha} \sum_{n=-\infty}^{\infty} \frac{i\omega_{p\alpha}^2}{k^2} \int \left\{ \frac{(n\omega_{c\alpha}/v_{\perp})\partial_{v_{\perp}} f_{\alpha 0} + k_{\|} \partial_{v_{\|}} f_{\alpha 0}}{s + i k_{\|} v_{\|} + i n \omega_{c\alpha}} \right\} J_n^2 (\frac{k_{\perp} v_{\perp}}{\omega_{c\alpha}}) d\mathbf{v} \qquad (4.1)$$

where the cylindrical coordinates system have been chosen and the propagation vector $\mathbf{k}$ is assumed to lie in the $x - z$ plane. Using the above dielectric constant we shall study the dispersion relation for pure dust Bernstein waves for non-Maxwellian distribution functions.

4.2.1 Dispersion relation of pure dust Bernstein waves for kappa distribution function

By employing kappa distribution in Eq.(4.1), we obtain the generalized dielectric constant as [79]

$$\begin{aligned}\varepsilon(k,\omega) &= 1+\sum_{\alpha}\sum_{n=-\infty}^{\infty}\frac{i4\omega_{p\alpha}^2}{\sqrt{\pi}k^2\theta_{\perp\alpha}^2\theta_{\|\alpha}}\left(\frac{(\kappa+1)\Gamma(\kappa+1)}{\kappa^{5/2}\Gamma(\kappa-(1/2))}\right)\\ &\times\int_{-\infty}^{\infty}\left\{\frac{(n\omega_{c\alpha}/\theta_{\perp\alpha}^2)+(k_{\|}v_{\|}/\theta_{\|\alpha}^2)}{s+ik_{\|}v_{\|}+in\omega_{c\alpha}}\right\}dv_{\|}\\ &\times\int_0^{\infty}v_{\perp}J_n^2(\frac{k_{\perp}v_{\perp}}{\omega_{c\alpha}})\left[1+\frac{v_{\|}^2}{\kappa\theta_{\|_\alpha}^2}+\frac{v_{\perp}^2}{\kappa\theta_{\perp_\alpha}^2}\right]^{-\kappa-2}dv_{\perp}\end{aligned}\tag{4.2}$$

Since the mass of the dust is much greater than that of ions and electrons, we may use asymptotic expansion of the Bessel function for dust species

$$J_n^2\left(\frac{k_{\perp}v_{\perp}}{\omega_{cd}}\right)=\frac{2\omega_{cd}}{\pi k_{\perp}v_{\perp}}\cos^2\left[\frac{k_{\perp}v_{\perp}}{\omega_{cd}}-\frac{n\pi}{2}-\frac{\pi}{4}\right]\ \text{for}\ \frac{k_{\perp}v_{\perp}}{\omega_{cd}}>1$$

An approximation is necessary for solving the plasma dispersion function which is given by [81]

$$\cos^2\left[\frac{k_{\perp}v_{\perp}}{\omega_{cd}}-\frac{n\pi}{2}-\frac{\pi}{4}\right]\simeq\frac{1}{2}$$

so that

$$J_n^2\left(\frac{k_{\perp}v_{\perp}}{\omega_{cd}}\right)=\frac{\omega_{cd}}{\pi k_{\perp}v_{\perp}}\tag{4.3}$$

Inserting this value in Eq.(4.2), we obtain the susceptibility constant for dust as

$$\begin{aligned}\chi_d &= \sum_{n=-\infty}^{\infty}\frac{4\omega_{pd}^2\omega_{cd}}{\pi^{3/2}k^2\theta_{\perp d}^2\theta_{\|d}k_{\perp}}\left(\frac{(\kappa+1)\Gamma(\kappa+1)}{\kappa^{5/2}\Gamma(\kappa-(1/2))}\right)\\ &\times\int_{-\infty}^{\infty}\left\{\frac{(n\omega_{cd}/\theta_{\perp d}^2)+(k_{\|}v_{\|}/\theta_{\|d}^2)}{-\omega+k_{\|}v_{\|}+n\omega_{cd}}\right\}\\ &\times\int_0^{\infty}\left[1+\frac{v_{\|}^2}{\kappa\theta_{\|d}^2}+\frac{v_{\perp}^2}{\kappa\theta_{\perp d}^2}\right]^{-\kappa-2}dv_{\perp}\end{aligned}\tag{4.4}$$

For the pure dust Bernstein waves $k_\parallel = 0$, and the integrals become

$$\int_0^\infty \left[1 + \frac{v_\parallel^2}{\kappa\theta_{\parallel d}^2} + \frac{v_\perp^2}{\kappa\theta_{\perp d}^2}\right]^{-\kappa-2} dv_\perp = \frac{\sqrt{\pi}\theta_{\perp d}}{2}\left(\frac{\sqrt{\kappa}\Gamma\left(\kappa+\frac{3}{2}\right)}{\Gamma\left(\kappa+2\right)}\right)\left(1 + \frac{v_\parallel^2}{\kappa\theta_{\parallel d}^2}\right)^{-\kappa-\frac{3}{2}}$$

$$\int_{-\infty}^\infty \left(1 + \frac{v_\parallel^2}{\kappa\theta_{\parallel d}^2}\right)^{-\kappa-\frac{3}{2}} dv_\parallel = \frac{\theta_{\parallel d}\sqrt{\pi\kappa}\Gamma\left(\kappa+1\right)}{\Gamma\left(\kappa+\frac{3}{2}\right)}$$

Thus χ_d simplifies to

$$\chi_d = -\sum_{n=1}^{\infty} \frac{4\omega_{pd}^2\omega_{cd}^3}{\sqrt{\pi}k_\perp^3\theta_{\perp d}^3}\left(\frac{\Gamma\left(\kappa+1\right)}{\kappa^{3/2}\Gamma(\kappa-(1/2))}\right)\left(\frac{n^2}{\omega^2 - n^2\omega_{cd}^2}\right)$$

where $\omega_{pd}^2 = \frac{4\pi Z_{d0}^2 e^2 n_{d0}}{m_d}$ and $\omega_{cd} = \frac{Z_{d0}eB_0}{m_d}$ are the dust plasma frequency and dust cyclotron frequency respectively. m_d is the mass of the dust and B_0 is the ambient magnetic field.

The susceptibilities for ions and electrons are given by

$$\begin{aligned}\chi_\alpha &= \sum_{n=-\infty}^{\infty} \frac{4\omega_{p\alpha}^2}{\sqrt{\pi}k^2\theta_{\perp\alpha}^2\theta_{\parallel\alpha}}\left(\frac{(\kappa+1)\Gamma(\kappa+1)}{\kappa^{5/2}\Gamma(\kappa-(1/2))}\right) \\ &\quad\times\int_{-\infty}^{\infty}\left\{\frac{(n\omega_{c\alpha}/\theta_{\perp\alpha}^2) + (k_\parallel v_\parallel/\theta_{\parallel\alpha}^2)}{-\omega + k_\parallel v_\parallel + n\omega_{c\alpha}}\right\} dv_\parallel \\ &\quad\times\int_0^\infty v_\perp J_n^2\left(\frac{k_\perp v_\perp}{\omega_{c\alpha}}\right)\left[1 + \frac{v_\parallel^2}{\kappa\theta_{\parallel\alpha}^2} + \frac{v_\perp^2}{\kappa\theta_{\perp\alpha}^2}\right]^{-\kappa-2} dv_\perp\end{aligned}$$

where $\alpha =$ ion, electron

Since the Larmor radii of these species are much smaller than the dust, we may treat the Bessel function argument to be small and therefore use the Neumann series expansion for the product of the Bessel function [76]. Resultantly the susceptibility can be written as

$$\chi_\alpha = -\sum_{\alpha=i,e}\sum_{n=1}^{\infty}\frac{4\omega_{p\alpha}^2}{k_\perp^2\theta_{\perp\alpha}^2}\sum_{m=0}^{\infty}\frac{C_{n,m}}{m!n!}\left(\frac{k_\perp^2\theta_{\perp\alpha}^2}{2^2\omega_{c\alpha}^2}\right)^{n+m}\left(\frac{\kappa^{n+m-1}\Gamma\left(\kappa+(1/2)-m-n\right)}{\Gamma(\kappa-(1/2))}\right) \times\left(\frac{n^2\omega_{c\alpha}^2}{\omega^2-n^2\omega_{c\alpha}^2}\right)$$

For low frequencies such as $\omega_{cd}<\omega<\omega_{ci}$, χ_α becomes

$$\chi_\alpha=\sum_{n=1}^{\infty}\sum_{m=0}^{\infty}\frac{4\omega_{p\alpha}^2}{k_\perp^2\theta_{\perp\alpha}^2}\frac{C_{n,m}}{m!n!}\left(\frac{k_\perp^2\theta_{\perp\alpha}^2}{2^2\omega_{c\alpha}^2}\right)^{n+m}\left(\frac{\kappa^{n+m-1}\Gamma\left(\kappa+(1/2)-m-n\right)}{\Gamma(\kappa-(1/2))}\right)$$

Thus the dielectric constant is written as

$$\varepsilon(k_\perp,\omega) = 1+\sum_{n=1}^{\infty}\sum_{m=0}^{\infty}\frac{4\omega_{pi}^2}{k_\perp^2\theta_{\perp i}^2}\frac{C_{n,m}}{m!n!}\left(\frac{k_\perp^2\theta_{\perp i}^2}{2^2\omega_{ci}^2}\right)^{n+m}\left(\frac{\kappa^{n+m-1}\Gamma\left(\kappa+(1/2)-m-n\right)}{\Gamma(\kappa-(1/2))}\right) -\sum_{n=1}^{\infty}\frac{4\omega_{pd}^2\omega_{cd}^3}{\sqrt{\pi}k_\perp^3\theta_{\perp d}^3}\left(\frac{\Gamma\left(\kappa+1\right)}{\kappa^{3/2}\Gamma(\kappa-(1/2))}\right)\left(\frac{n^2}{\omega^2-n^2\omega_{cd}^2}\right) \quad (4.5)$$

where we have neglected the electron dynamics since $m_e << m_i$. This is the generalized dielectric constant of pure dust Bernstein waves in terms of kappa distribution function. It is straight forward to check that the above relation is reduced to the Maxwellian distribution case in the limit of $\kappa\to\infty$, as given below

$$\varepsilon(k_\perp,\omega)=1+\sum_{n=1}^{\infty}\sum_{m=0}^{\infty}\frac{4\omega_{pi}^2}{k_\perp^2v_{T_{\perp i}}^2}\frac{C_{n,m}}{m!n!}\left(\frac{k_\perp^2v_{T_{\perp i}}^2}{2^2\omega_{ci}^2}\right)^{n+m}-\sum_{n=1}^{\infty}\frac{4\omega_{pd}^2\omega_{cd}^3}{\sqrt{\pi}k_\perp^3v_{\perp d}^3}\left(\frac{n^2}{\omega^2-n^2\omega_{cd}^2}\right) \quad (4.6)$$

We have plotted the dispersion relation for pure dust Bernstein waves (Eq.(4.5)) in Fig (4-1) Graphs are plotted for normalized wave number squared $\left(K=\frac{k_\perp^2}{k_d^2}\right)$ vs normalized frequency $\left(\Omega=\frac{\omega}{\omega_{cd}}\right)$ for different values of kappa $\kappa=3,5,7,10,100$ with $b=\frac{k_\perp^2v_{T_{\perp d}}^2}{2\omega_{cd}^2}=10$ and $\frac{\omega_{pi}^2}{\omega_{ci}^2}=0.01$. We observe that the K - variation domain depends upon the choice of b value, large value of b restricts the domain while smaller values widen it. We also notice

that the propagation band which is rather narrow in general widens for higher harmonics. Similarly the departure from Maxwellian curve is enlarged as we move towards higher harmonics. It is evident from the plots that for large kappa e.g.; ($\kappa = 100$), the dispersion curves approach the Maxwellian curve as expected. Fig (4-2) displays normalized frequency $\left(\Omega = \frac{\omega}{\omega_{cd}}\right)$ vs b, for the lowest harmonics with parameters $\frac{\omega_{pi}^2}{\omega_{ci}^2} = 0.01$, dust to ion mass ratio $\left(\frac{m_d}{m_i} = 10^6\right)$, electron/ion equilibrium density ratio $\left(\frac{n_{e0}}{n_{i0}} = 0.5\right)$. Fig. shows graphs with dust charge values ($Z_d = 3000, 5000, 10000$) keeping $\kappa = 3$ fixed. We observe that the high charge values lower the frequency domains as b increases, the frequency curves settle down at same common low frequency value. In other words, for large b the Z_d variation has little effect on frequency domain. In Fig (4-3) graphs are plotted for normalized frequency $\left(\Omega = \frac{\omega}{\omega_{cd}}\right)$ vs b, for different values of $\frac{n_{d0}}{n_{i0}} = 1.5 \times 10^{-4}$, 10^{-4}, 5×10^{-5} choosing $\kappa = 3$, $\frac{\omega_{pi}^2}{\omega_{ci}^2} = 0.01$, $\frac{m_d}{m_i} = 10^6$ and $Z_d = 3000$. Here we notice that with the increase of dust content $\left(\frac{n_{d0}}{n_{i0}}\right)$ dispersion curves shift to higher frequencies. If the dust content $\left(\frac{n_{d0}}{n_{i0}}\right)$ exceeds the value of 1.5×10^{-4}, the dispersion curve may jump to the next harmonic.

4.2.2 Dispersion relation of pure dust Bernstein waves for (r, q) distribution function

Inserting the value of generalized (r, q) distribution in Eq.(4.1), we obtain the generalized dielectric constant as [79]

$$\begin{aligned}
\varepsilon(k,\omega) &= 1 + \sum_{\alpha} \sum_{n=-\infty}^{\infty} \frac{i3\omega_{p\alpha}^2}{k^2 \psi_{\perp\alpha}^2 \psi_{\parallel\alpha}} \left(\frac{q\,(1+r)\,\Gamma(q)}{(q-1)^{1+\frac{3}{2+2r}} \Gamma(q - \frac{3}{2+2r}) \Gamma(1 + \frac{3}{2+2r})} \right) \\
&\quad \int_{-\infty}^{\infty} \left\{ \frac{(n\omega_{c\alpha}/\psi_{\perp\alpha}^2) + (k_{\parallel} v_{\parallel}/\psi_{\parallel\alpha}^2)}{s + ik_{\parallel} v_{\parallel} + in\omega_{c\alpha}} \right\} dv_{\parallel} \\
&\quad \times \int_0^{\infty} v_{\perp} J_n^2 (\frac{k_{\perp} v_{\perp}}{\omega_{c\alpha}}) \left(\frac{v_{\parallel}^2}{\psi_{\parallel\alpha}^2} + \frac{v_{\perp}^2}{\psi_{\perp\alpha}^2} \right)^r
\end{aligned}$$

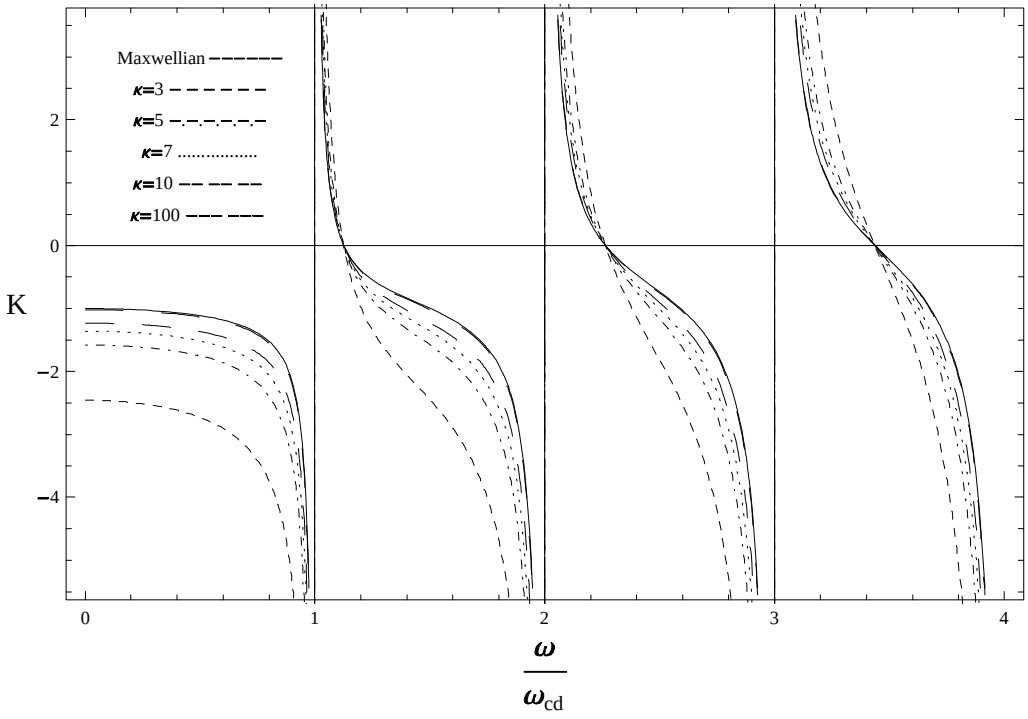

Figure 4-1: Dispersion plots of the pure dust Bernstein waves for $K\left(=\frac{k_{\perp}^2}{k_D^2}\right)$ versus $\Omega\left(=\frac{\omega}{\omega_{cd}}\right)$ using kappa velocity distribution.

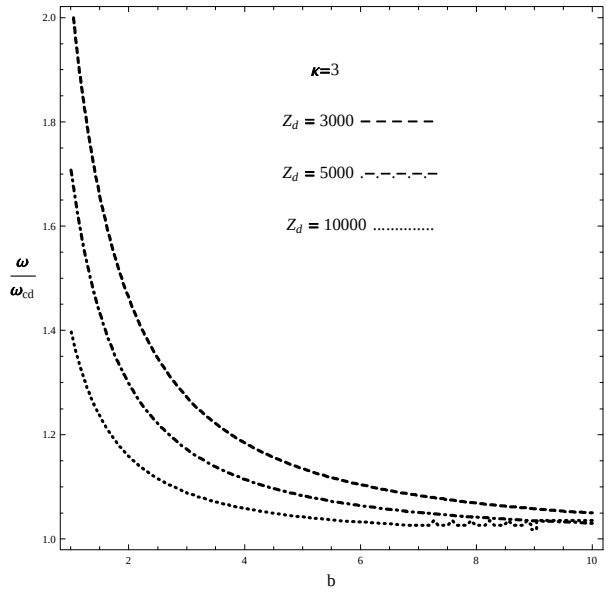

Figure 4-2: Plots of the pure dust Bernstein waves for $\Omega\left(=\frac{\omega}{\omega_{cd}}\right)$ versus b with different values of Z_d and $\kappa = 3$ fixed.

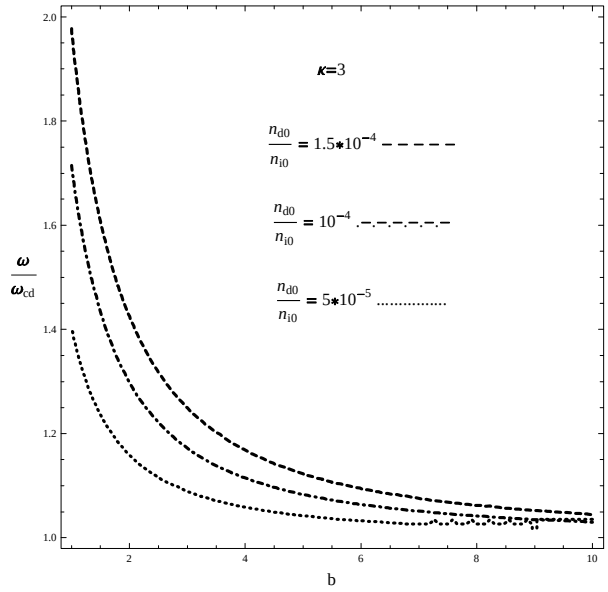

Figure 4-3: Plots of the pure dust Bernstein waves for $\Omega\left(=\frac{\omega}{\omega_{cd}}\right)$ versus b with different values of dust to ion ratio $(\frac{n_{d0}}{n_{i0}})$ and $\kappa = 3$ fixed.

$$\times \left[1+\frac{1}{(q-1)}\left(\frac{v_{\parallel}^2}{\psi_{\parallel\alpha}^2}+\frac{v_{\perp}^2}{\psi_{\perp\alpha}^2}\right)^{r+1}\right]^{-q-1} dv_{\perp}$$

In dust Bernstein mode, we have used the large argument expansion of $J_n^2(\frac{k_\perp v_\perp}{\omega_{c\alpha}})$ for dust and the small argument expansion of the $J_n^2(\frac{k_\perp v_\perp}{\omega_{c\alpha}})$ for ions. This assumption is valid due to the large mass of dust as compared with ions and electrons.

The dust susceptibility in terms of (r,q) distribution is written as

$$\begin{aligned}\chi_d &= \sum_{n=1}^{\infty}\frac{3\omega_{pd}^2\omega_{cd}}{\pi k_\perp^3\psi_{\perp d}^4\psi_{\parallel d}}\left(\frac{q\,(1+r)\,\Gamma(q)}{(q-1)^{1+\frac{3}{2+2r}}\Gamma(q-\frac{3}{2+2r})\Gamma(1+\frac{3}{2+2r})}\right)\left(\frac{-2n^2}{\omega^2-n^2\omega_{cd}^2}\right)\\ &\int_{-\infty}^{\infty}\int_0^{\infty}\left(\frac{v_{\parallel}^2}{\psi_{\parallel d}^2}+\frac{v_{\perp}^2}{\psi_{\perp d}^2}\right)^{r}\times\left[1+\frac{1}{(q-1)}\left(\frac{v_{\parallel}^2}{\psi_{\parallel d}^2}+\frac{v_{\perp}^2}{\psi_{\perp d}^2}\right)^{r+1}\right]^{-q-1} dv_{\perp}\end{aligned}$$

Performing the perpendicular integration we obtain

$$\begin{aligned}&\int_0^{\infty}\left(\frac{v_{\parallel}^2}{\psi_{\parallel d}^2}+\frac{v_{\perp}^2}{\psi_{\perp d}^2}\right)^{r}\times\left[1+\frac{1}{(q-1)}\left(\frac{v_{\parallel}^2}{\psi_{\parallel d}^2}+\frac{v_{\perp}^2}{\psi_{\perp d}^2}\right)^{r+1}\right]^{-q-1} dv_{\perp}\\ &= \psi_{\perp d}\left(\frac{v_{\parallel}^2}{\psi_{\parallel d}^2}\right)^{\frac{-1}{2}-q-qr}\left(\frac{{}_2F_1\left[q+1,q+\frac{1}{2+2r};q+1+\frac{1}{2+2r},-(q-1)\left(\frac{v_{\parallel}^2}{\psi_{\parallel d}^2}\right)^{-1-r}\right]}{(q-1)^{-q-1}\,(2q+2qr+1)}\right)\end{aligned}$$

where ${}_2F_1$ is the standard hypergeometric function. The susceptibility for the dust becomes

$$\begin{aligned}\chi_d &= -\sum_{n=1}^{\infty}\frac{3\omega_{pd}^2\omega_{cd}^3}{\pi k_\perp^3\psi_{\perp d}^3\psi_{\parallel d}}\left(\frac{q\,(1+r)\,\Gamma(q)}{(q-1)^{-q+\frac{3}{2+2r}}\Gamma(q-\frac{3}{2+2r})\Gamma(1+\frac{3}{2+2r})}\right)\left(\frac{2n^2}{\omega^2-n^2\omega_{cd}^2}\right)\\ &\int_{-\infty}^{\infty}\left(\frac{v_{\parallel}^2}{\psi_{\parallel d}^2}\right)^{\frac{-1}{2}-q-qr}\times\end{aligned}$$

$$ {}_2F_1\left[q+1, q+\frac{1}{2+2r}; q+1+\frac{1}{2+2r}, -(q-1)\left(\frac{v_\parallel^2}{\psi_{\parallel d}^2}\right)^{-1-r}\right] dv_\parallel \qquad (4.7) $$

The parallel integration gives

$$ \int_{-\infty}^{\infty}\left(\frac{v_\parallel^2}{\psi_{\parallel d}^2}\right)^{\frac{-1}{2}-q-qr} {}_2F_1\left[q+1, q+\frac{1}{2+2r}; q+1+\frac{1}{2+2r}, -(q-1)\left(\frac{v_\parallel^2}{\psi_{\parallel d}^2}\right)^{-1-r}\right] dv_\parallel $$

$$ = \frac{\psi_{\parallel d}(q-1)^{-q}(2q+2qr+1)}{q(1+r)} $$

Substituting the value of parallel integration in Eq.(4.7) we get

$$ \begin{aligned} \chi_d &= -\sum_{n=1}^{\infty}\frac{3\omega_{pd}^2\omega_{cd}^3}{\pi k_\perp^3\psi_{\perp d}^3}\left(\frac{2n^2}{\omega^2-n^2\omega_{cd}^2}\right) \\ &\quad\times\left(\frac{\Gamma(q)}{(q-1)^{\left(\frac{3}{2+2r}\right)}\Gamma(q-\frac{3}{2+2r})\Gamma(1+\frac{3}{2+2r})}\right) \end{aligned} $$

Using the small argument of the Bessel function and performing the perpendicular and parallel integration, we obtain the susceptibility for the ions

$$ \begin{aligned} \chi_i &= \sum_{n=1}^{\infty}\frac{3\omega_{pi}^2}{k_\perp^2\psi_{\perp i}^2}\sum_{m=0}^{\infty}\frac{C_{n,m}}{m!n!}\left(\frac{k_\perp^2\psi_{\perp i}^2}{2^2\omega_{ci}^2}\right)^{n+m} \\ &\quad\times\sum_{p=0}^{n+m}\left(\frac{2(-1)^p}{p!\,(n+m-p)!\,(2p+1)}\right) \\ &\quad\times\left(\frac{\Gamma\left(\frac{3+2n+2m+2r}{2+2r}\right)\Gamma\left(q-\left(\frac{1+2n+2m}{2+2r}\right)\right)}{(q-1)^{\frac{1-n-m}{1+r}}\Gamma(q-\frac{3}{2+2r})\Gamma(1+\frac{3}{2+2r})(1+r)}\right) \end{aligned} $$

So the dielectric constant for pure dust Bernstein waves for (r, q) velocity distribution becomes

$$\varepsilon(k_\perp,\omega) = 1+\sum_{n=1}^{\infty}\frac{3\omega_{pi}^2}{k_\perp^2\psi_{\perp i}^2}\sum_{m=0}^{\infty}\frac{C_{n,m}}{m!n!}\left(\frac{k_\perp^2\psi_{\perp i}^2}{2^2\omega_{ci}^2}\right)^{n+m}\sum_{p=0}^{n+m}\left(\frac{2(-1)^p}{p!\,(n+m-p)!\,(2p+1)}\right)\left(\frac{\Gamma\left(\frac{3+2n+2m+2r}{2+2r}\right)\Gamma\left(q-\left(\frac{1+2n+2m}{2+2r}\right)\right)}{(q-1)^{\frac{1-n-m}{1+r}}\Gamma(q-\frac{3}{2+2r})\Gamma(1+\frac{3}{2+2r})\,(1+r)}\right) - \sum_{n=1}^{\infty}\frac{3\omega_{pd}^2\omega_{cd}^3}{\pi k_\perp^3\psi_{\perp d}^3}\left(\frac{2n^2}{\omega^2-n^2\omega_{cd}^2}\right)\left(\frac{\Gamma(q)}{(q-1)^{\frac{3}{2+2r}}\,\Gamma(q-\frac{3}{2+2r})\Gamma(1+\frac{3}{2+2r})}\right) \quad (4.8)$$

The contribution of electrons is neglected due to the small mass as compared to ions and dust. One can easily show that the above relation will reduce to the kappa result in the limit of $r=0$, $q=\kappa+1$, and to that of the Maxwellian in the limit of $r=0$, $q\to\infty$.

The dispersion relation of pure dust Bernstein waves (Eq.(4.8)) is plotted in Fig (4-4) for normalized waves number squared $\left(K=\frac{k_\perp^2}{k_d^2}\right)$ vs normalized frequency $\left(\Omega=\frac{\omega}{\omega_{cd}}\right)$ with $b=10$ and $\frac{\omega_{pi}^2}{\omega_{ci}^2}=0.01$. Dispersion curves are plotted for different r values ($r=1,2,3$) keeping $q=4$ fixed and then compared with the Maxwellian curve. With increasing r values, the departure from the Maxwellian curve is pronounced as expected. Fig (4-5) displays normalized frequency $\left(\Omega=\frac{\omega}{\omega_{cd}}\right)$ vs b, for the lowest harmonic and with the parameters $\frac{\omega_{pi}^2}{\omega_{ci}^2}=0.01$, $\frac{m_d}{m_i}=10^6$, $\frac{n_{e0}}{n_{i0}}=0.5$. Fig (4-5) shows the plots for dust charge values ($Z_d=3000,5000,10000$) for $r=1$ and $q=4$. It is evident that with increasing dust charge value the dispersion curves go to the lower side of the Ω. Similarly Fig (4-6) exhibits graphs for different values of $\frac{n_{d0}}{n_{i0}}=1.5\times10^{-4}$, 10^{-4}, 5×10^{-5} for $r=1$, $q=4$, $\frac{\omega_{pi}^2}{\omega_{ci}^2}=0.01$, $\frac{m_d}{m_i}=10^6$ and $Z_d=3000$. Dispersion curves shift to the lower side of frequency Ω for lower values of $\frac{n_{d0}}{n_{i0}}$.

4.3 Summary and Conclusion

We have investigated the pure dust Bernstein waves using non-Maxwellian kappa and (r,q) distribution functions in a collisionless, uniform magnetized dusty plasma using the kinetic model. Dispersion relations are derived for frequency of the order of dust

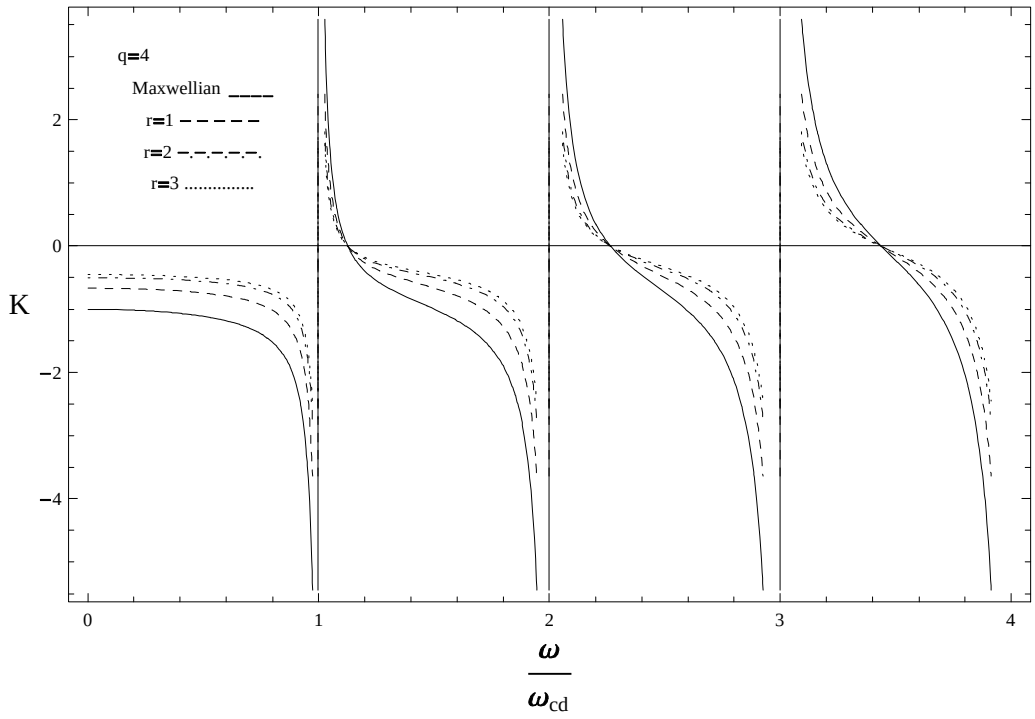

Figure 4-4: Dispersion plots of the pure dust Bernstein waves for $K\left(=\frac{k_{\perp}^2}{k_D^2}\right)$ versus $\Omega\left(=\frac{\omega}{\omega_{cd}}\right)$ varying the values of r with fixed $q=4$ using the Generalized (r,q) distribution.

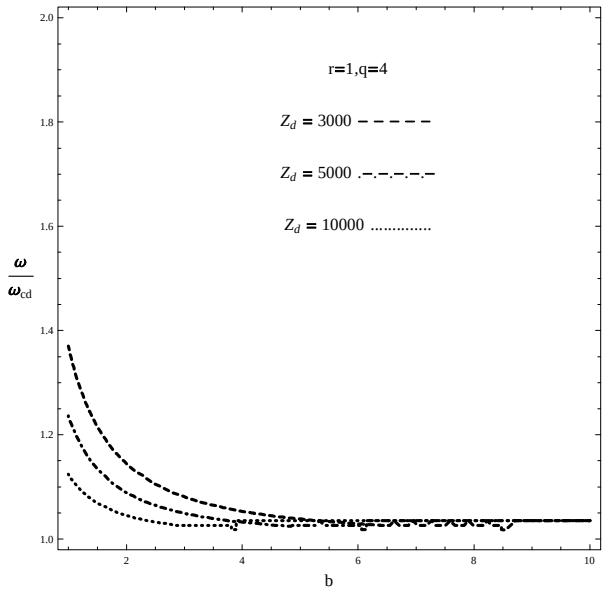

Figure 4-5: Plots of the pure dust Bernstein waves for $\Omega\left(=\frac{\omega}{\omega_{cd}}\right)$ versus b with different values of Z_d and $r = 1$, $q = 4$ fixed.

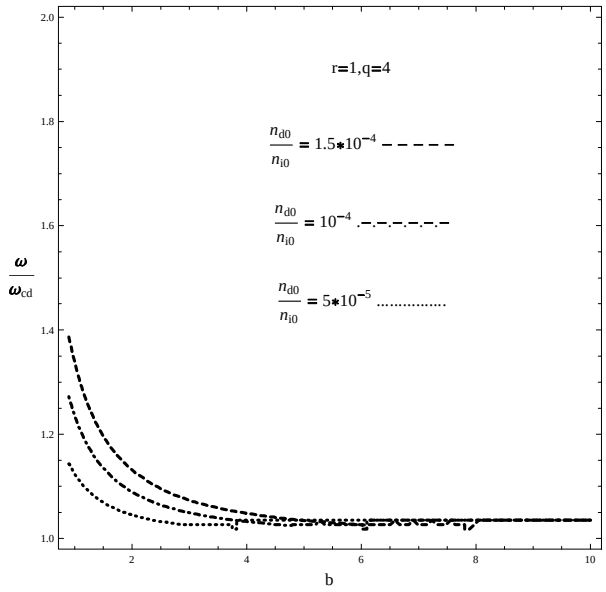

Figure 4-6: Plots of the pure dust Bernstein waves for $\Omega\left(=\frac{\omega}{\omega_{cd}}\right)$ versus b with different values of dust to ion ratio $(\frac{n_{d0}}{n_{i0}})$ and $r = 1$, $q = 4$ fixed.

cyclotron frequency and the wavelength of the order of dust Larmor radius. For deriving the dispersion relation, contribution of electrons is neglected due to its small mass as compared to ions and dust. Dispersion curves are plotted for kappa and (r, q) distribution functions by choosing specific values of the spectral indices and then the results are compared with Maxwellian distribution. It is found that for large values of spectral index kappa (κ), the dispersion curves approach the Maxwellian curves. With (r, q) distribution, the dispersion curves reduce to kappa curves for $r = 0$ but show deviation from Maxwellian curves for $r = 1, 2, 3$. Comparing dust Bernstein waves with electron Bernstein waves we notice that the propagation band for the former is rather narrow as compared with the latter. However the band width increases for higher harmonics for both kappa and (r, q) distributions. Effect of dust charge on dispersion curves is also studied and we observe that with increasing dust charge, the dispersion curves shift toward the lower frequencies. We also observe that increasing the dust to ion density ratio $\left(\frac{n_{d0}}{n_{i0}}\right)$ causes the dispersion curve to shift toward the higher frequencies. All these effects are discussed in detail in the subsections (4.2.1) and (4.2.2). Relevance of this work can be found in space and astrophysical dusty plasmas (for instance, interstellar media, planetary magnetospheres, cometary tails, asteroid zones, ionosphere, etc.), where non-Maxwellian distribution is present along with the dust particles.

Chapter 5

Summary of the Results and Recommendations for Future Research Work

The electrostatic potentials (Debye and wake) and energy loss due to a charged projectile propagating through an unmagnetized collisionless dusty plasma are derived employing kappa and generalized (r, q) velocity distributions for the Dust Acoustic Wave (DAW). It is found that these quantities in general differ from their Maxwellian counterparts and are sensitive to the values of spectral index, κ in case of kappa distribution and to r, q in case of generalized (r, q) distribution. The amplitudes of these quantities are less for small values of the spectral index (κ, $r = 0$, q) but approach to the Maxwellian in the limit $\kappa \longrightarrow \infty$ (for kappa distribution) and for $r = 0$, $q \rightarrow \infty$ (for generalized (r, q) distribution). For any non-zero value of r, the potential and the energy loss grow beyond the Maxwellian results. The effect of kappa and generalized (r, q) distributions on potential and energy loss is also studied numerically and the results are compared with those of the Maxwellian distribution [50].

A generalized dielectric constant for the electron Bernstein waves using non-Maxwellian distribution functions is derived in a collisionless, uniform magnetized plasma. Using

Neumann's series expansion for the products of Bessel functions, we can derive dispersion relations for both kappa and the generalized (r, q) distributions in a straight forward manner. The dispersion relations now become dependent upon the spectral indices κ and (r, q) for the kappa and the generalized (r, q) distribution respectively. Our results show how the non-Maxwellian dispersion curves deviate from the Maxwellian depending upon the values of the spectral indices chosen. It may be noted that the (r, q) dispersion relation is reduced to the Kappa distribution for $r = 0$, $q = \kappa + 1$, which, in turn, is further reduceable to the Maxwellian distribution for $\kappa \to \infty$ [79].

Pure dust Bernstein waves are investigated using non-Maxwellian kappa and (r, q) distribution functions in a collisionless, uniform magnetized dusty plasma. Dispersion relations for both distributions are derived considering waves whose frequency is of the order of dust cyclotron frequency and dispersion curves are plotted. It is observed that the propagation band for dust Bernstein waves is rather narrow as compared with the electron Bernstein waves. However the band width increases for higher harmonics, for both kappa and (r, q) distributions. Effect of dust charge on dispersion curves is also studied and one observes that with increasing dust charge, the dispersion curves shift toward the lower frequencies. Increasing the dust to ion density ratio $\left(\frac{n_{d0}}{n_{i0}}\right)$ causes the dispersion curve to shift toward the higher frequencies. It is also found that for large values of spectral index kappa (κ), the dispersion curves approach to the Maxwellian curves. (r, q) distribution approaches to kappa for $r = 0$, whereas for $r > 0$, dispersion curves show deviation from Maxwellian curves as expected. Relevance of this work can be found in astrophysical dusty plasmas where non-Maxwellian distribution is present along with the dust particles [80].

The dielectric constant which is derived for the Bernstein waves for non-Maxwellian velocity distributions can also be used to calculate the Debye and wake potentials in a magnetized dusty plasma. Once we have potentials we can further extend this work for the calculation of the energy loss of a test charge particle moving through a magnetized dusty plasma.

Bibliography

[1] F. F. Chen, Introduction to Plasma Physics and Controlled Fusion, Volume I: Plasma Physics, 2 ed. (Plenum Press, New York, 1990).

[2] P. M. Bellan Fundamentals of Plasma Physics, (Cambridge University Press, London, 2006).

[3] T. J. M. Boyd and J. J. Sanderson, The Physics of Plasmas, (Cambridge University Press, New York, 2003).

[4] D. G. Swanson, Plasma Waves, 2nd Edition, (Institute of Physics Publishing, London, 2003).

[5] W. Baumjohann and R. A. Treumann, Basic Space Plasma Physics, (Imperial College Press, London, 1997).

[6] R. A. Treumann and W. Baumjohann, Advanced Space Plasma Physics, (Imperial College Press, London, 2001).

[7] P. K. Shukla and A AMamun, Introduction to Dusty Plasma Physics, (Institute of Physics Publishing, London 2002).

[8] D. Summers and R. M. Thorne, Phys. Fluids B **3,** 1835 (1991).

[9] V. M. Vasyliunas, J. Geophys. Res. **73**, 2839 (1968).

[10] R. L. Mace, M. A. Helberg and R. A. Treumann, J. Plasma Phys. **59**, 393 (1998).

[11] R. L. Mace and M. A. Helberg, Phys. Plasmas **2**, 2098 (1995).

[12] M. N. S. Qureshi, H. A. Shah, G. Murtaza, S. J. Schwartz and F. Mahmood, Phys. Plasmas **11**, 3819 (2004).

[13] R. L. Mace, Phys. Plasmas, **10**, 2181 (2003).

[14] R. J. Dumonta, C. K. Phillips and D. N. Smithe, Phys. Plasmas, **12**, 042508 (2005).

[15] C. K. Goertz, Rev. Geophys., **27**, 271 (1989).

[16] D. A. Mendis and M. Rosenberg, IEEE Trans. Plasma Sci., **20**, 929 (1992).

[17] D. A. Mendis and M. Rosenberg, Annu. Rev. Astron. Astrophys., **32**, 419 (1994).

[18] D. A. Mendis, in Advances in Dusty Plasmas, edited by P. K. Shukla, D. A. Mendis, and T. Desai (World Scientific, Singapore, 1997).

[19] S. Barabash and R. Lundin, IEEE Trans. Plasma Sci. 22, 173 (1994).

[20] P. Bliokh, V. Sinitsin and V. Yaroshenko, Dusty and Self-Gravitational Plasmas in Space, (Kluwer Academic, Dordrecht, 1995).

[21] E. Grün, et al., Science, **274**, 399 (1996).

[22] P. K. Shukla, et al., The Physics of Dusty Plasmas (World Scientific, Singapore, 1996).

[23] R. Bingham and V. N. Tsytovich, Astropart. Phys., **12**, 35 (1999).

[24] A. L. Graps et al., Nature, London, **405**, 48 (2000).

[25] F. Verheest, Waves in Dusty Space Plasmas, (Kluwer Academic, Dordrecht, 2000).

[26] B. T. Tsurutani et al., Geophys. Res. Lett., **30**, 2134 (2003).

[27] D. A. Gurnett, et al., Icarus, **53**, 236 (1983).

[28] D. A. Gurnett, et al., Geophys. Res. Lett., **24**, 3125 (1997).

[29] D. Tsintikidis, et al., Geophys. Res. Lett., **23**, 997 (1996).

[30] M. Horányi, Phys. Plasmas, **7**, 3847 (2000).

[31] M. Horányi, et al., Rev. Geophys. 42, RG4002 (2004).

[32] G. S. Selwyn, et al., J. Vac. Sci. Technol. A, **7**, 2758 (1989).

[33] S. V. Vladimirov and K. Ostrikov, Phys. Rep., **393**, 175 (2004).

[34] I. Levchenko, et al., Phys. Plasmas, **14**, 063502 (2007).

[35] A. F. Pal', et al., Plasma Phys. Rep., **33**, 43 (2007).

[36] G. Nishimaru, et al., Diamond Relat. Mater. **12**, 374 (2003).

[37] J. Winter, Plasma Phys. Controlled Fusion, **40**, 1201 (1998).

[38] W. P. West, et al., Plasma Phys. Rep. **48**, 1661 (2006).

[39] M. Nambu and H. Akama, Phys. Fluids **28**, 2300 (1985).

[40] M. Nambu, S. V. Vladimirov and P. K. Shukla, Phys. Lett. A **203**, 40 (1995).

[41] K. Takahashi, T. Oishi, K. I. Shimomai, Y. Hayashi and S. Nishino, Phys. Rev. E **58**, 7805 (1998).

[42] M. H. Nasim, A. M. Mirza, G. Murtaza and P. K. Shukla, Phys. Scr. **61**, 628 (2000).

[43] M. H. Nasim, A. M. Mirza, M. S. Qaisar, G. Murtaza and P. K. Shukla, Phys. Plasmas **5**, 3581 (1998).

[44] M. H. Nasim, A. M. Mirza, M. S. Qaisar, G. Murtaza and P. K. Shukla, Phys. Plasmas **7**, 762 (2000).

[45] S. Ali, M. H. Nasim and G. Murtaza, Phys. Plasmas **10**, 4207 (2003).

[46] S. Zaheer, G. Murtaza and H. A. Shah, Phys. Plasmas **11**, 2246 (2004).

[47] M. A. Sarwar and A. M. Mirza, Phys. Plasmas **12**, 062108 (2005)

[48] N. Rubab and G. Murtaza, Phys. Scr. **73**, 178 (2006).

[49] N. Rubab and G. Murtaza, Phys. Scr. **74**, 145 (2006).

[50] F. Deeba, Z. Ahmad and G. Murtaza, Phys. Plasmas, **13**, 082108 (2006).

[51] J. C. Wright, P. T. Bonoli, A. E. Schmidt, C. K. Phillips, E. J. Valeo, R. W. Harvey, and M. A. Brambilla, Phys. Plasmas, **16**, 072502 (2009).

[52] V. Krivenski, Fusion Eng. and Design, **53**, 23 (2001).

[53] A. Mueck, L. Curchod, Y. Camenen, S. Coda, T. P. Goodman, H. P. Laqua, A. Pochelon, L. Porte, and F. Volpe, Phys. Rev. Lett., **98**, 175004 (2007).

[54] T. H. Stix, Waves in Plasmas (Springer-Verlag, New York, 1992).

[55] I. Bernstein, Phys. Rev., **109**, 10 (1958).

[56] R. A. Cairns and C. N. Lashmore-Davies, Phys. Plasmas, **7**, 4126 (2000).

[57] S. J. Diem, G. Taylor, J. B. Caughman, P. C. Efthimion, H. Kugel, B. P. LeBlanc, C. K. Phillips, J. Preinhaelter, S. A. Sabbagh, J. Urban and J. B.Wilgen, Nucl. Fusion, **49,** 095027 (2009)

[58] V. Shevchenko, Y. Baranov, M. O'Brien, and A. Saveliev, Phys. Rev. Lett., **89**, 265005 (2002).

[59] P. C. Efthimion, J.C. Hosea, R. Kaita, R. Majeski and G. Taylore, Rev. Sci. Instrum., **70,** 1018 (1999).

[60] F. Crawford, J. Res. of the National Bureau of Standards, Section D- Radio Science, **D 69**, 789 (1965).

[61] F. Leuterer, Plasma Physics, **11**, 615 (1969).

[62] M. Moncuquet, N. Meyervernet and S. Hoang, J. Geophys. Res., **100**, 21697 (1995).

[63] R. L. Mace, Phys. Plasmas, **11**, 507 (2004).

[64] N. Meyer-Vernet, S. Hoang, and M. Moncuquet, J. Geophys. Res. **98**, 21163 (1993).

[65] L. D. Landau, J. Phys. USSR, **10**, 25 (1946).

[66] A. I. Sukhorukov and P. Stubbe, Phys. Plasmas, **4**, 2497 (1997).

[67] F. Valentini, P. Veltri and A. Mangeney, Phys. Rev. E, **71**, 016402 (2005).

[68] F. Valentini and R. D'Agosta, Phys. Plasmas, **14**, 092111 (2007).

[69] M. Ono, Phys. Fluids B, **5** 241 (1993).

[70] M. Salimullah, Phys. Lett., A **215**, 296 (1996).

[71] F. Verheest and T. Cattaert, IEEE Trans. Plasma Sci., **32**, 653 (2004).

[72] M. Salimullah, M. Salahuddin, B. Dasgupta and M. S. Janaki, Phys. Scr., **58**, 271 (1998)

[73] A. Melzer, V. A. Schweigert, and A. Piel, Phys. Rev. Lett. **83**, 3194 (1999).

[74] M. H. Nasim, P. K. Shukla and G. Murtaza, Phys. Plasmas, **6**, 1409 (1999).

[75] M. Moncuquet, N. Meyer-Vernet, S. Hoang, R. J. Forsyth, and P. Canu , J. Geophys. Res., **102**, 2373 (1997).

[76] M. Brambilla, Kinetic Theory of Plasma Waves Homogeneous Plasmas (Oxford University Press Inc., New York, 1998)

[77] D. C. Montgomery and D. A. Tidman, Plasma Kinetic Theory (McGraw-Hill Book Company, New Yark, 1964).

[78] M. A. Raadu, IEEE Trans. Plasma Sci. **29**, 182 (2001)

[79] F. Deeba, Z. Ahmad and G. Murtaza, Phys. Plasmas, **17**, 102114 (2010)

[80] F. Deeba, Z. Ahmad and G. Murtaza, Phys. Plasmas, Submitted (2011)

[81] S. P. Gary, J. Plasma Phys., **7**, 417 (1972)